On primordial black holes

Savvas M. Koushiappas

BROWN
Department of Physics

With Alex Geringer-Sameth, Kyriakos Vattis, Ross Kliegman, Matthew Walker, and Avi Loeb

What I hope to talk about

- Primordial black holes as dark matter and dwarf galaxies constraints.
- What is the robustness of these constraints.
- The primordial black hole WIMP conflict.
- The growth of supermassive black holes (in the context of PBHs).
- How to distinguish baryonic from primordial black holes.

Fundamental questions about primordial black holes

- When and how are they form?
- When and how can we infer their existence?

Fundamental questions about primordial black holes

- When and how are they form?
- When and how can we infer their existence?

What would it take to establish their existence?

- Direct observation (e.g., gravitational waves)
- Indirect observation (e.g., effects in the early universe, CMB, energetic backgrounds, lensing, stellar dynamics, merger rates, etc….

Fundamental questions about primordial black holes

- When and how are they form?
- When and how can we infer their existence?

What would it take to establish their existence?

- Direct observation (e.g., gravitational waves)
- Indirect observation (e.g., effects in the early universe, CMB, energetic backgrounds, lensing, **stellar dynamics**, **merger rates**, etc….

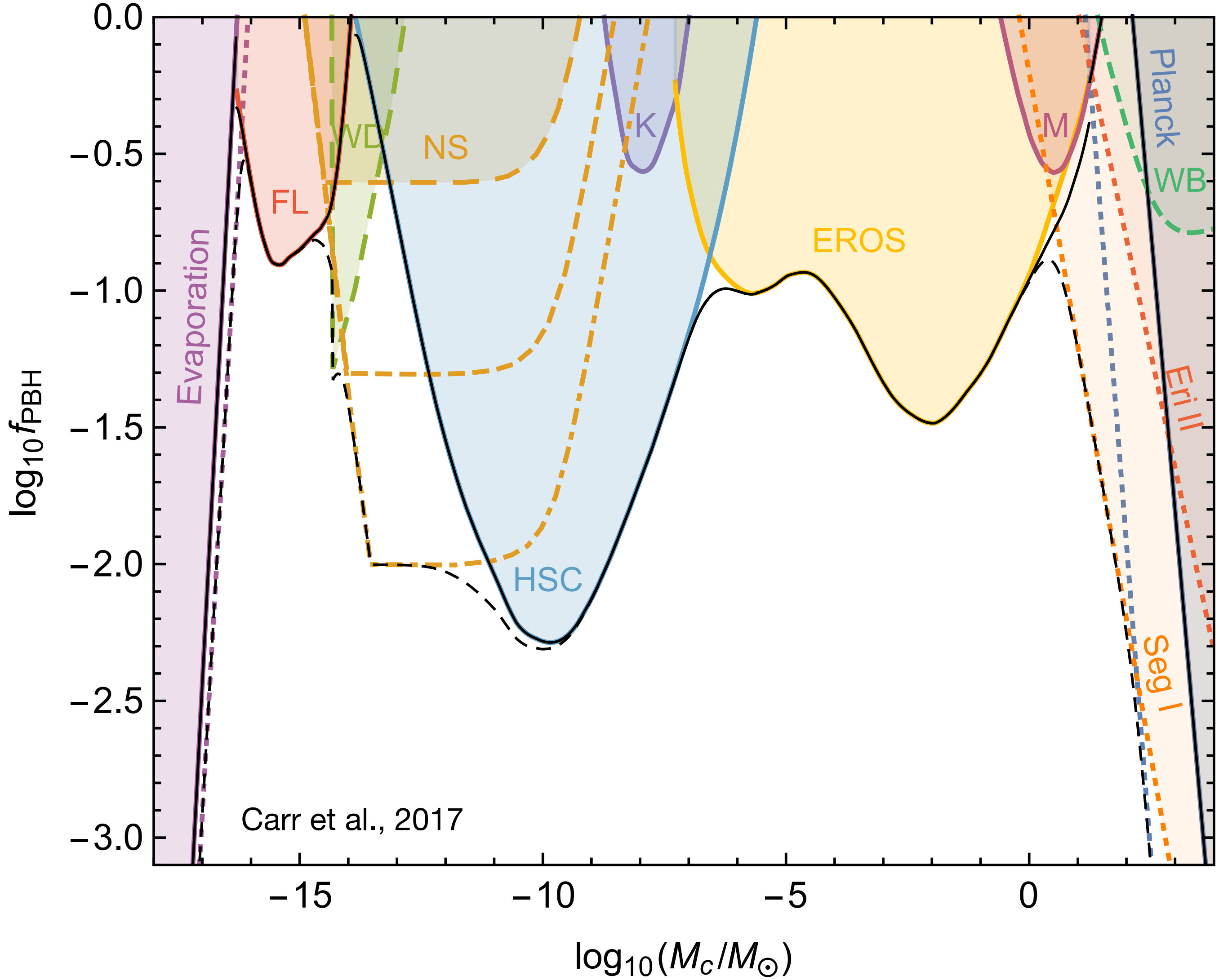

Evaporation
FL
WD
NS
K
HSC
EROS
M
Planck
WB
Eri II
Seg I
Carr et al., 2017
0.0
−0.5
−1.0
−1.5
−2.0
−2.5
−3.0
−15
−10
−5
0
$\log_{10} f_{\rm PBH}$
$\log_{10}(M_c/M_\odot)$

Constraints from dwarf galaxies

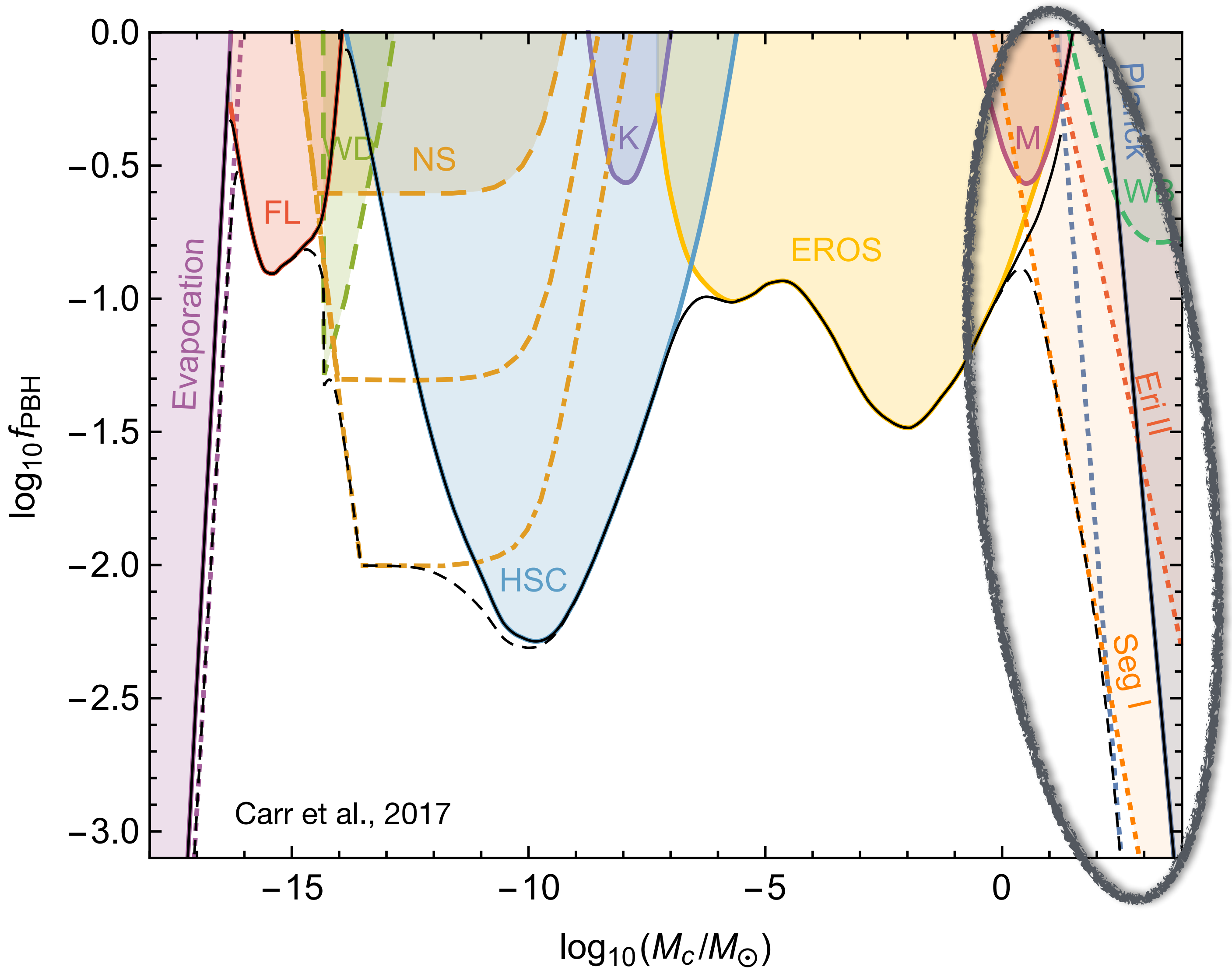

Dwarf galaxies — state of the art constraints on thermal cross section

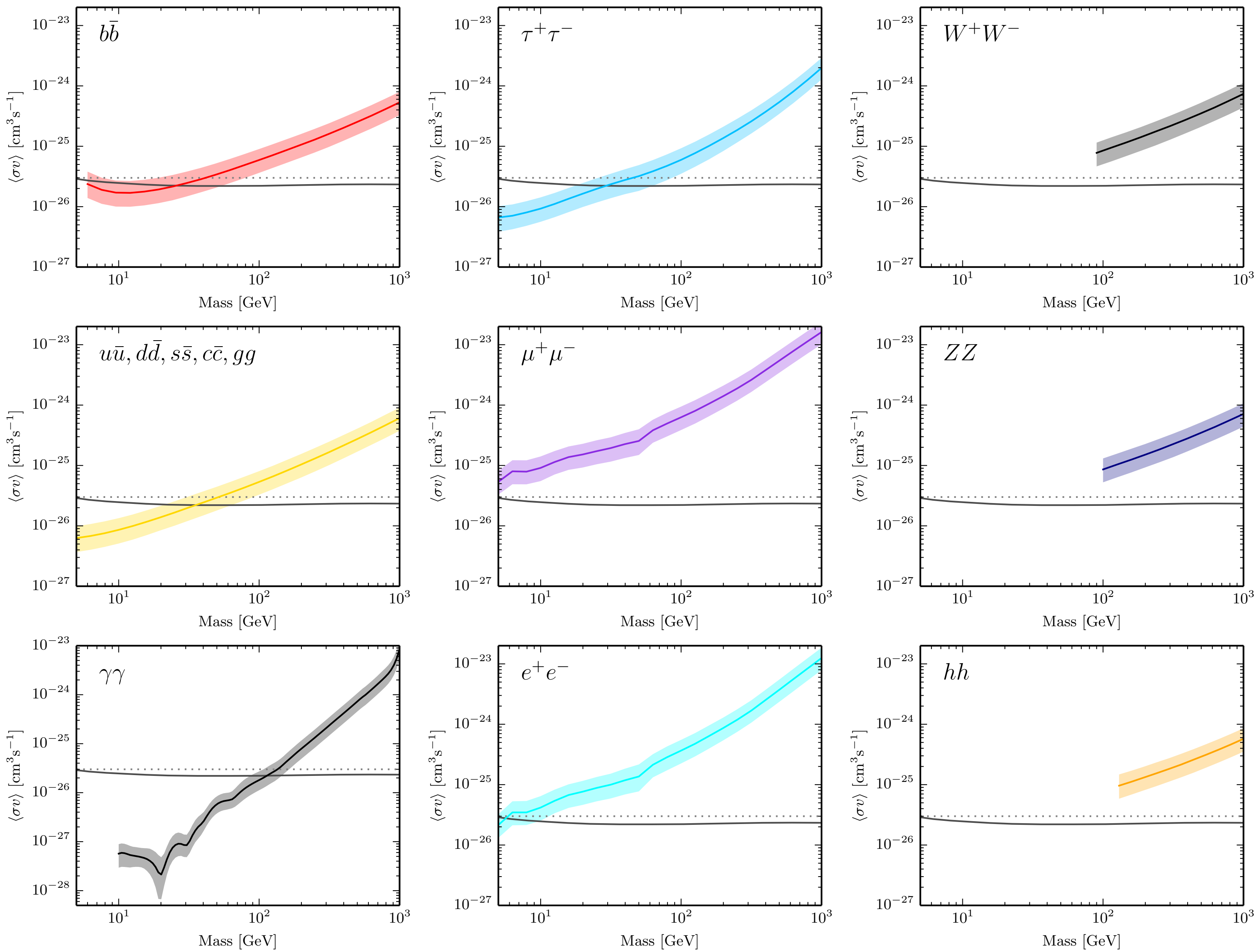

The structure of substructure

Small scales collapse first. The smaller the perturbation the earlier it collapses, the higher its density.

Dark matter halos contain **high density dark matter** substructure

The structure of substructure

The spectrum of dark matter subhalo properties originates from the host assembly history — a random realization set by initial conditions.

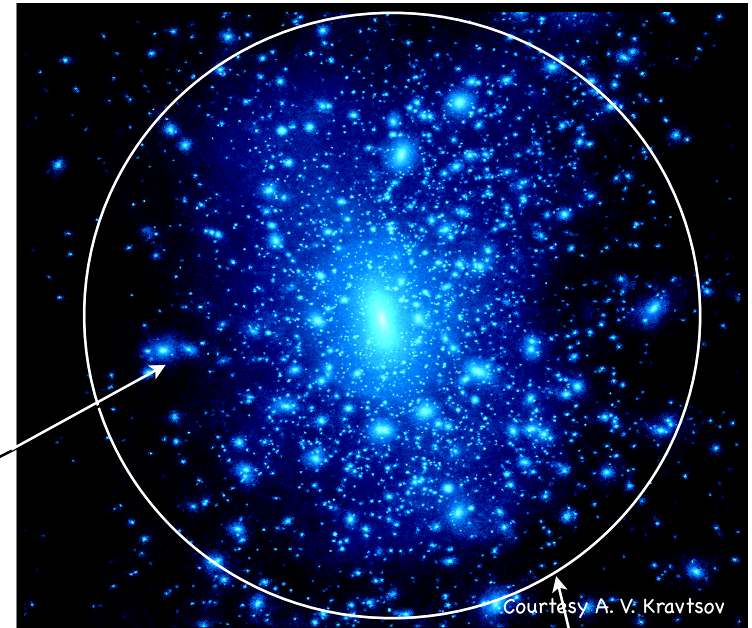

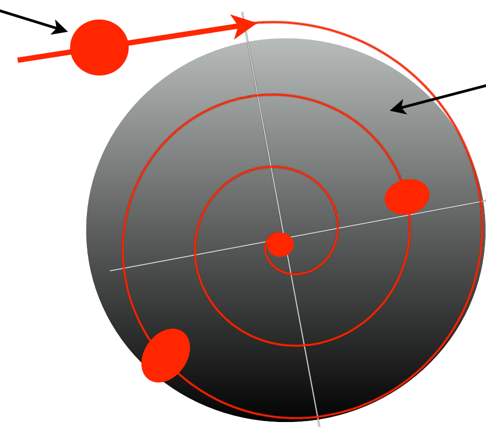

Koushiappas, Zentner & Walker, PRD 69, 043501 (2004), but see also Baltz, Tayor & Wai, ApJ 659, L125 (2006), Kuhlen, Diemand & Madau , arXiv:0805.4416

The structure of substructure

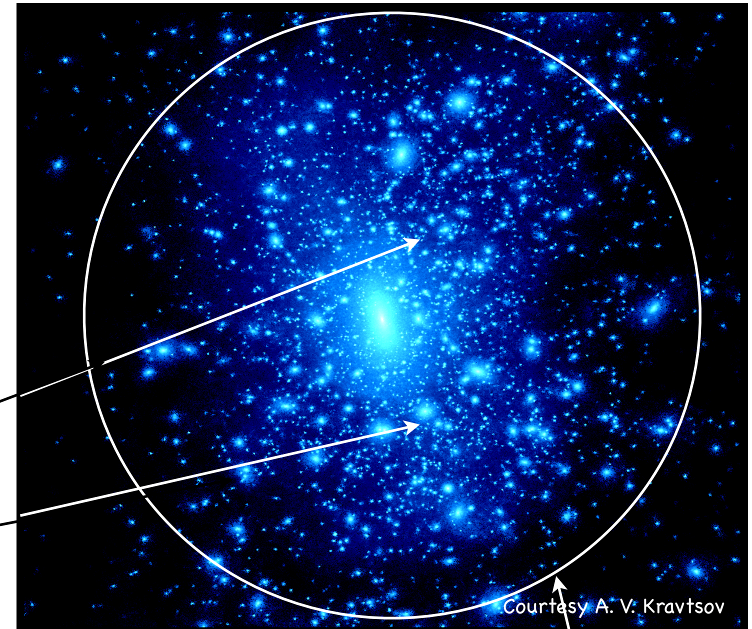

The spectrum of dark matter subhalo properties originates from the host assembly history — a random realization set by initial conditions.

These two may have the **same mass**, but different history

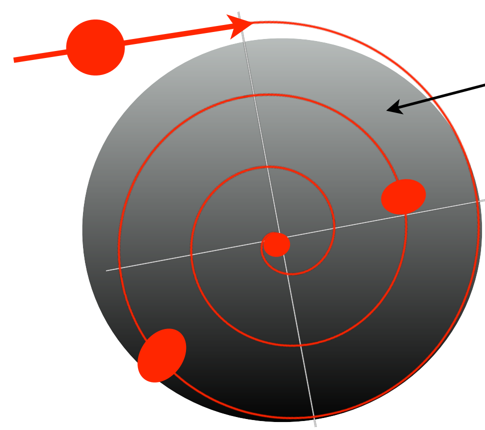

Koushiappas, Zentner & Walker, PRD 69, 043501 (2004), but see also Baltz, Tayor & Wai, ApJ 659, L125 (2006), Kuhlen, Diemand & Madau , arXiv:0805.4416

The structure of substructure

The spectrum of dark matter subhalo properties originates from the host assembly history — a random realization set by initial conditions.

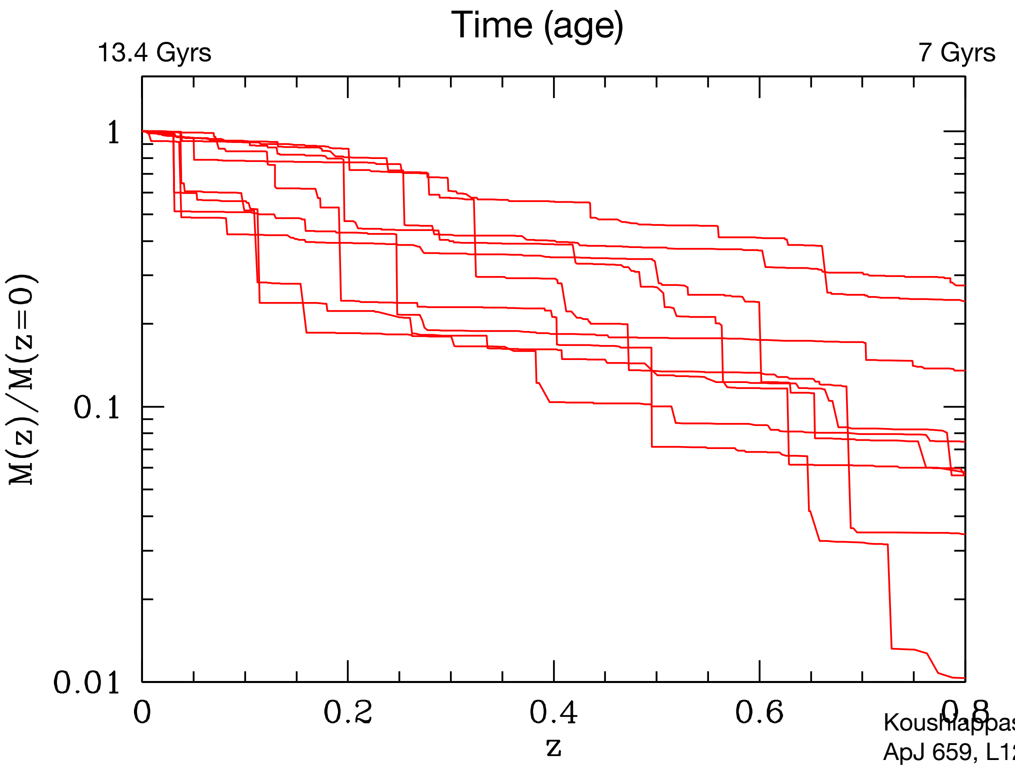

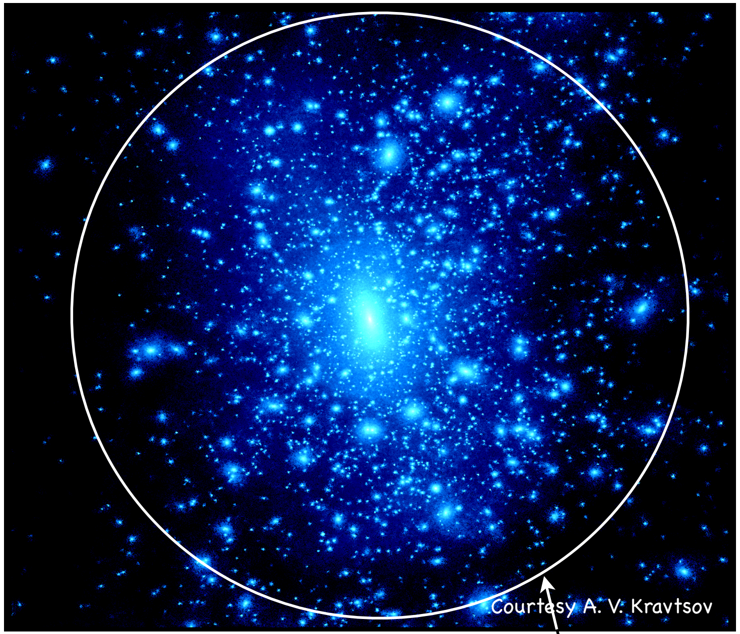

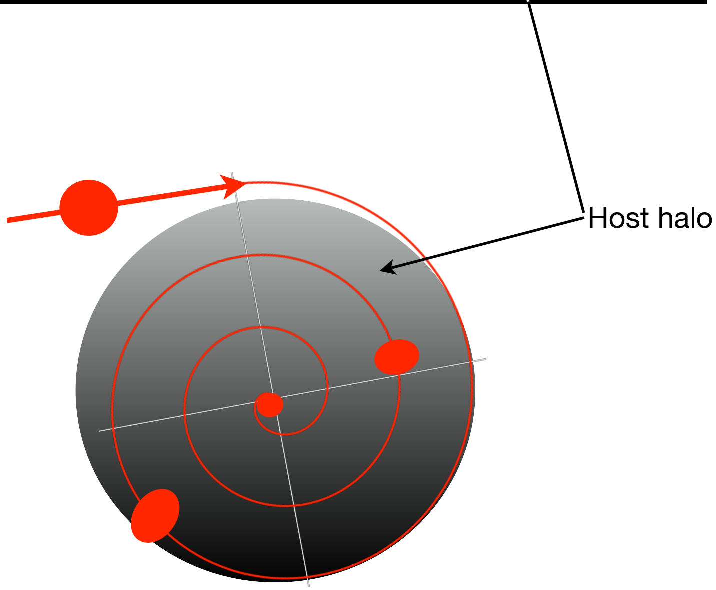

Koushiappas, Zentner & Walker, PRD 69, 043501 (2004), but see also Baltz, Tayor & Wai, ApJ 659, L125 (2006), Kuhlen, Diemand & Madau , arXiv:0805.4416

The structure of substructure

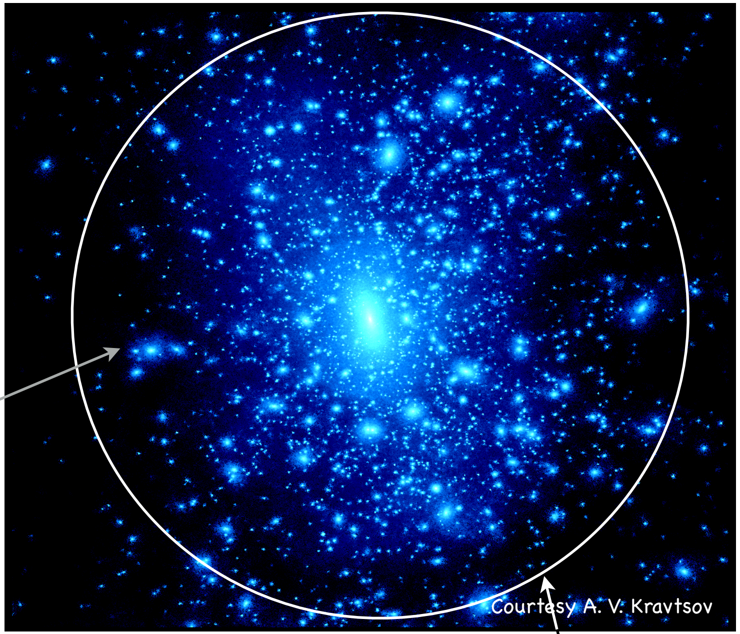

If these dark matter potential wells contain stars we call them **dwarf galaxies**

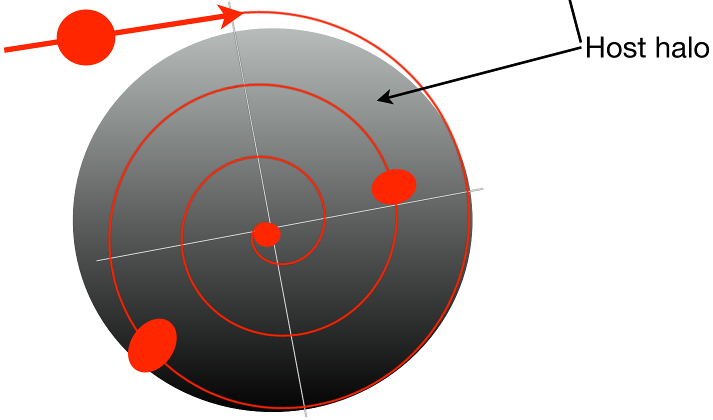

Koushiappas, Zentner & Walker, PRD 69, 043501 (2004), but see also Baltz, Tayor & Wai, ApJ 659, L125 (2006), Kuhlen, Diemand & Madau , arXiv:0805.4416

Dwarf galaxies

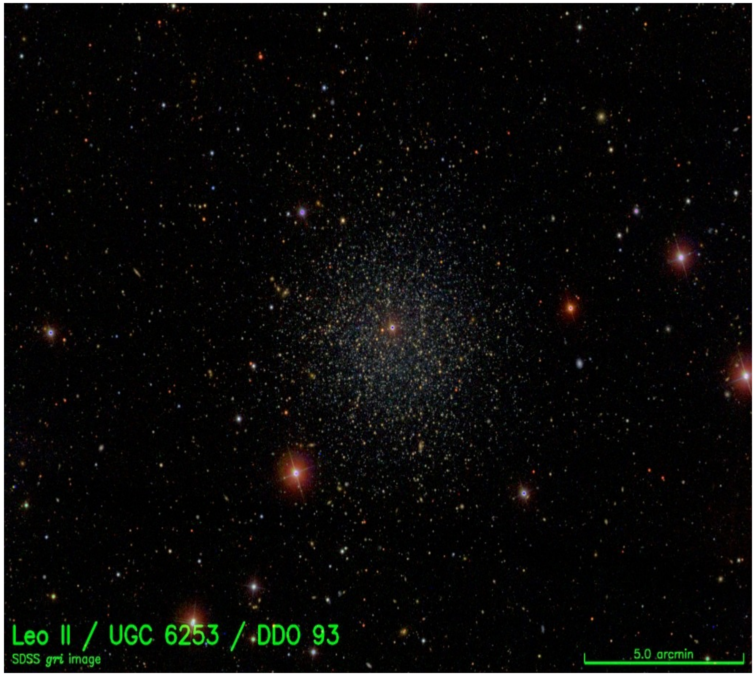

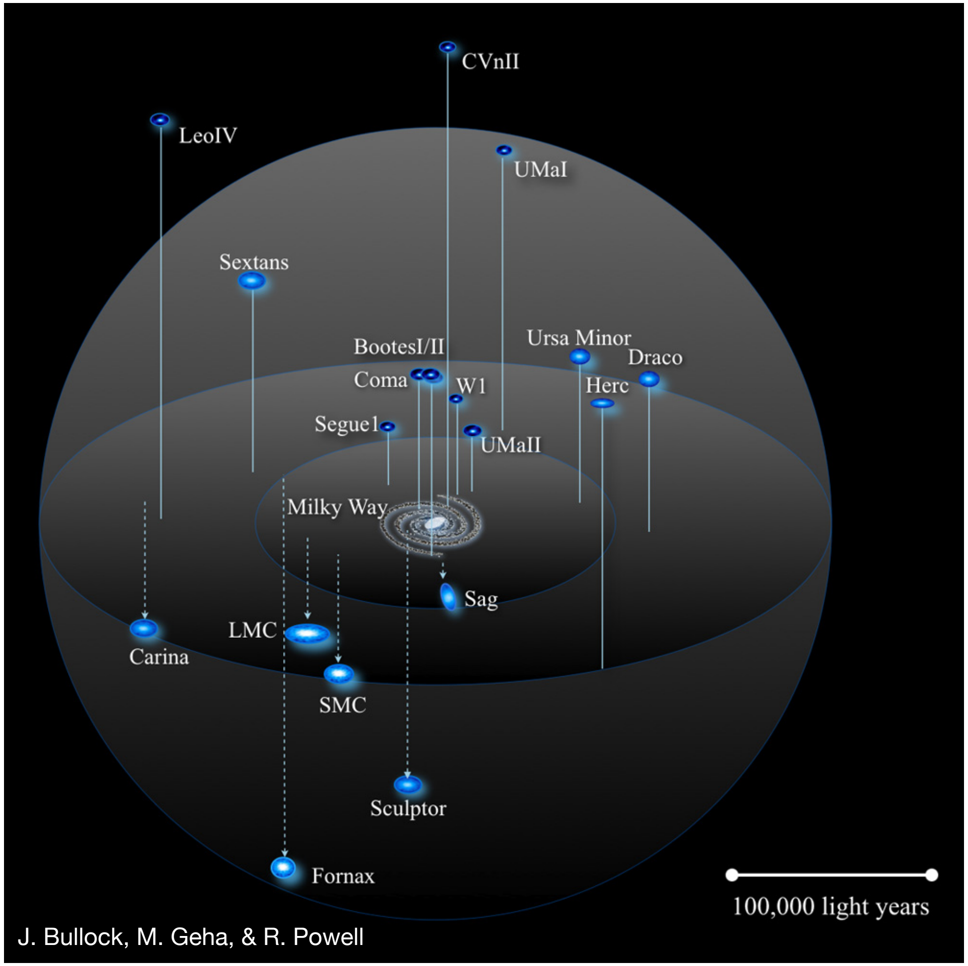

- High mass-to-light ratio (i.e., dark matter dominated, very few stars)
- No known astrophysical background (no gas, stars are old)

Dwarf galaxies

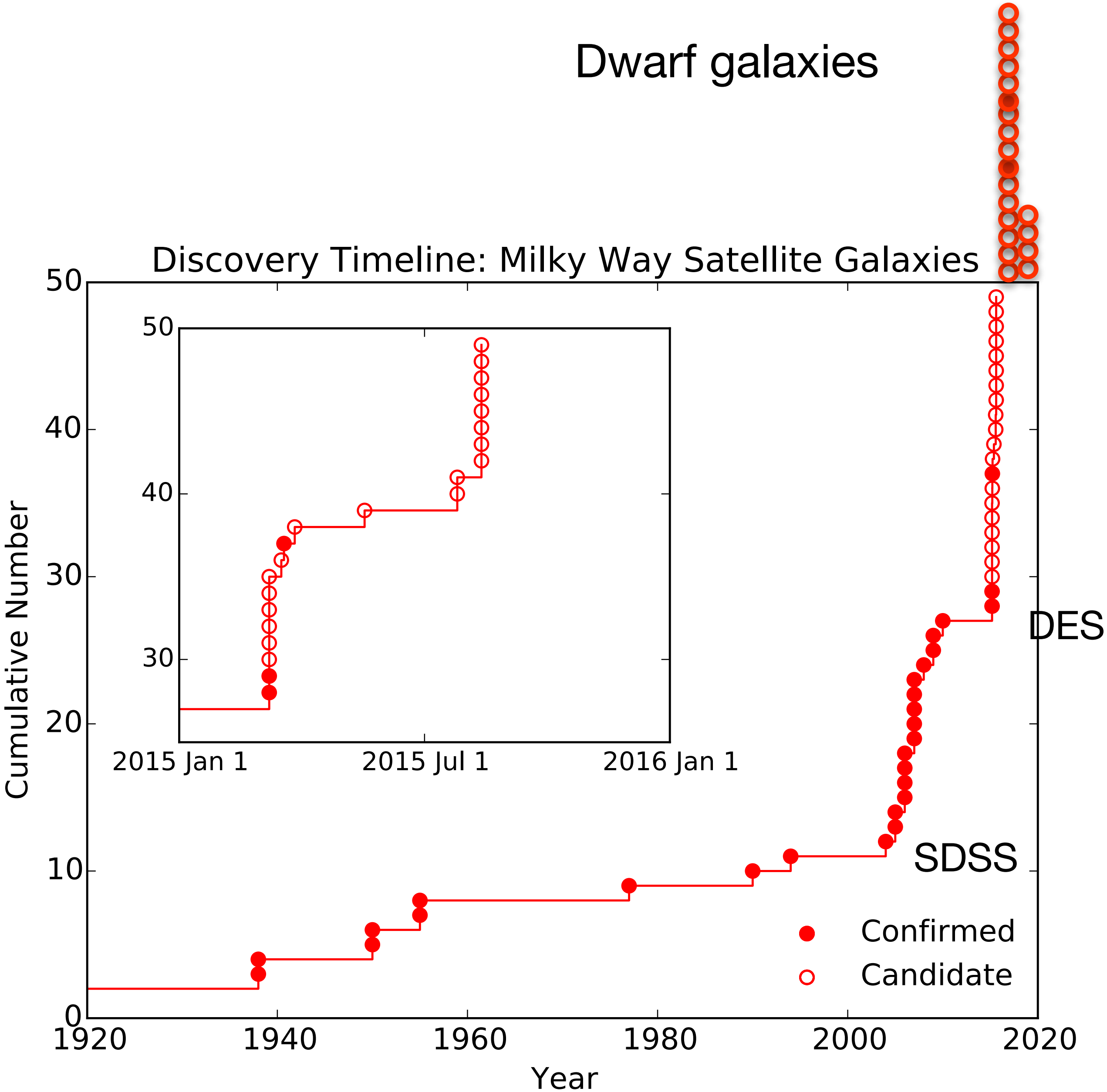

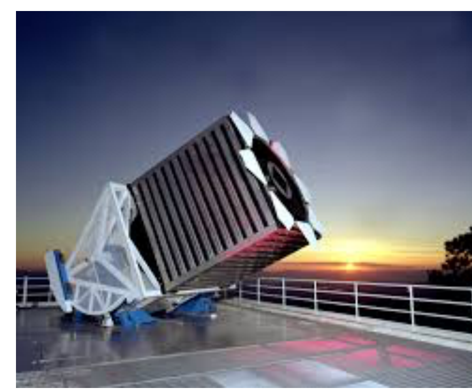

From Keith Bechtol's talk TAUP 2015

Dwarf galaxies: **Dark matter** dominated systems with few stars

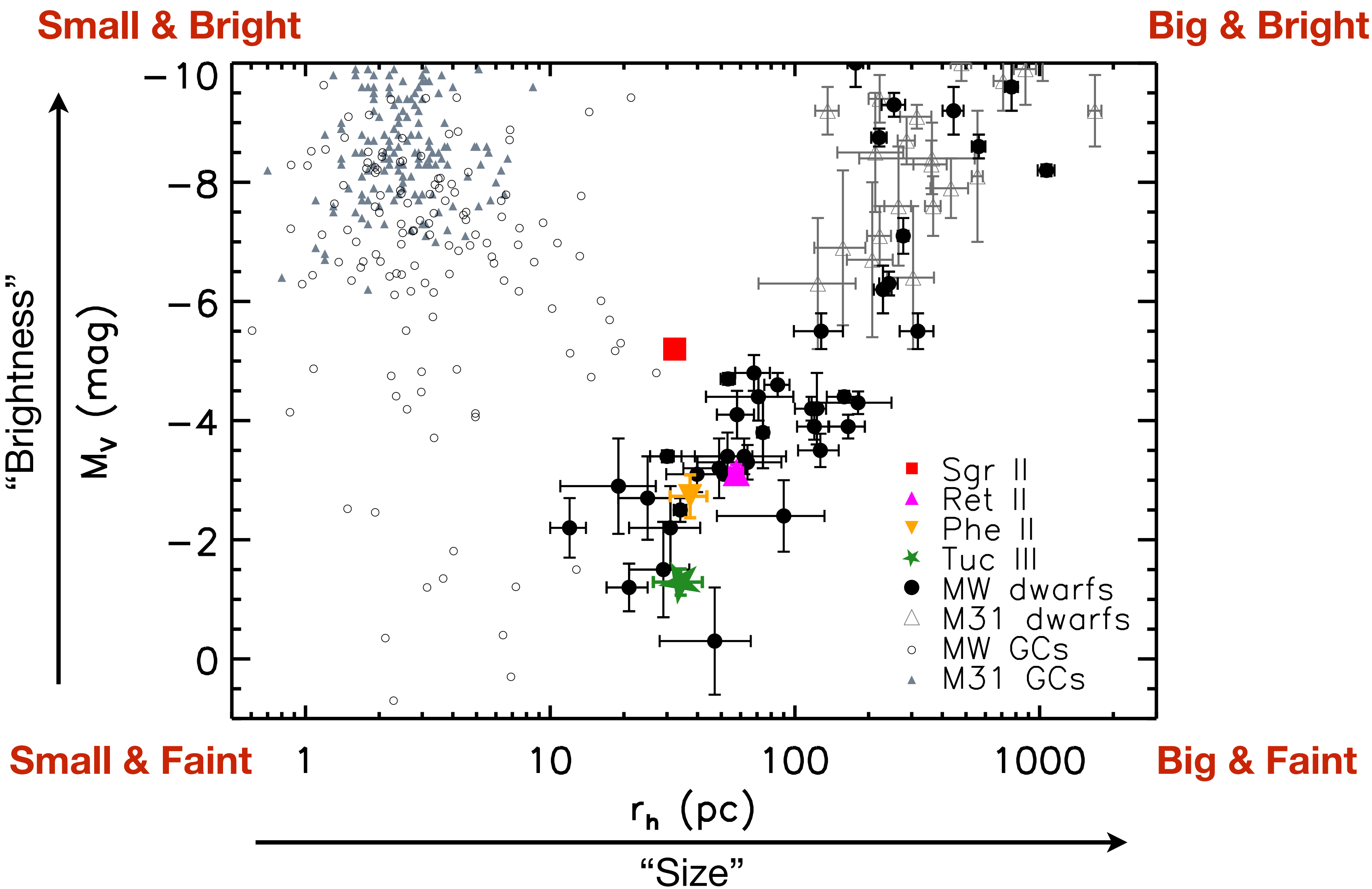

Dwarf galaxies: **Dark matter** dominated systems with few stars

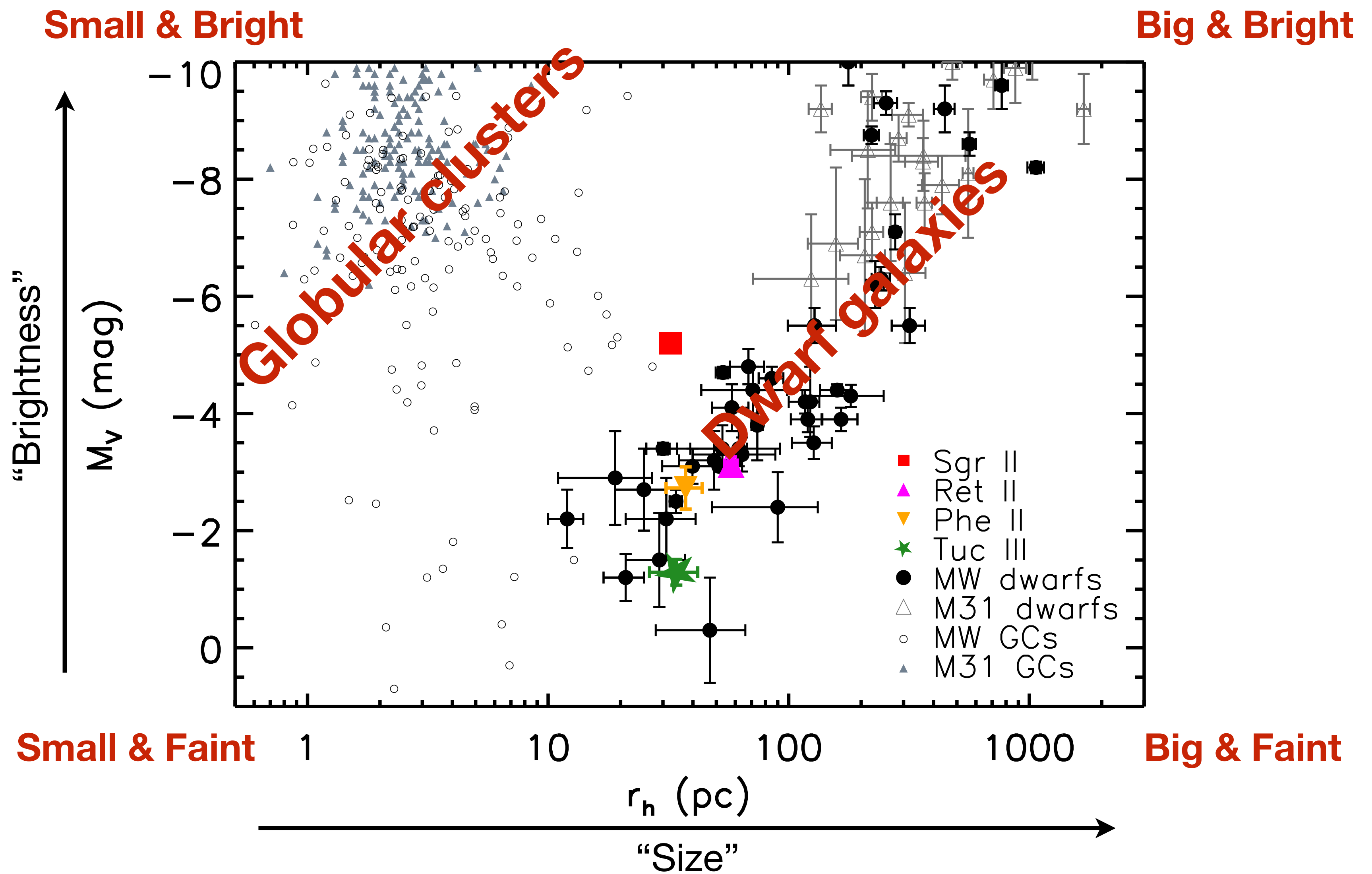

Dwarf galaxies: **Dark matter** dominated systems with few stars

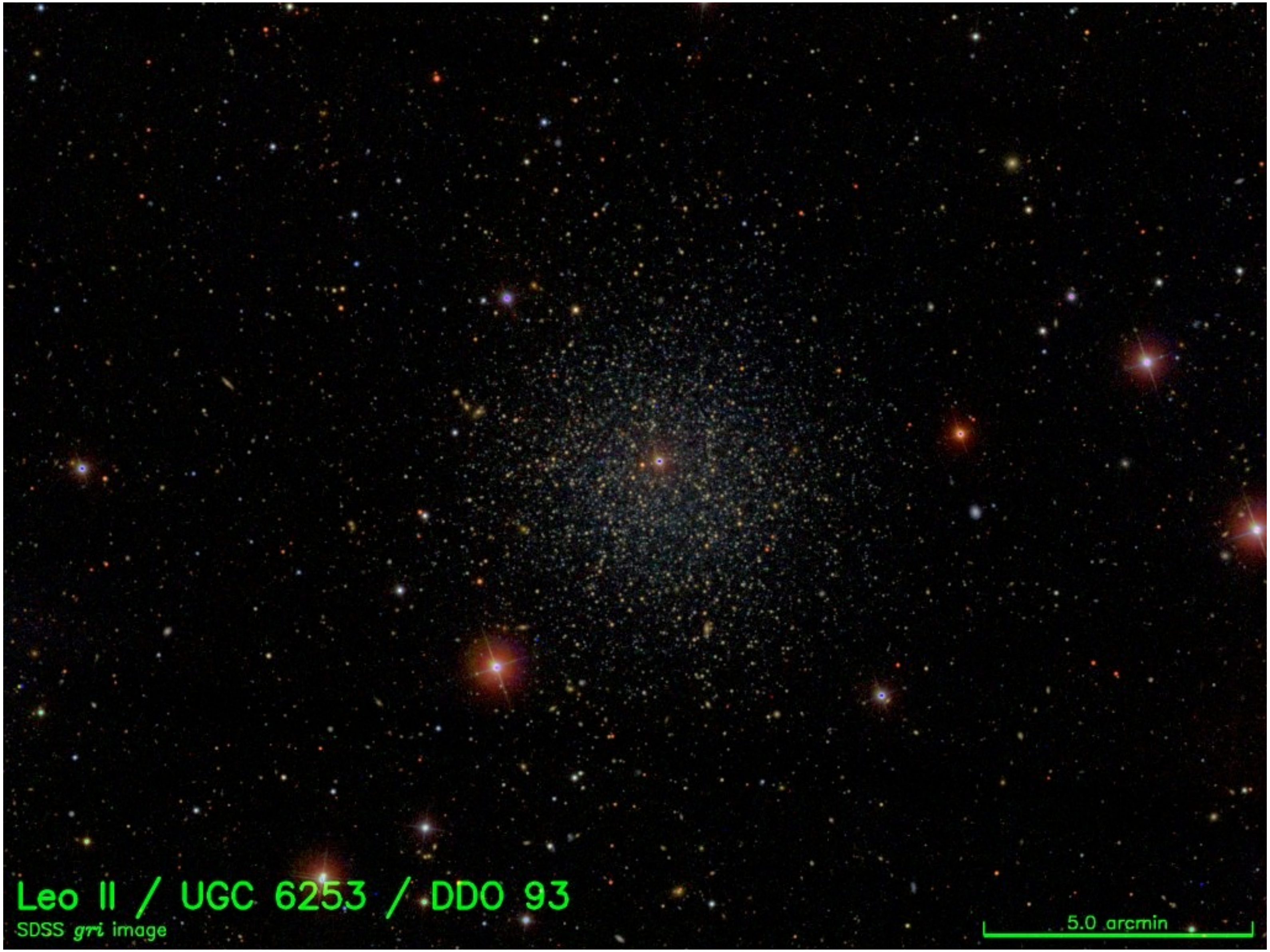

Primordial black hole

Dwarf galaxies: ~~Dark matter~~ dominated systems with few stars

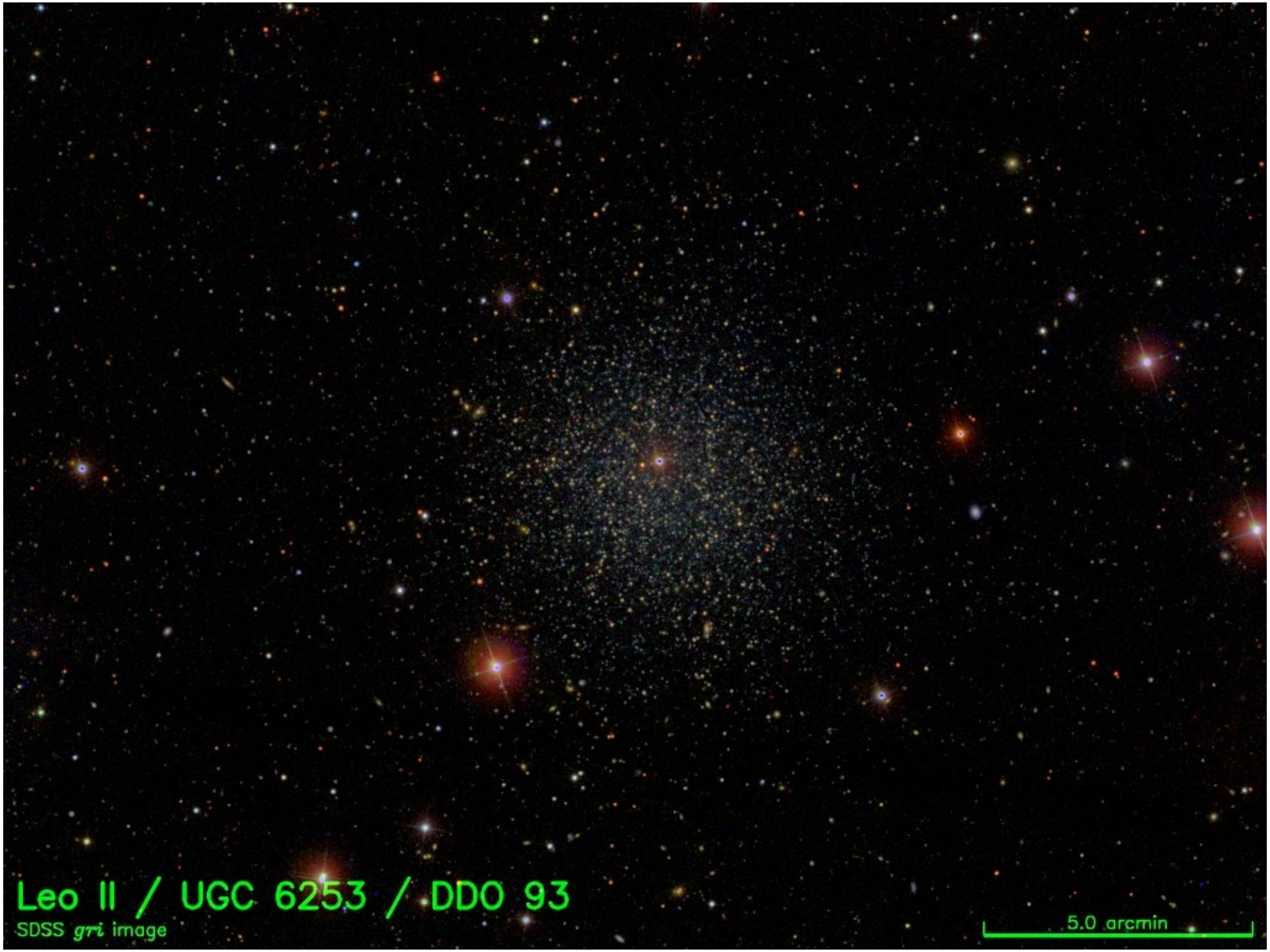

Dwarf galaxies: **Primordial black hole** dominated systems with few stars

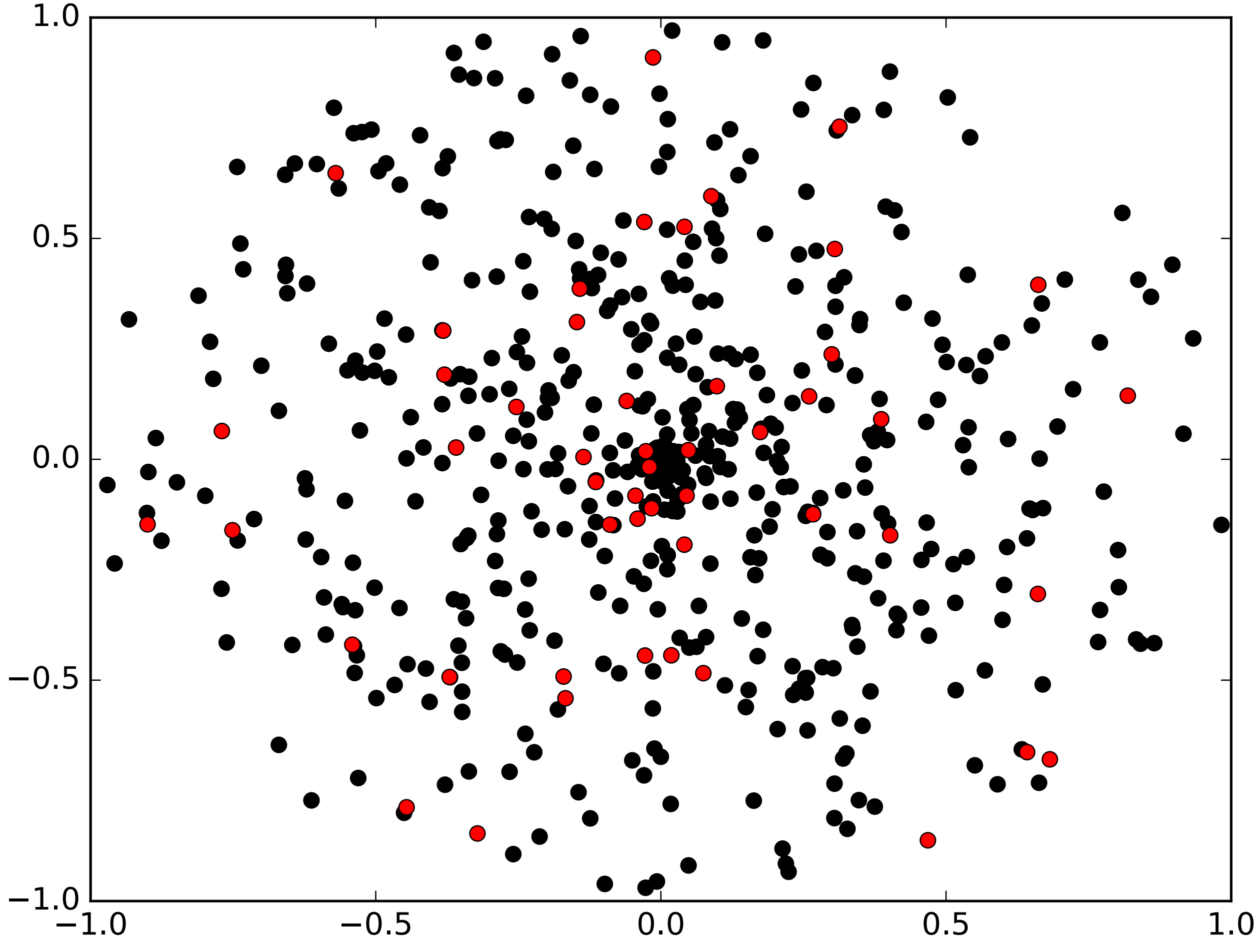

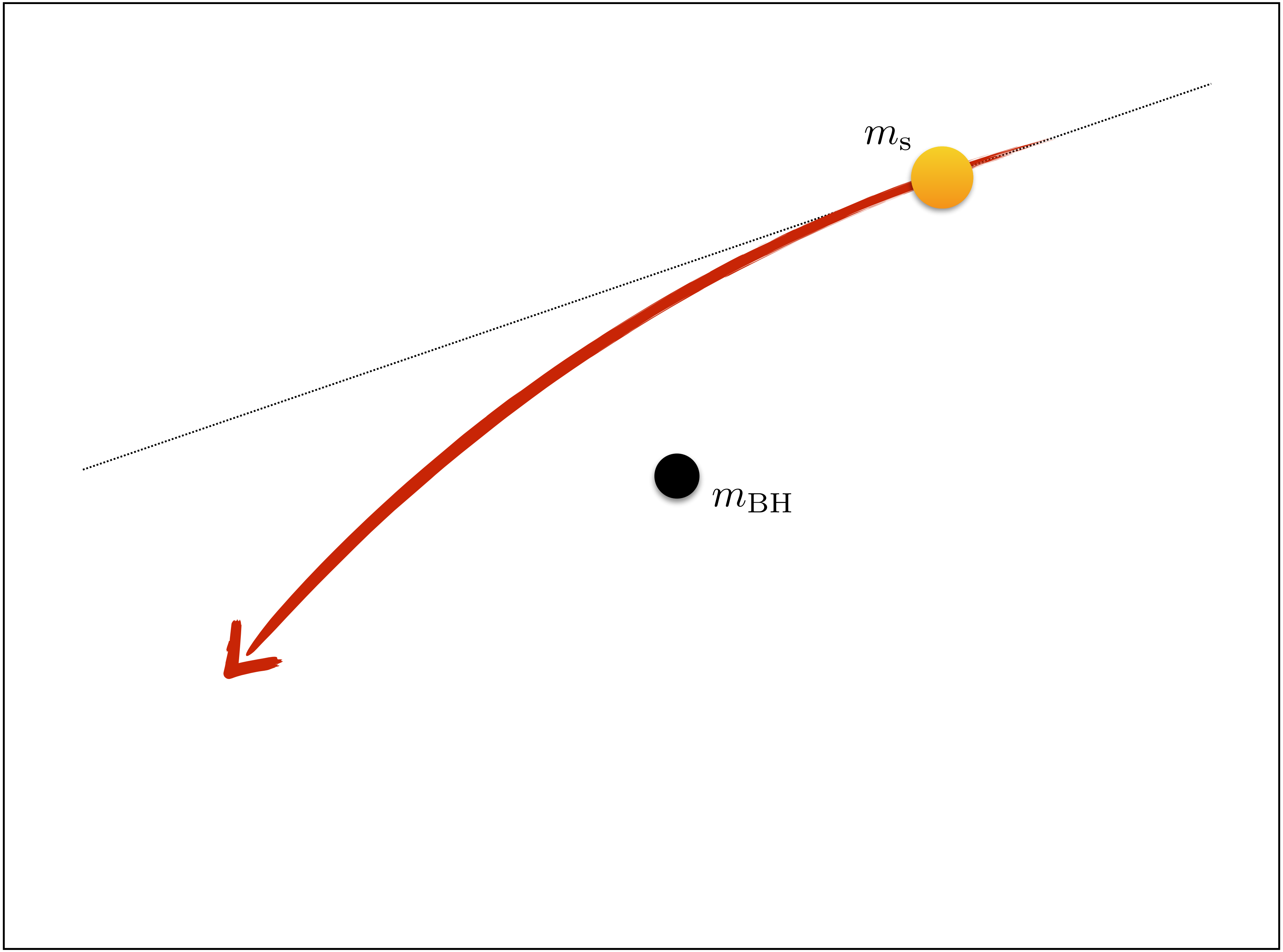
m_s
m_BH

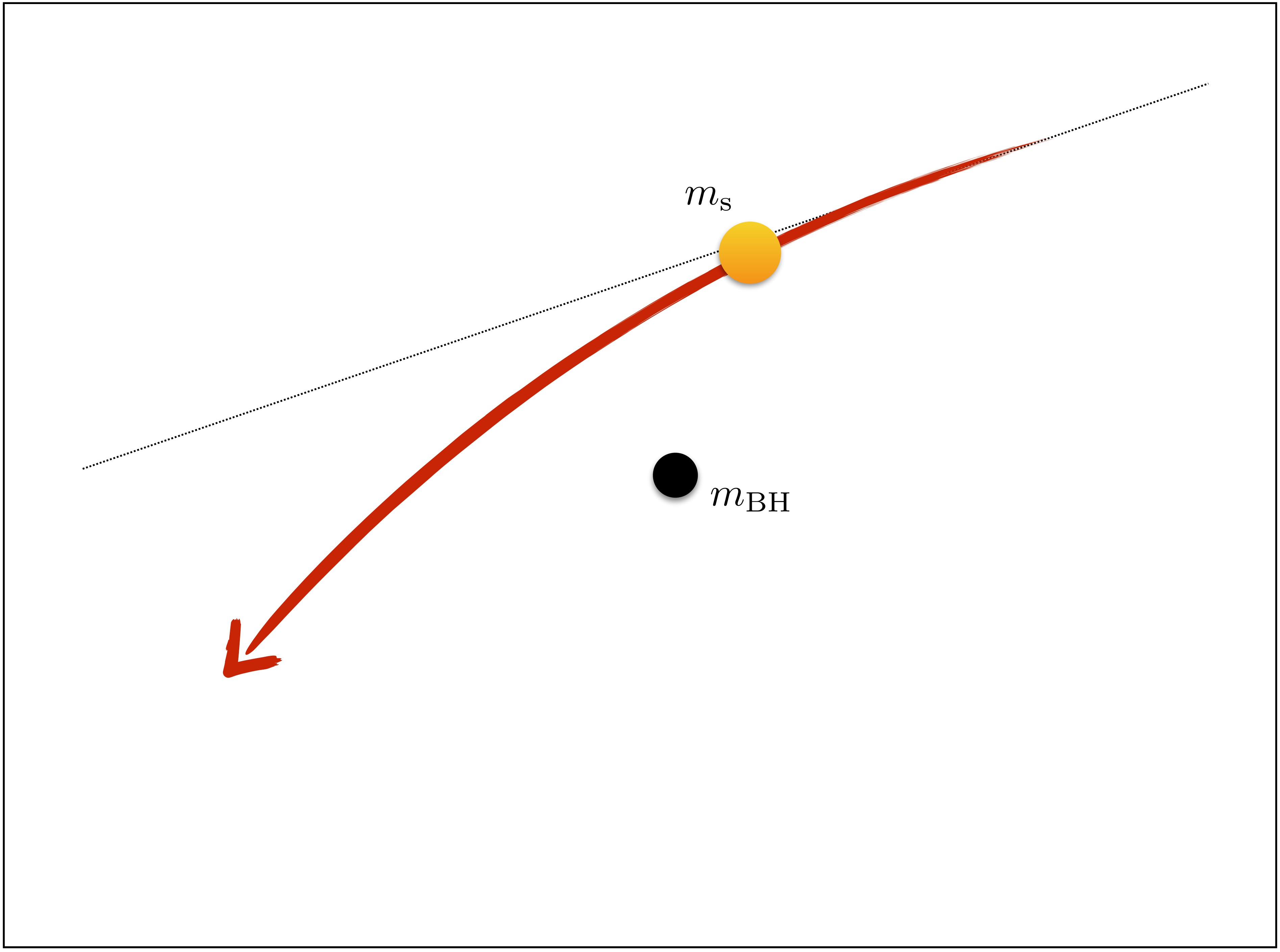
m_s
m_{BH}

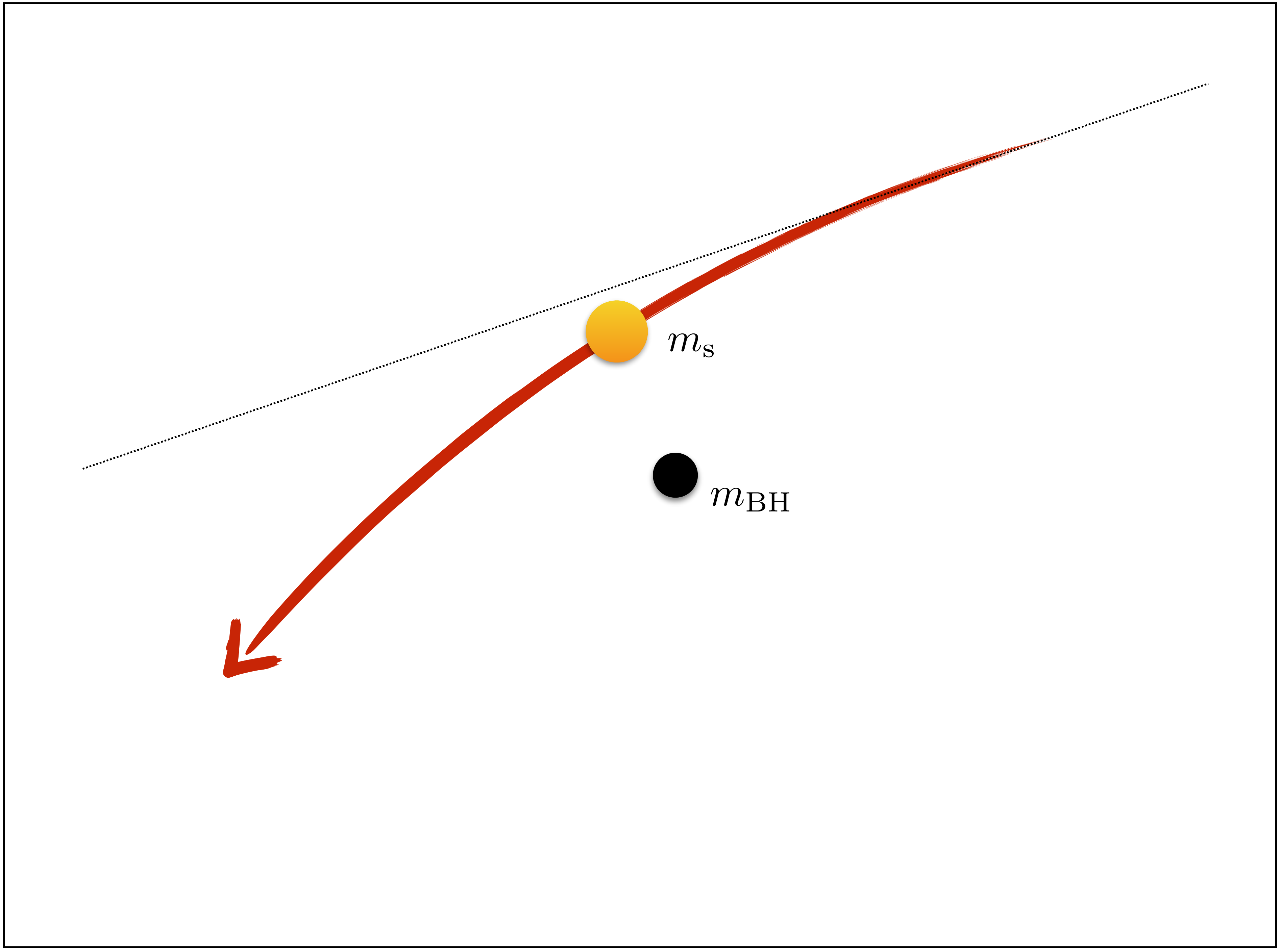
$m_{\rm s}$
$m_{\rm BH}$

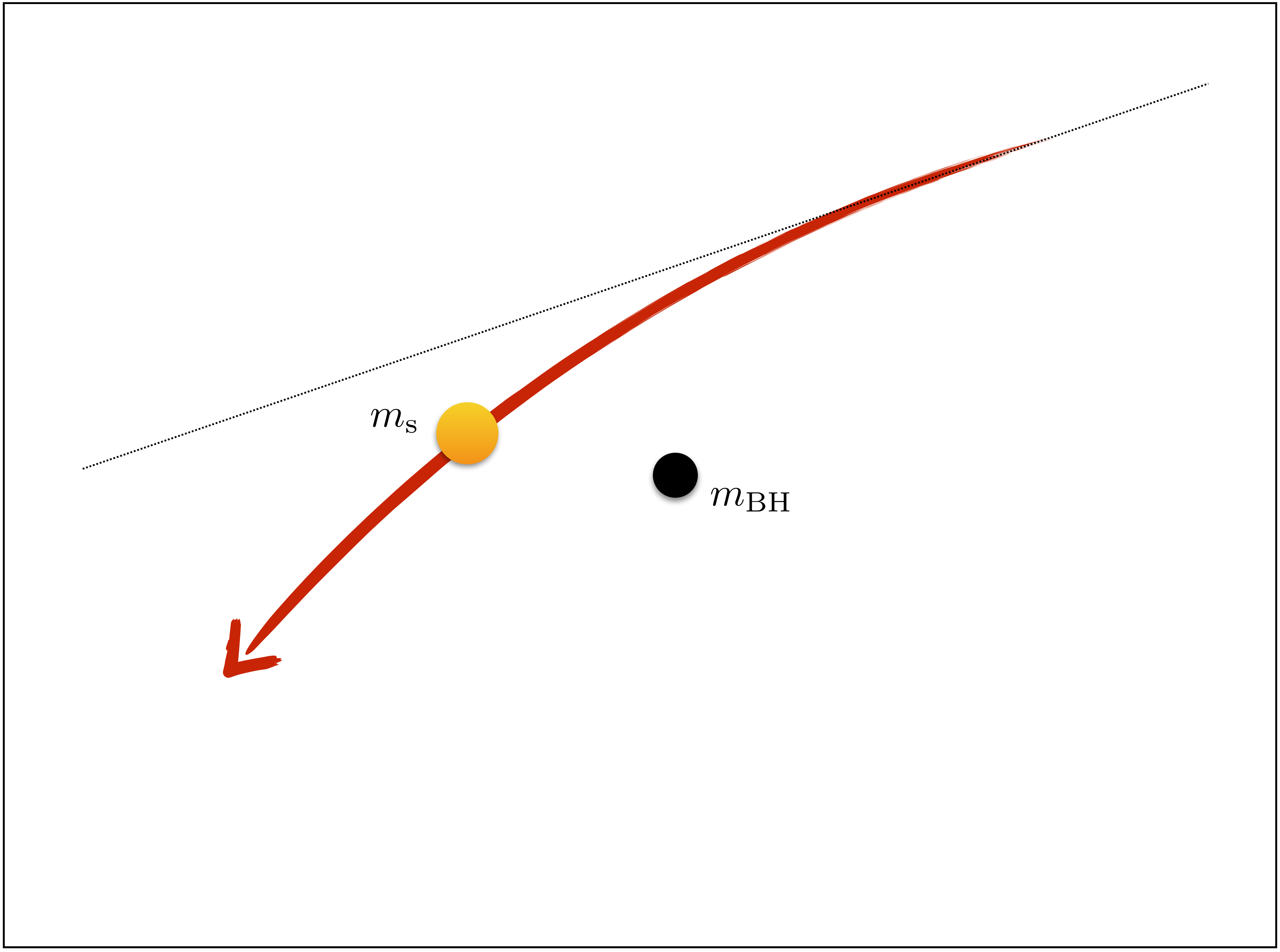

$m_{\rm s}$
$m_{\rm BH}$

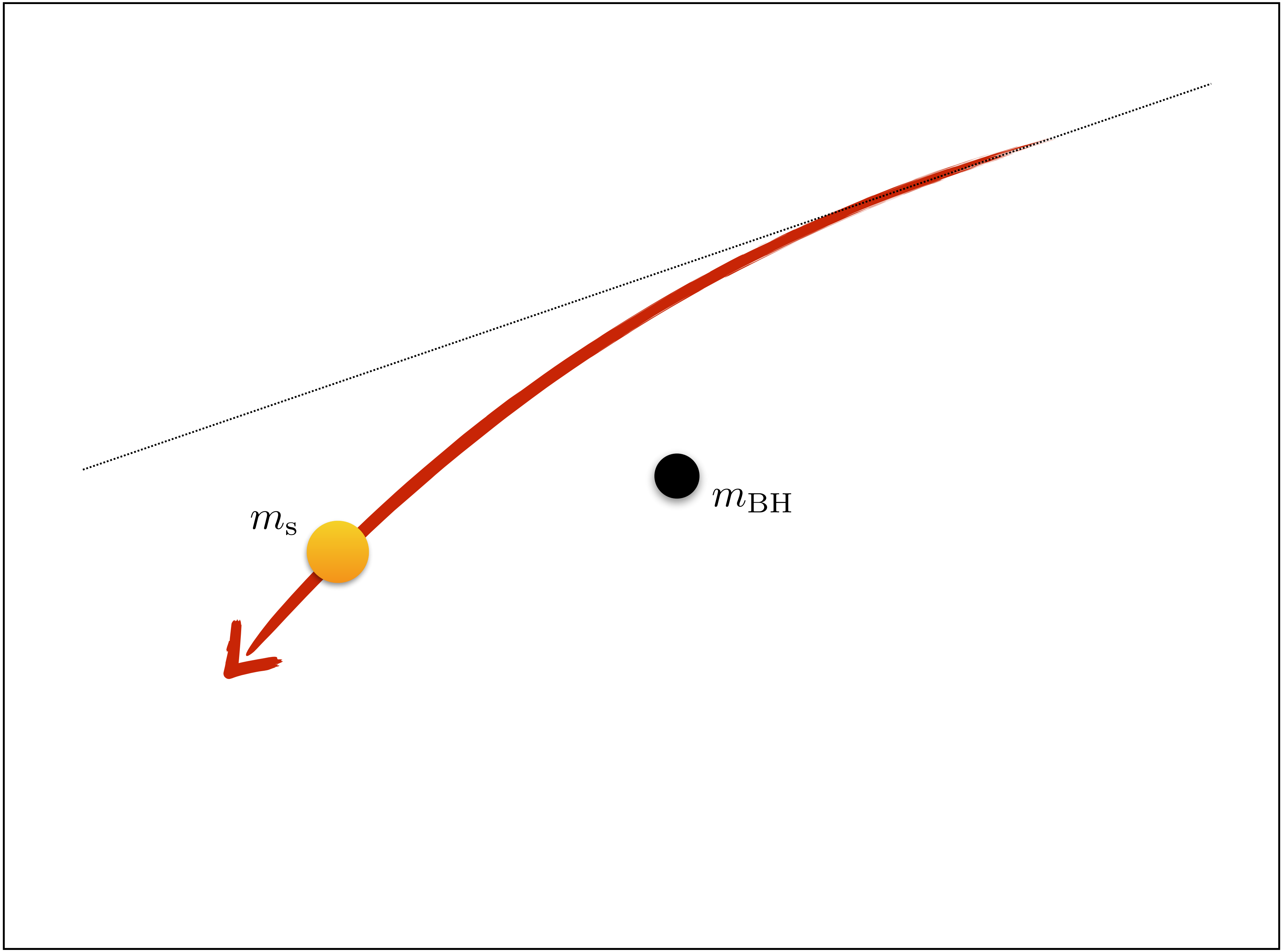
$m_{\rm s}$
$m_{\rm BH}$

Average change in kinetic energy (per unit mass and time) for single interaction

$$\langle \Delta E \rangle_s = v_s \langle \Delta v_{s,\parallel} \rangle + \frac{1}{2} \langle (\Delta v_{s,\parallel})^2 \rangle + \frac{1}{2} \langle (\Delta v_{s,\perp})^2 \rangle$$
$$= \frac{4\pi G^2 m_{\rm BH} \rho_{\rm BH} \ln \Lambda}{v_s}$$
$$\times \left[-\frac{m_s}{m_{\rm BH}} \mathrm{erf}(X) + \left(1 + \frac{m_s}{m_{\rm BH}}\right) X \mathrm{erf}'(X) \right], \qquad X \equiv v_s / \sqrt{2 \langle v_{\rm BH}^2 \rangle}$$

Change of energy in stellar population

$$\frac{dE_s}{dt} = \sqrt{\frac{2}{\pi}} \frac{1}{\sigma_s^3} \int_0^\infty m_s \langle \Delta E \rangle_s v_s^2 e^{-v_s^2/2\sigma_s^2} dv_s$$

$$= \frac{\sqrt{96\pi} G^2 m_s \rho_{\rm BH} \ln \Lambda}{[\langle v_s^2 \rangle + \langle v_{\rm BH}^2 \rangle]^{3/2}} [m_{\rm BH} \langle v_{\rm BH}^2 \rangle - m_s \langle v_s^2 \rangle]$$

Average change in kinetic energy (per unit mass and time) for single interaction

$$\langle \Delta E \rangle_s = v_s \langle \Delta v_{s,\parallel} \rangle + \frac{1}{2} \langle (\Delta v_{s,\parallel})^2 \rangle + \frac{1}{2} \langle (\Delta v_{s,\perp})^2 \rangle$$

$$= \frac{4\pi G^2 m_{\rm BH} \rho_{\rm BH} \ln \Lambda}{v_s}$$

$$\times \left[-\frac{m_s}{m_{\rm BH}} \mathrm{erf}(X) + \left(1 + \frac{m_s}{m_{\rm BH}}\right) X \mathrm{erf}'(X) \right], \qquad X \equiv v_s / \sqrt{2 \langle v_{\rm BH}^2 \rangle}$$

Change of energy in stellar population

$$\frac{dE_s}{dt} = \sqrt{\frac{2}{\pi}} \frac{1}{\sigma_s^3} \int_0^\infty m_s \langle \Delta E \rangle_s v_s^2 e^{-v_s^2/2\sigma_s^2} dv_s$$

$$= \frac{\sqrt{96\pi} G^2 m_s \rho_{\rm BH} \ln \Lambda}{[\langle v_s^2 \rangle + \langle v_{\rm BH}^2 \rangle]^{3/2}} [m_{\rm BH} \langle v_{\rm BH}^2 \rangle - m_s \langle v_s^2 \rangle]$$

Take a note of that -- more on this later

Time over which equipartition takes place

$$t_{\mathrm{r}} = \frac{E_s}{dE_s/dt}$$

Virial theorem →

$$t_r \approx (N/8 \ln N)\tau_c$$

Crossing time

$$\tau_c = r/\sigma$$

Time over which equipartition takes place

$$t_{\rm r} = \frac{E_s}{dE_s/dt} \xrightarrow{\text{Virial theorem}} t_r \approx (N/8 \ln N)\tau_c$$

Crossing time

$$\tau_c = r/\sigma$$

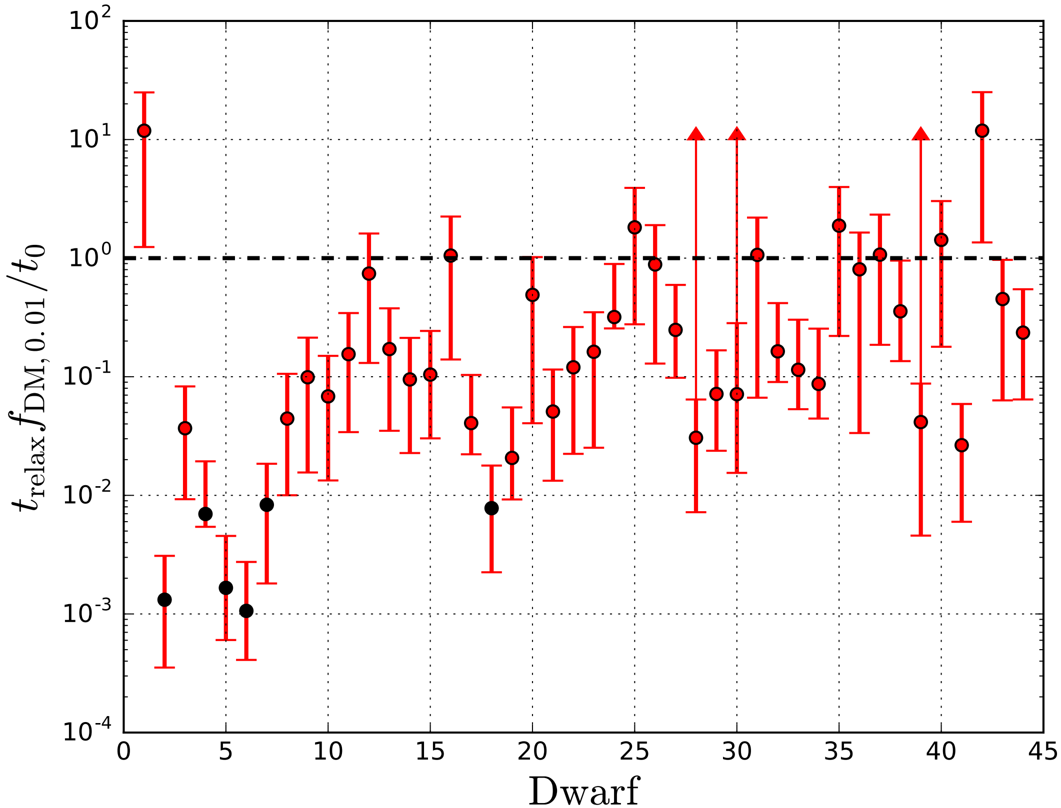

Dwarfs with smallest relaxation time

Segue 1
Boötes II
Segue II
Wilman 1
Coma Berenices
Canes Venatici II

Time over which equipartition takes place

$$t_{\rm r} = \frac{E_s}{dE_s/dt} \xrightarrow{\text{Virial theorem}} t_r \approx (N/8\ln N)\tau_c$$

Crossing time

$$\tau_c = r/\sigma$$

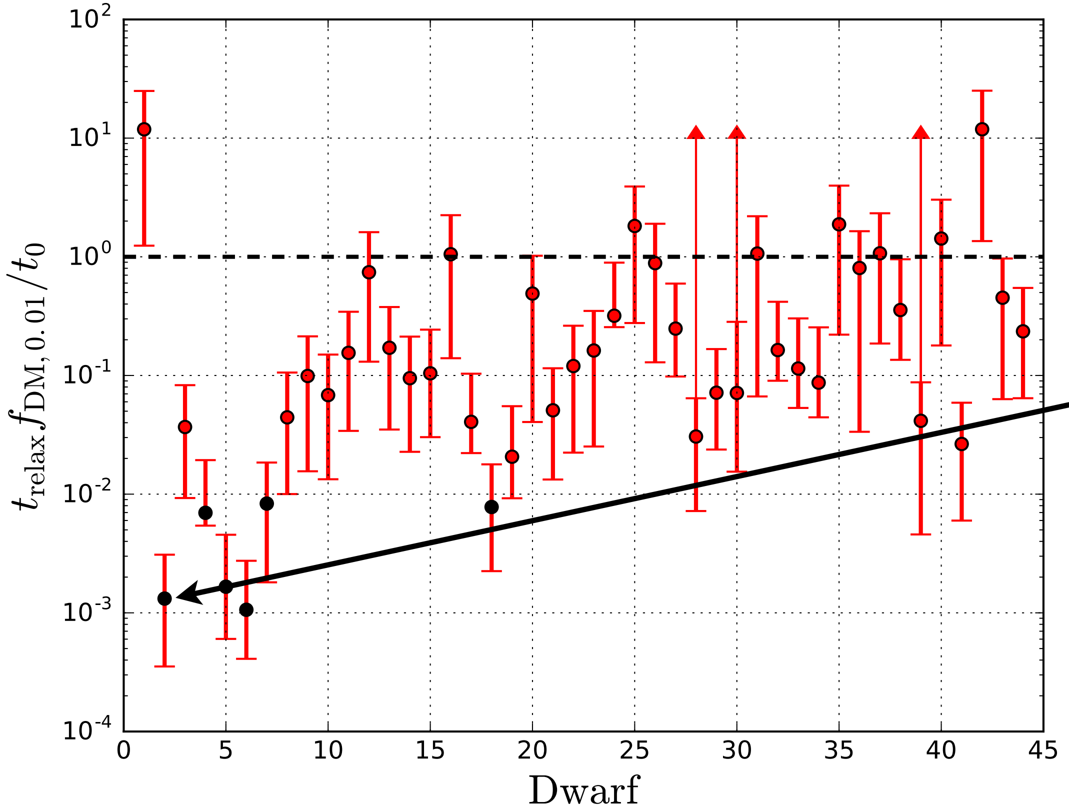

Dwarfs with smallest relaxation time

Segue 1

Boötes II

Segue II

Wilman 1

Coma Berenices

Canes Venatici II

The Astrophysical Journal, 733:46 (20pp), 2011 May 20
doi:10.1088/0004-637X/733/1/46

A COMPLETE SPECTROSCOPIC SURVEY OF THE MILKY WAY SATELLITE SEGUE 1: THE DARKEST GALAXY*

Joshua D. Simon[1], Marla Geha[2], Quinn E. Minor[3], Gregory D. Martinez[3], Evan N. Kirby[4,8], James S. Bullock[3], Manoj Kaplinghat[3], Louis E. Strigari[5,8], Beth Willman[6], Philip I. Choi[7], Erik J. Tollerud[3], and Joe Wolf[3]

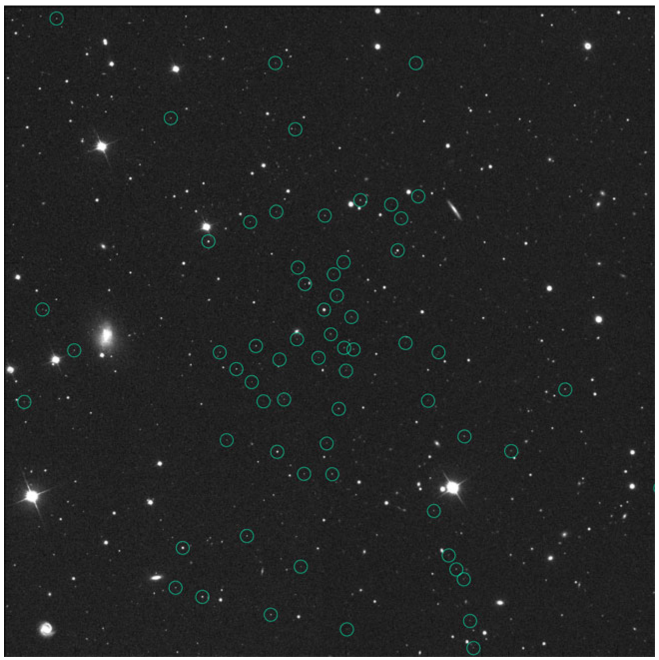

Table 1
Summary of Properties of Segue 1

Row	Quantity	Value
(1)	R.A. (J2000) (h m s)	$10{:}07{:}03.2 \pm 1^{\rm s}.7$
(2)	Decl. (J2000) (° ′ ″)	$+16{:}04{:}25 \pm 15''$
(3)	Distance (kpc)	23 ± 2
(4)	M_V	$-1.5^{+0.6}_{-0.8}$
(5)	L_V ($L_\odot$)	340
(6)	ϵ	$0.48^{+0.10}_{-0.13}$
(7)	$\mu_{V,0}$ (mag arcsec^{-2})	$27.6^{+1.0}_{-0.7}$
(8)	$r_{\rm eff}$ (pc)	29^{+8}_{-5}
(9)	$V_{\rm hel}$ (km s^{-1})	208.5 ± 0.9
(10)	$V_{\rm GSR}$ (km s^{-1})	113.5 ± 0.9
(11)	σ (km s^{-1})	$3.7^{+1.4}_{-1.1}$
(12)	Mass ($M_\odot$)	$5.8^{+8.2}_{-3.1} \times 10^5$
(13)	M/L_V ($M_\odot/L_\odot$)	3400
(14)	Mean [Fe/H]	-2.5

The Astrophysical Journal, 801:74 (18pp), 2015 March 10
doi:10.1088/0004-637X/801/2/74

DWARF GALAXY ANNIHILATION AND DECAY EMISSION PROFILES FOR DARK MATTER EXPERIMENTS

Alex Geringer-Sameth[1,2], Savvas M. Koushiappas[1], and Matthew Walker[2]

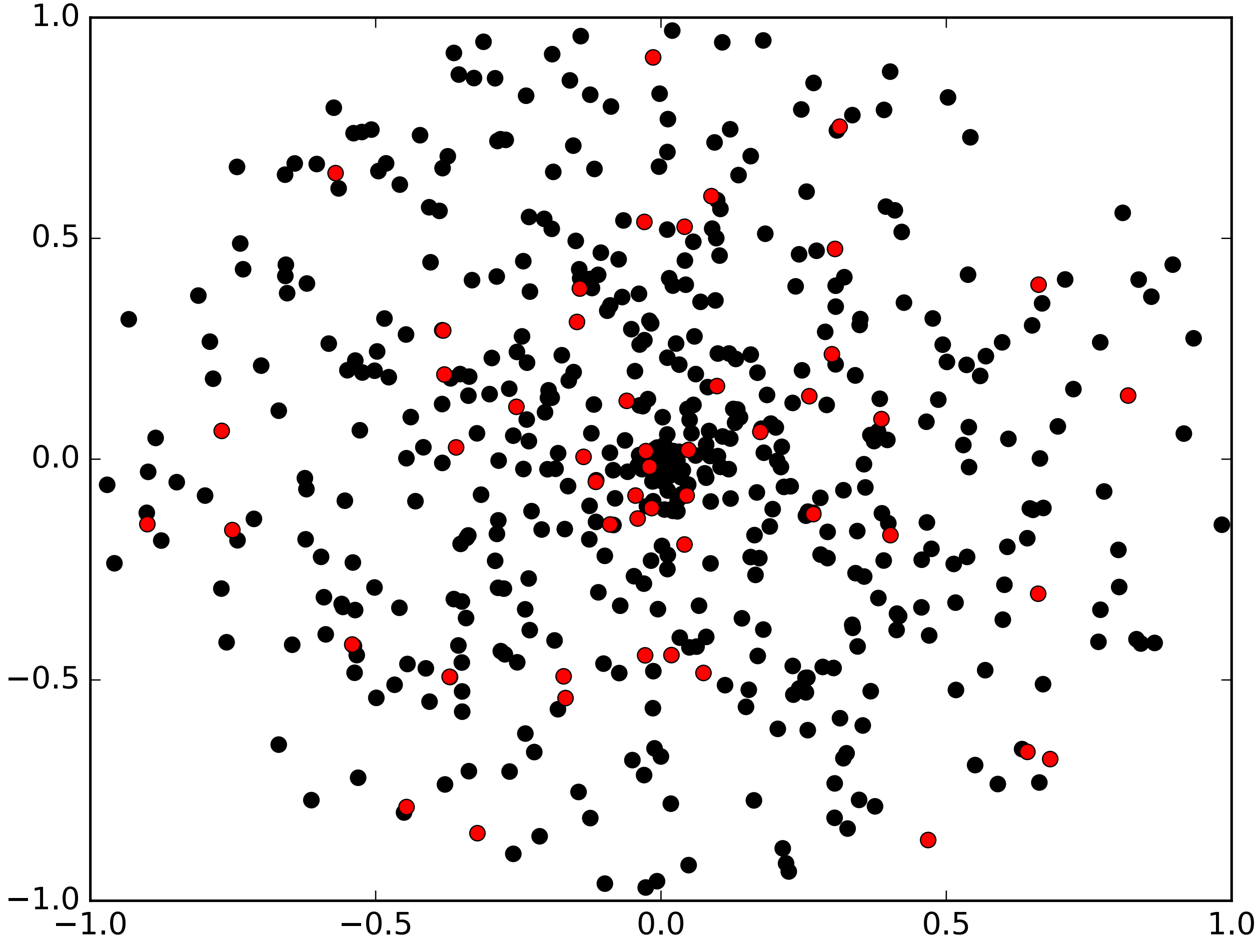

Koushiappas & Loeb PRL 119, 041102 (2017)

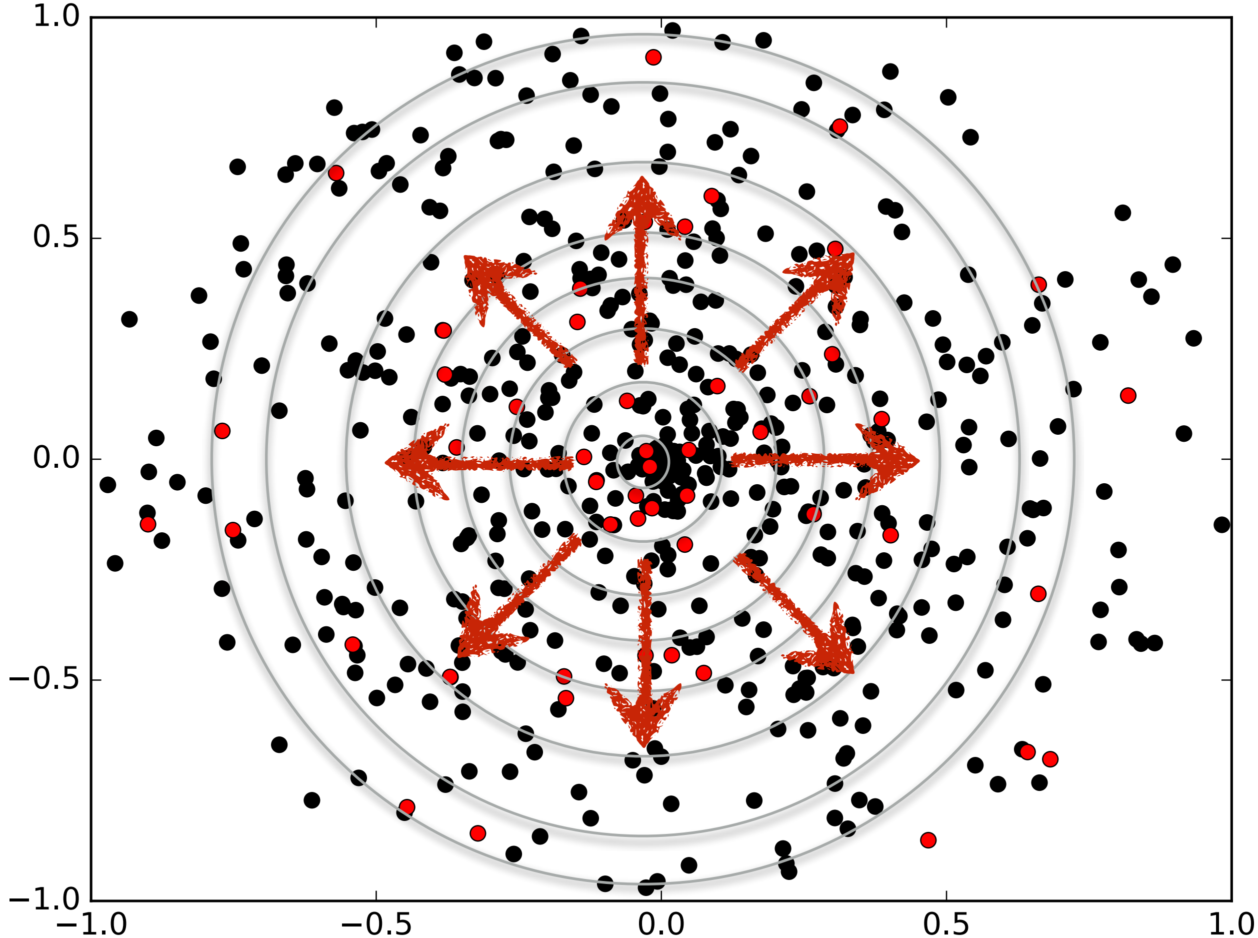

Koushiappas & Loeb PRL 119, 041102 (2017)

Equipartition leads to the depletion of stars from the center of the dwarf

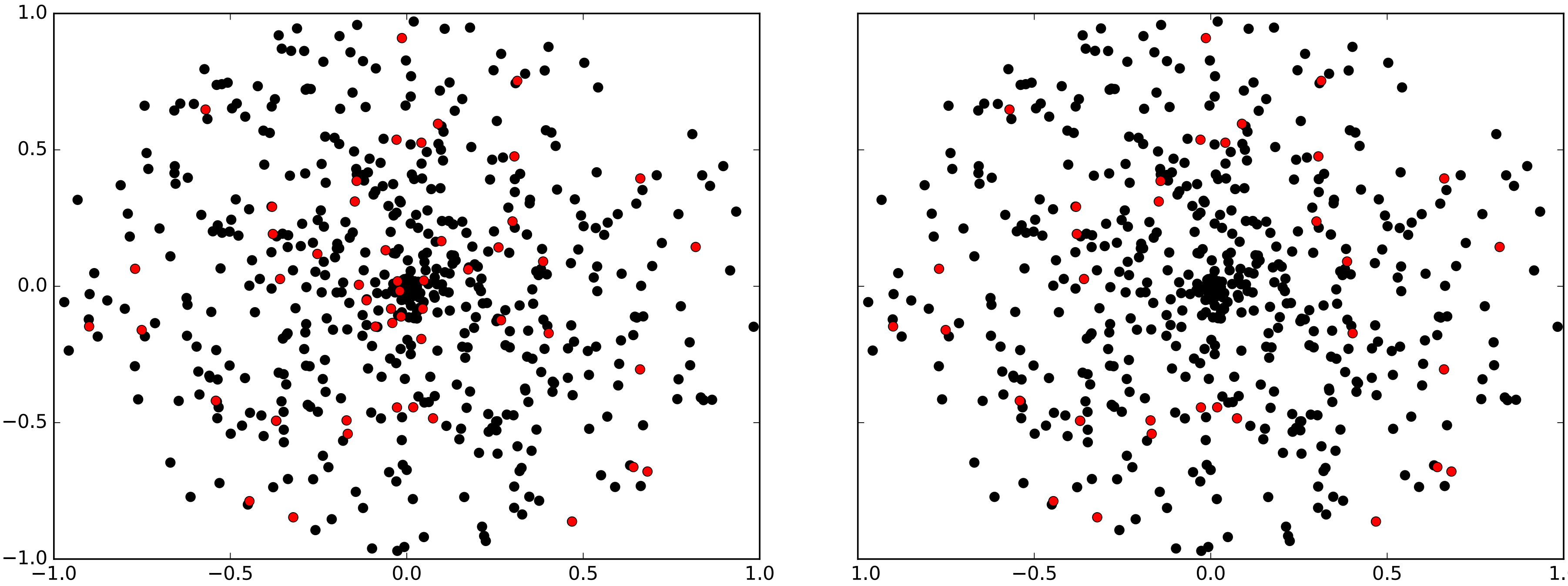

Koushiappas & Loeb PRL 119, 041102 (2017)

Evolution of density profile when 1% of dark matter is in 20 solar mass black holes

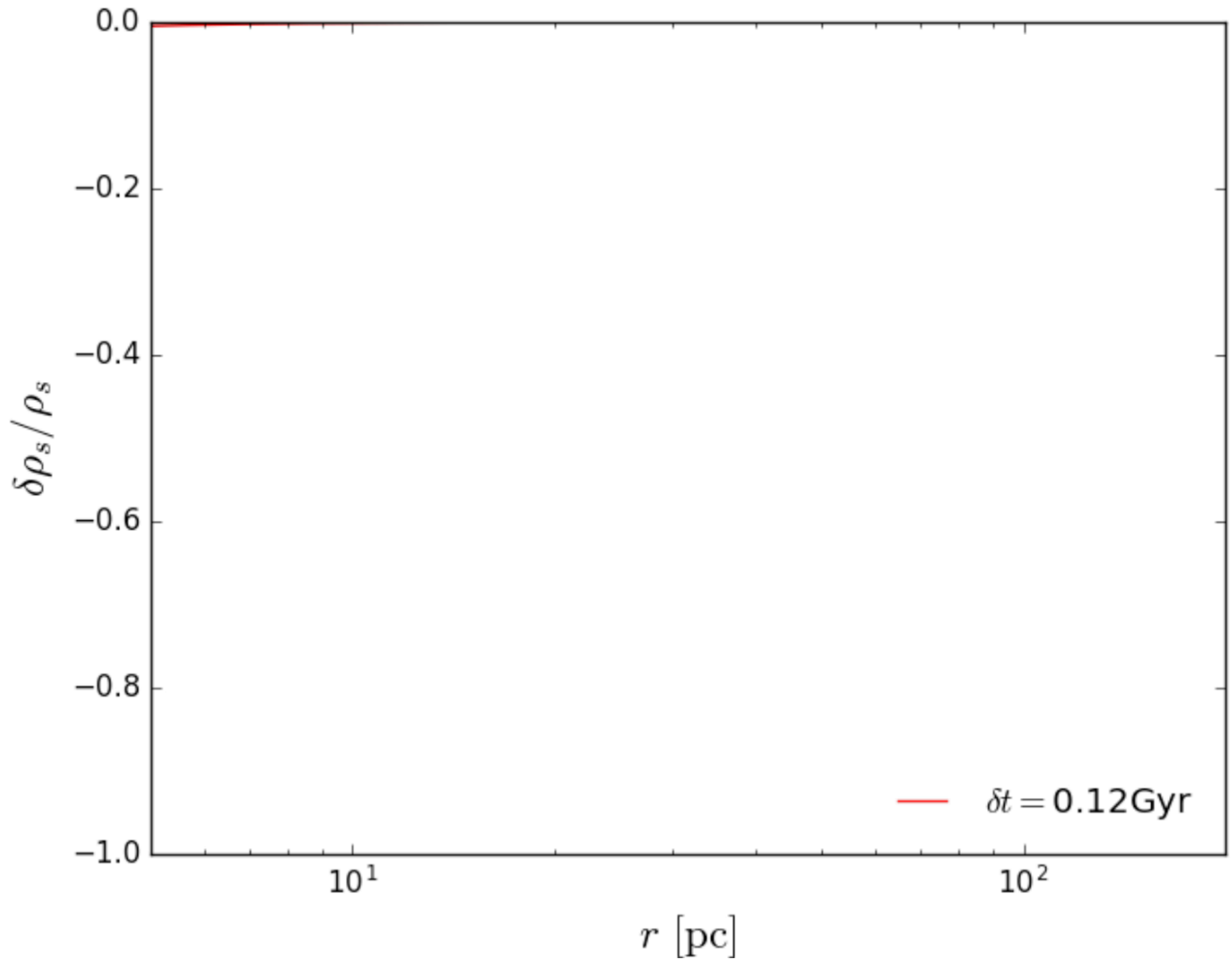

Koushiappas & Loeb PRL 119, 041102 (2017)

Evolution of density profile over 12 Gigayears

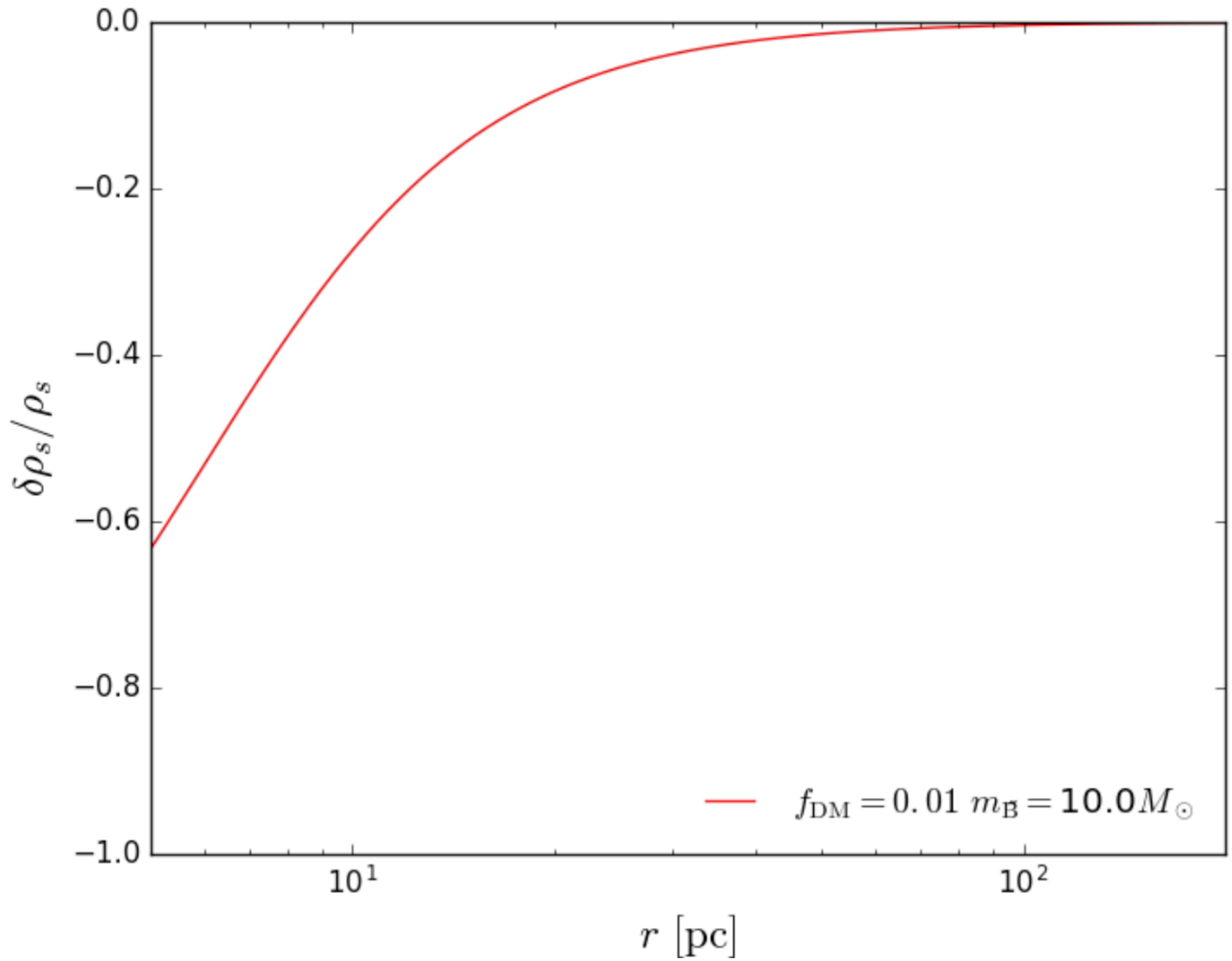

Koushiappas & Loeb PRL 119, 041102 (2017)

Depletion of stars in the inner regions

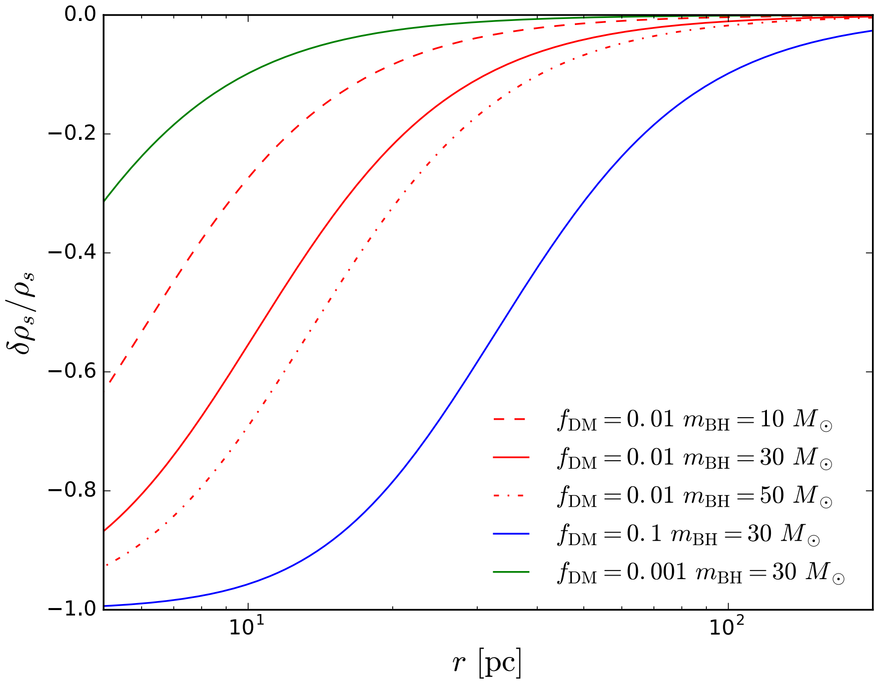

$$\frac{\delta\rho_s}{\rho_s} = \frac{r^3(t)}{r^3(0)} - 1$$

Koushiappas & Loeb PRL 119, 041102 (2017)

Depletion of stars in the inner regions

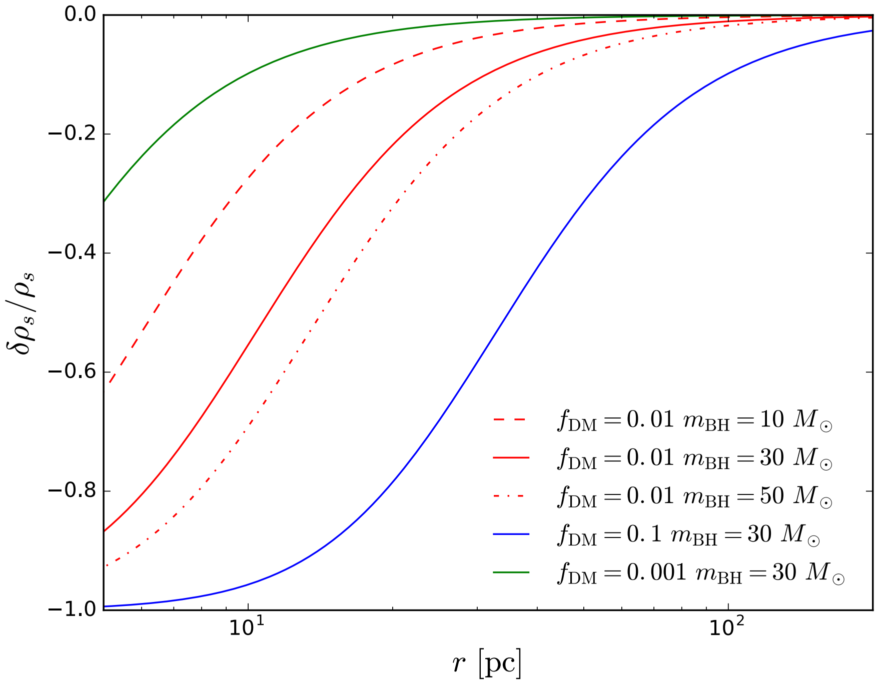

Prediction of a **stellar ring** in projection

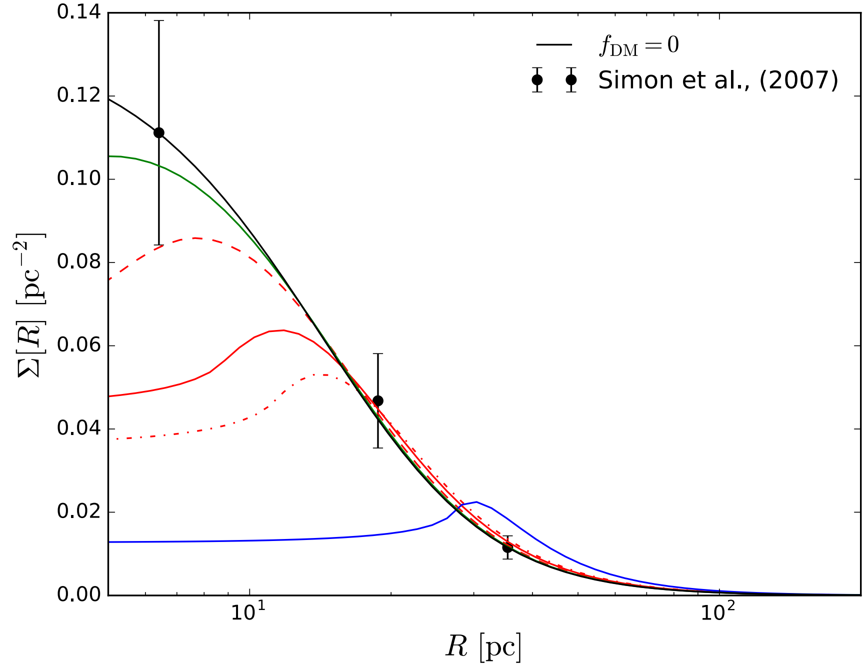

$$\frac{\delta\rho_s}{\rho_s} = \frac{r^3(t)}{r^3(0)} - 1$$

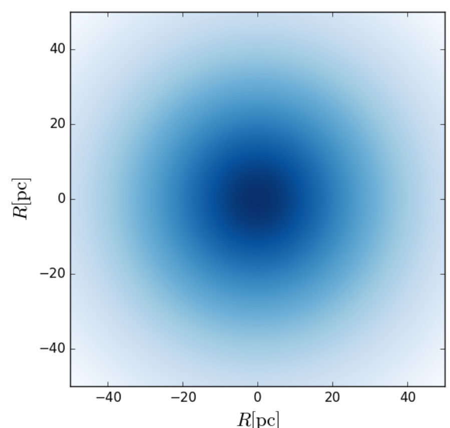

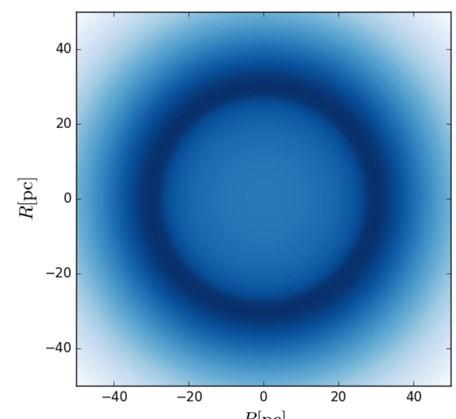

Koushiappas & Loeb PRL 119, 041102 (2017)

Primordial black hole constraints from the whole stellar population of Segue 1

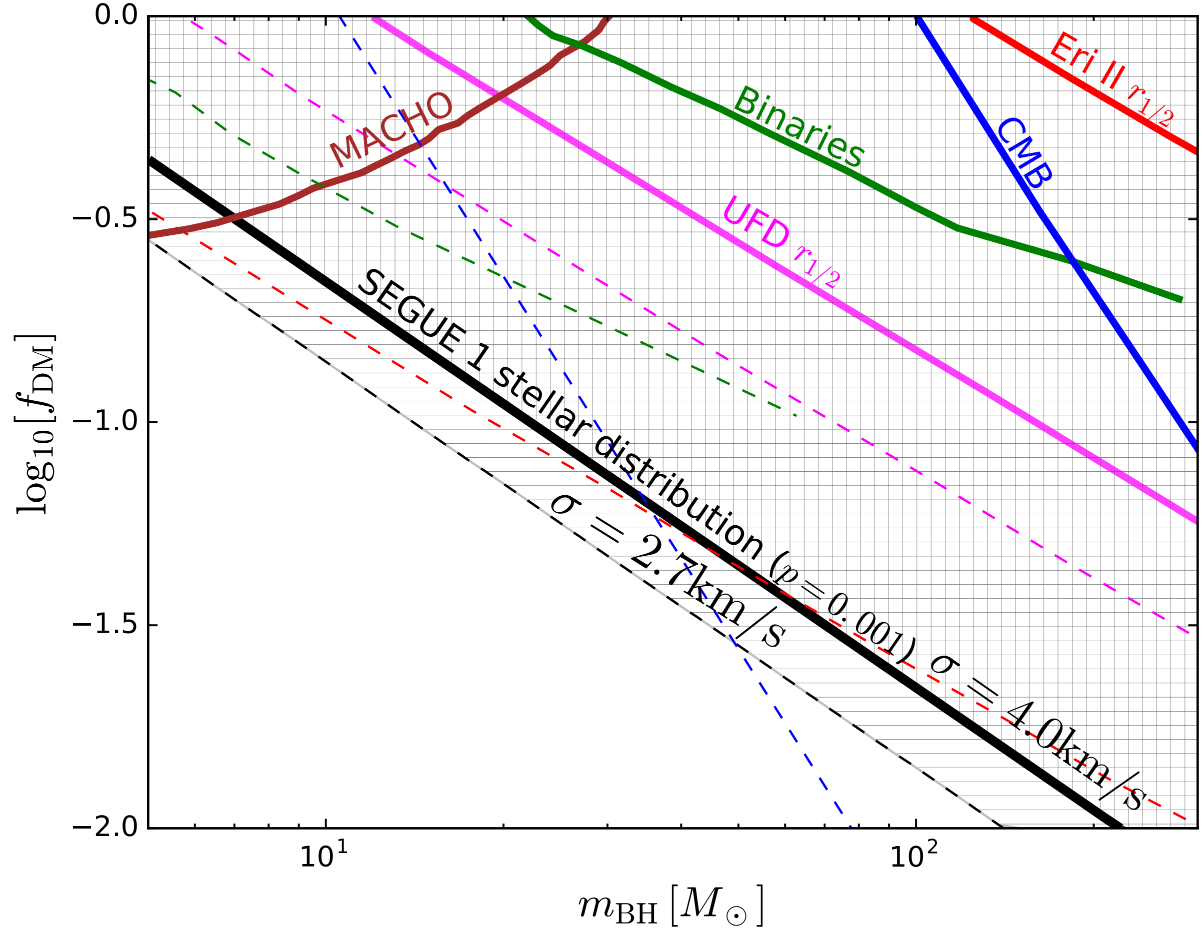

Eridanus II

Velocity dispersion unknown
Dark matter distribution unknown
Use 1/2-light radius of the central cluster only

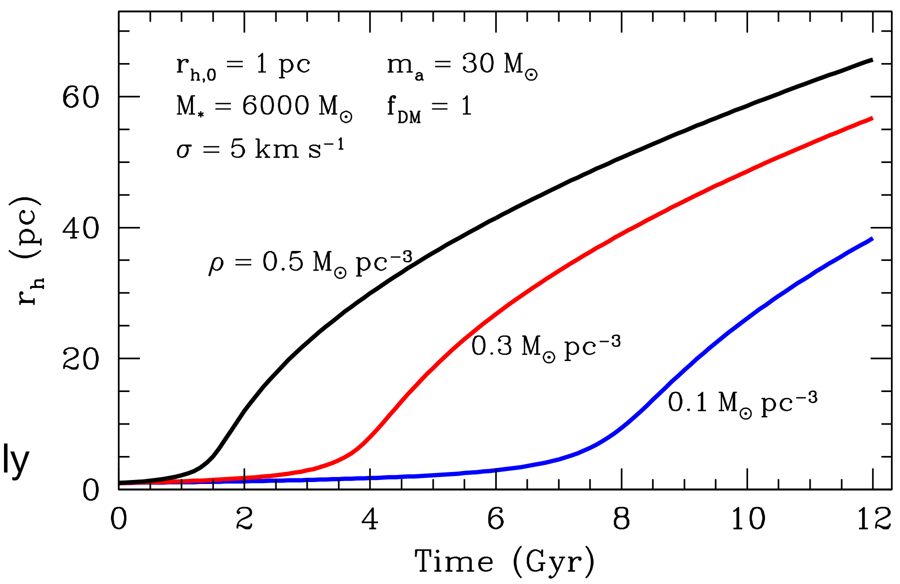

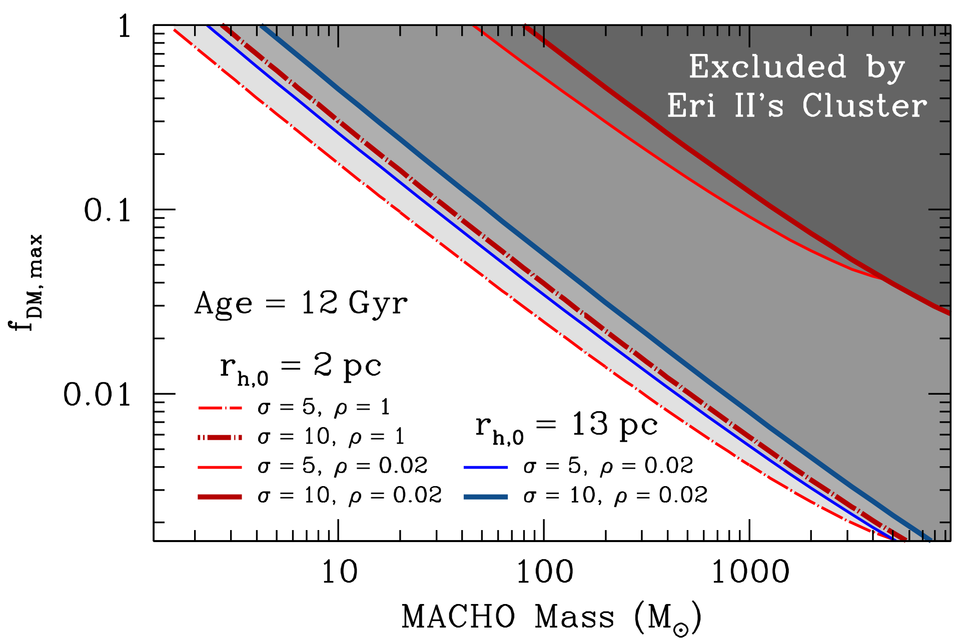

T. D. Brandt, Astrophys. J. Lett. **824**, L31 (2016)

Primordial black hole constraints from the whole stellar population of Segue 1

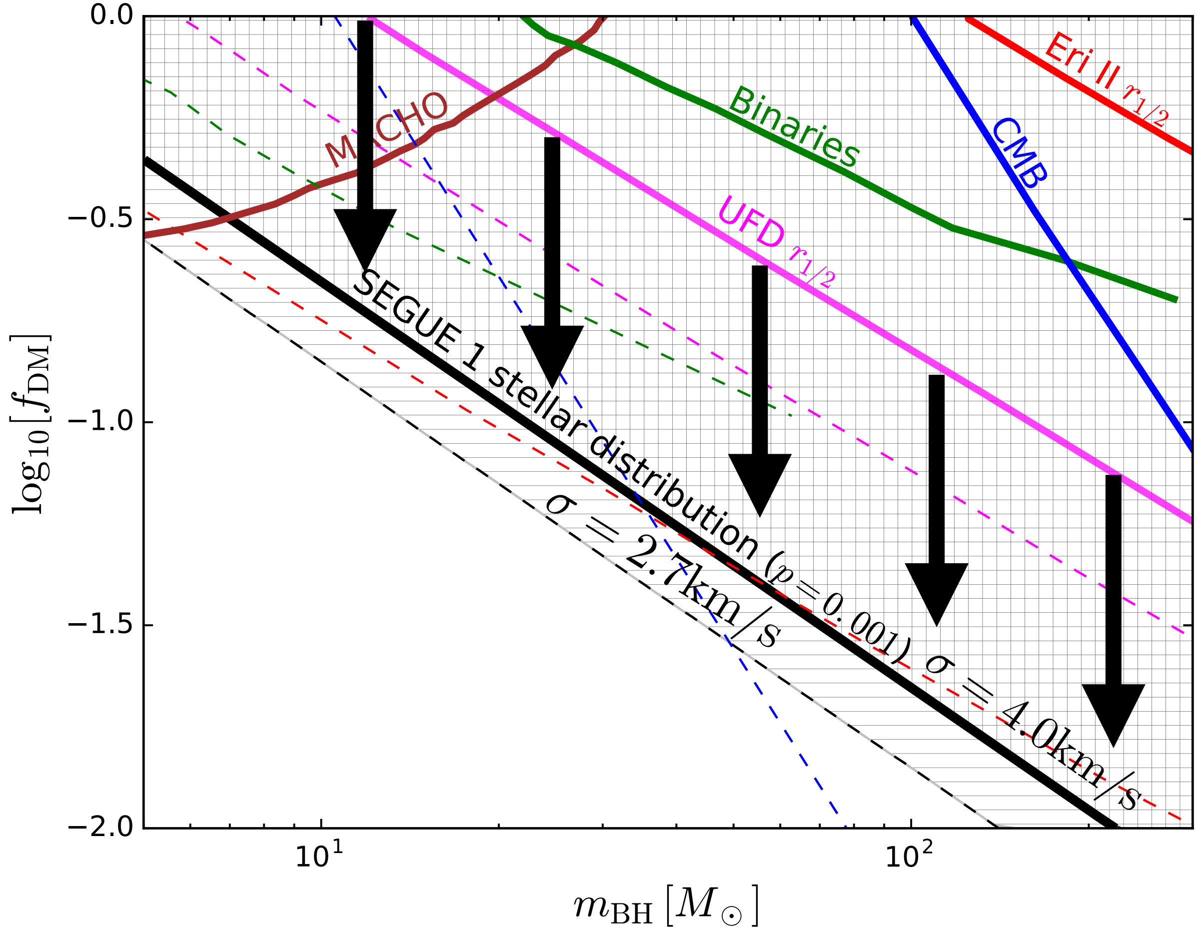

Depletion of stars in the inner regions

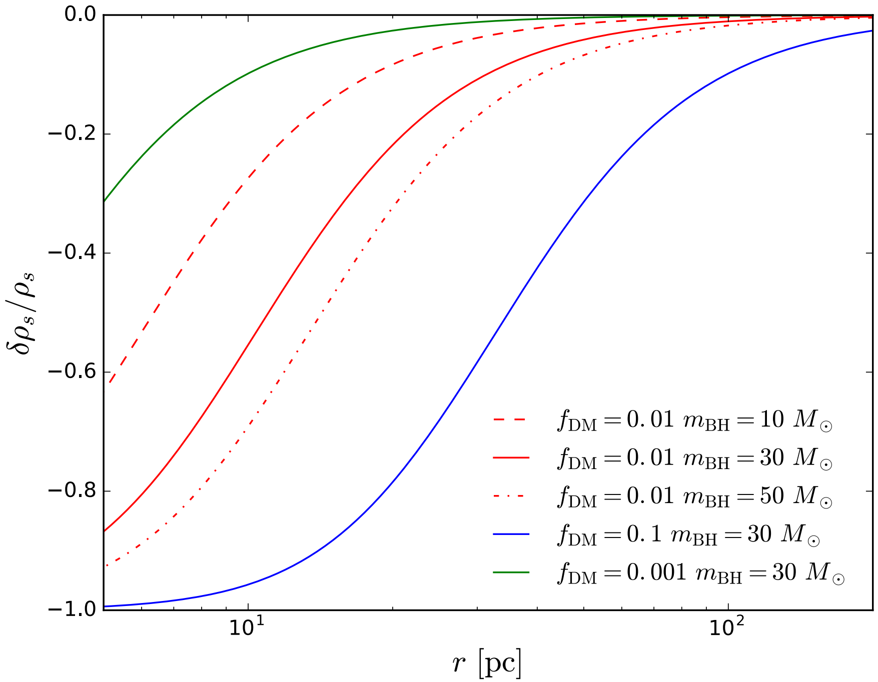

$$\frac{\delta\rho_s}{\rho_s} = \frac{r^3(t)}{r^3(0)} - 1$$

Prediction of a **stellar ring** in projection

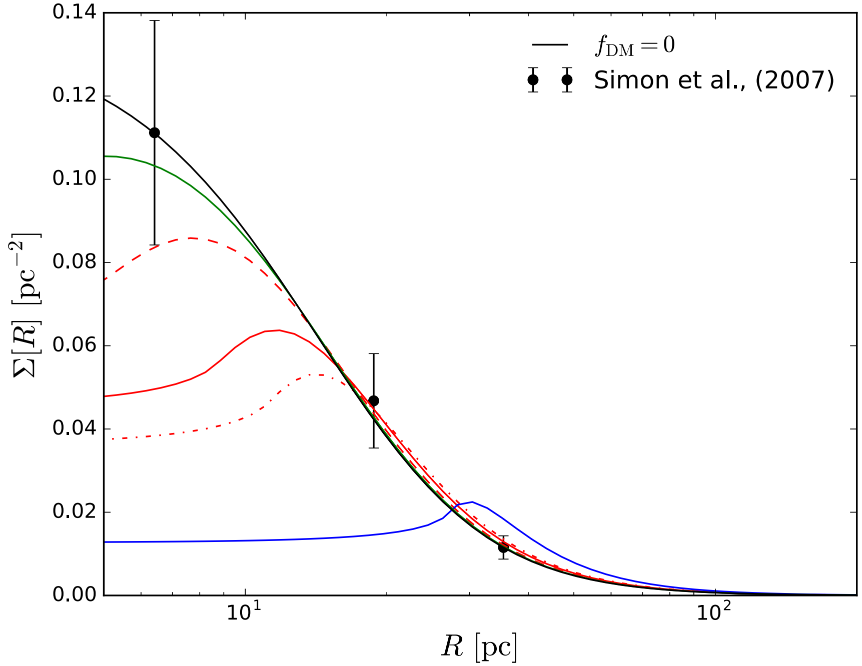

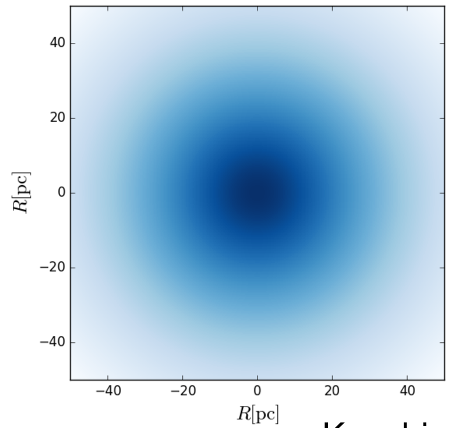

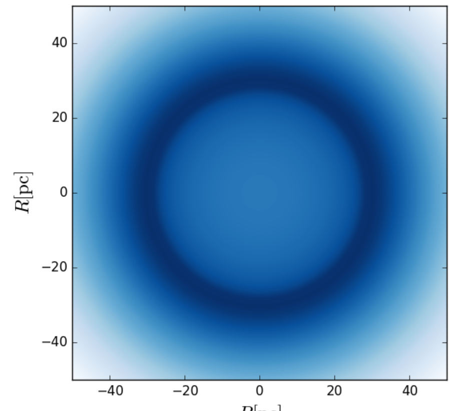

Koushiappas & Loeb PRL 119, 041102 (2017)

No black holes

1% dark matter in
10 solar mass black holes

10% of dark matter in
30 solar mass black holes

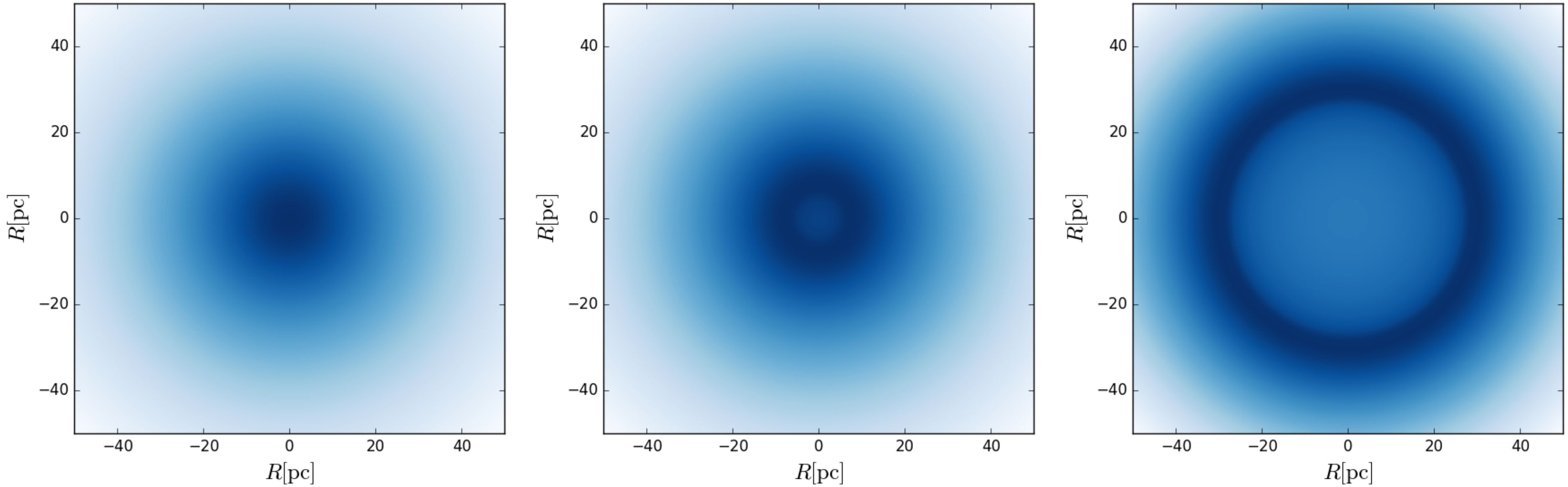

Both of these consistent with current observations

Ruled out

No black holes

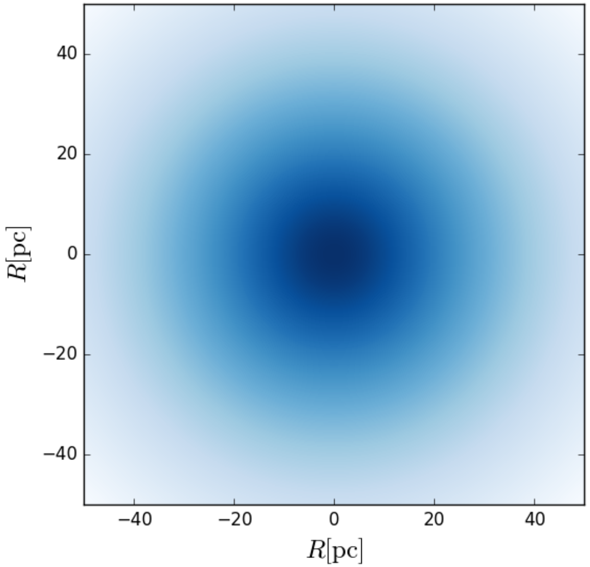

1% dark matter in
10 solar mass black holes

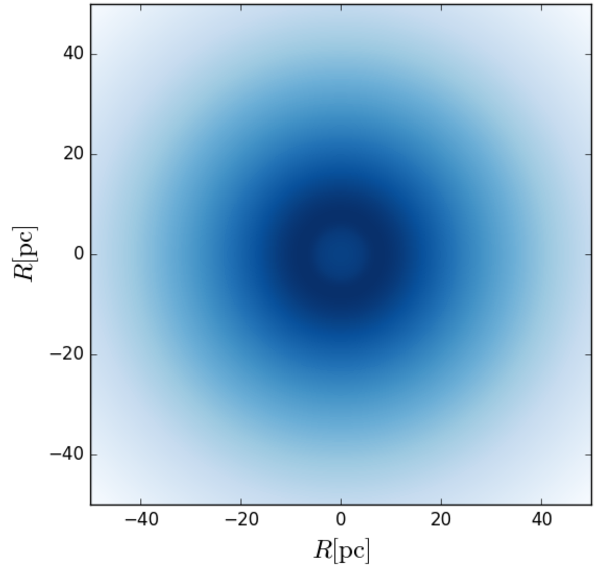

10% of dark matter in
30 solar mass black holes

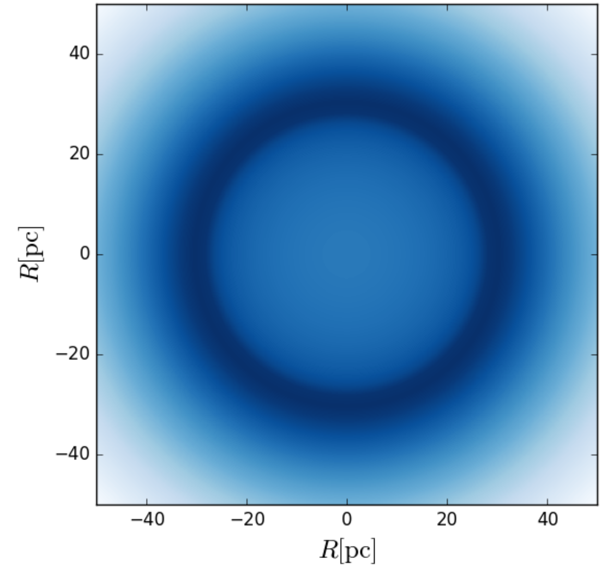

Both of these consistent with current observations

Ruled out

Subaru Telescope
National Astronomical Observatory of Japan

Thanks to Masahiro Takada!!

Fokker-Planck treatment of the same problem

Primordial black holes as dark matter: constraints from compact ultra-faint dwarfs

Qirong Zhu ✉, Eugene Vasiliev, Yuexing Li, Yipeng Jing

Monthly Notices of the Royal Astronomical Society, Volume 476, Issue 1, May 2018, Pages 2–11,
https://doi.org/10.1093/mnras/sty079

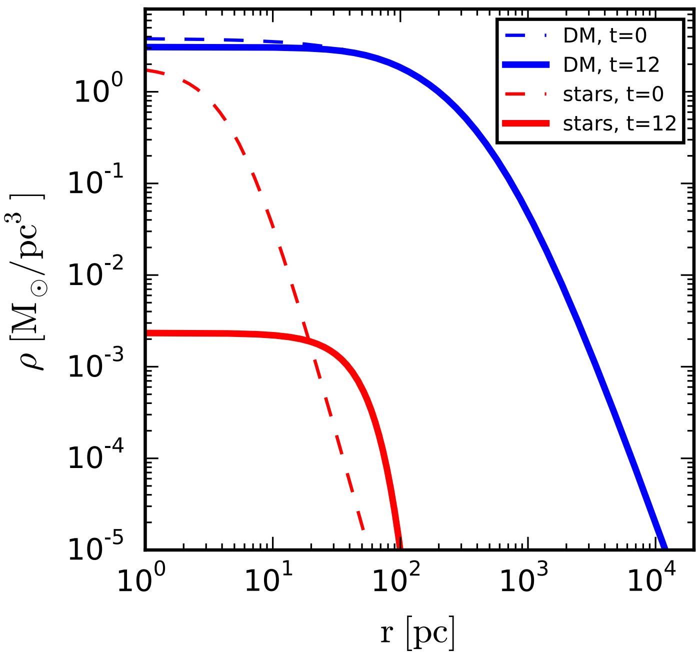

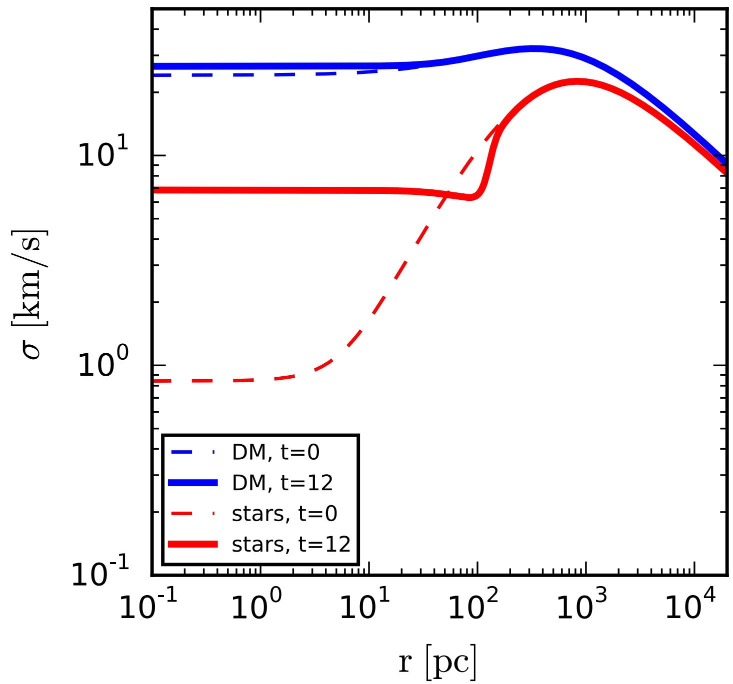

Fokker-Planck treatment of the same problem

Improved constraints from ultra-faint dwarf galaxies on primordial black holes as dark matter

Jakob Stegmann,[1,2]⋆ Pedro R. Capelo,[3] Elisa Bortolas[3] and Lucio Mayer[3]
[1] Department of Physics, ETH Zurich, Otto-Stern-Weg 1, 8093 Zurich, Switzerland
[2] School of Physics and Astronomy, Cardiff University, Cardiff, CF24 3AA, United Kingdom
[3] Center for Theoretical Astrophysics and Cosmology, Institute for Computational Science, University of Zurich, Winterthurerstrasse 190, 8057 Zurich, Switzerland

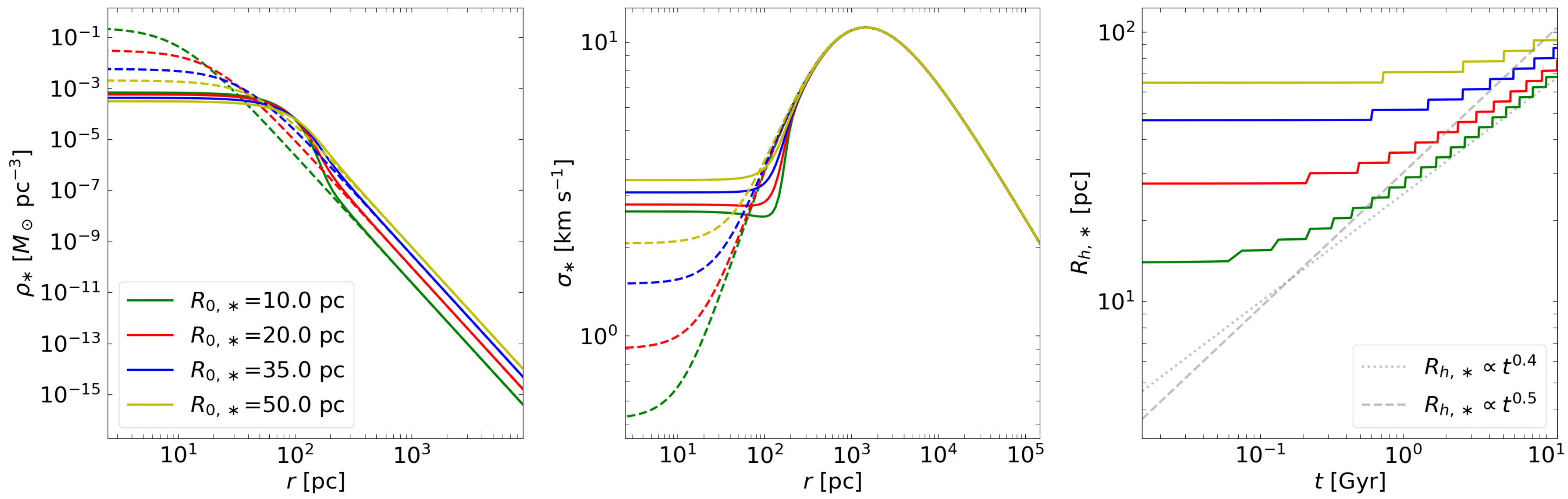

Constraints from dwarf galaxies

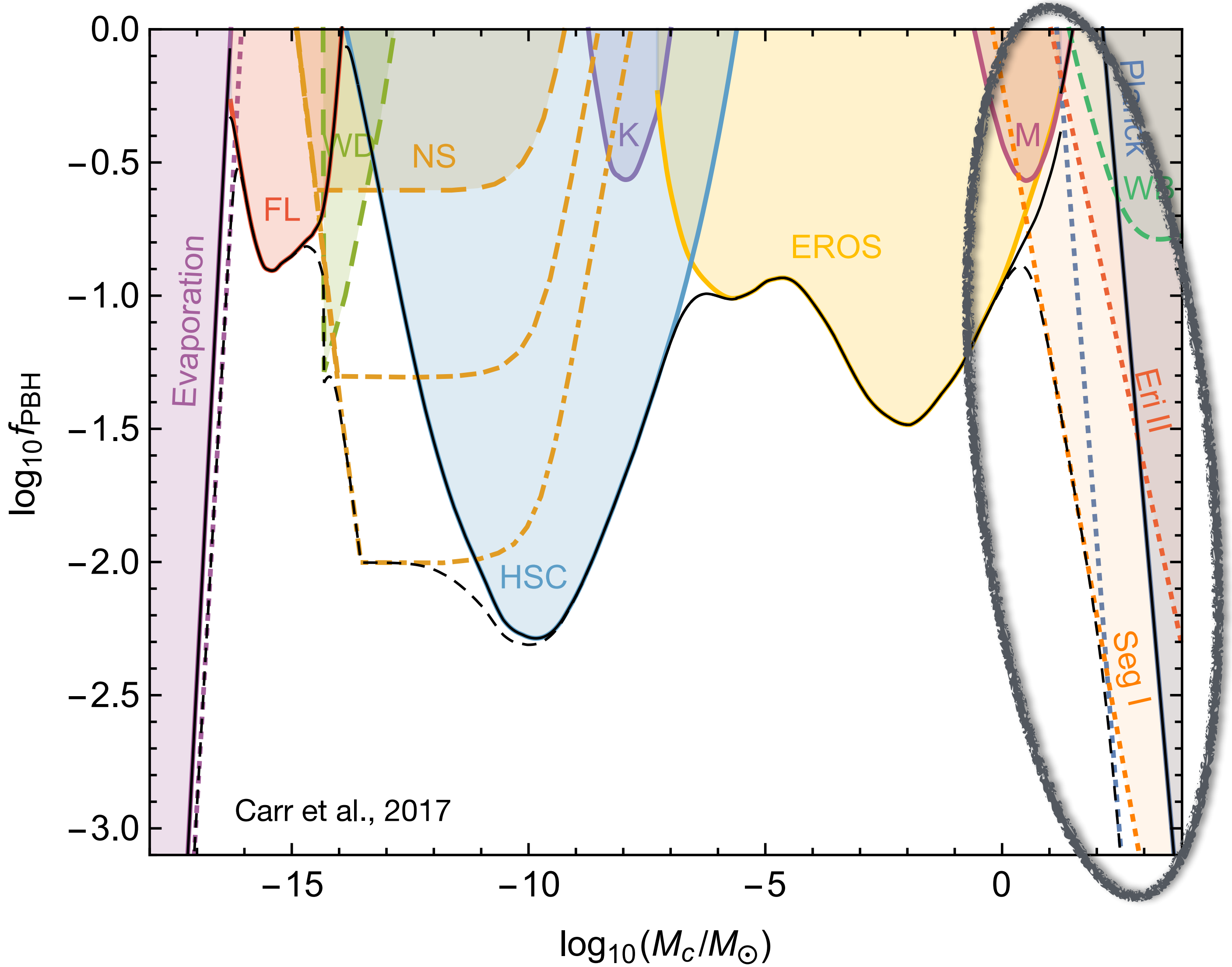

Grain of salt

Reconstructing the potential of dwarf galaxies using stellar kinematics

Reconstructing the potential of dwarf galaxies using stellar kinematics

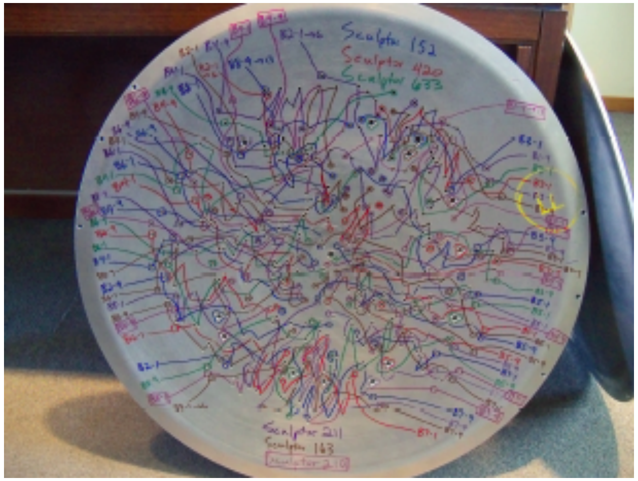

Reconstructing the potential of dwarf galaxies using stellar kinematics

- Fit mass and/or concentration (based on analytic forms derived in dissipantionless cosmological simulations (Strigari et al. 2008, Martinez et al, 2009, Martinez 2013).
- Assume dwarfs have cored profiles (Cholis & Salucci 2012, Salucci et al, 2012)
- Agnostic — fit a flexible density profile that is not restricted to the form used to describe simulated halos (Charmonnier et al. 2011, Geringer-Sameth et al, 2014, 2015, 2017).

Error propagation

- Errors are log-normal and folded into the likelihood (Ackermann et al 2011, Albert et al 2015).
- Separate systematics from statistical uncertainties (Geringer-Sameth, et al. 2011, 2015, 2018).

Flexible profile

$$\rho(r) = \frac{\rho_s}{(r/r_s)^\gamma \left[1 + (r/r_s)^\alpha\right]^{(\beta-\gamma)/\alpha}}.$$

Split power-law

$$d \log \rho / d \log r|_{r \ll r_s} = -\gamma$$

$$d \log \rho / d \log r|_{r \gg r_s} = -\beta$$

Transition takes place at r_s and α describes its sharpness

The NFW is recovered if $(\alpha, \beta, \gamma) = (1, 3, 1)$

"Cusped" profiles $(\gamma > 1)$

"Cored" profiles $(\gamma \sim 0)$

Collisionless stellar systems — phase space density describes potential

Stellar density profile $$\nu(r) \equiv \int f(\mathbf{r}, \mathbf{u})\; d^3\mathbf{u},$$

Velocity dispersion profile $$\overline{u^2}(r) = \overline{u_r^2}(r) + \overline{u_\theta^2}(r) + \overline{u_\phi^2}(r)$$

$$= \frac{1}{\nu(r)} \int u^2 f(\mathbf{r}, \mathbf{u})\; d^3\mathbf{u}.$$

Assume dynamic equilibrium & spherical symmetry

Jeans equation $$\frac{1}{\nu(r)} \frac{d}{dr}\left[\nu(r)\overline{u_r^2}(r)\right] + 2\frac{\beta_a(r)\overline{u_r^2}(r)}{r} = -\frac{d\Phi}{dr} = -\frac{GM(r)}{r^2}$$

Enclosed mass $$M(r) = 4\pi \int_0^r s^2 \rho(s) ds$$

Orbital anisotropy $$\beta_a(r) \equiv 1 - \frac{2\overline{u_\theta^2}(r)}{\overline{u_r^2}(r)}$$

General solution to the Jeans equation

$$\nu(r)\overline{u_r^2}(r) = \frac{1}{f(r)} \int_r^\infty f(s)\,\nu(s)\,\frac{GM(s)}{s^2}\,ds.$$

$$f(r) = 2\,f(r_1)\,\exp\left[\int_{r_1}^{r} \beta_a(s)s^{-1}\,ds\right]$$

Projecting along the line of sight

$$\sigma^2(R)\,\Sigma(R) = 2\int_R^\infty \left(1 - \beta_a(r)\frac{R^2}{r^2}\right)\frac{\nu(r)\,\overline{u_r^2}(r)\,r}{\sqrt{r^2 - R^2}}\,dr$$

Line of sight velocity dispersion

Projected stellar density

Both are observables -> Use them to constrain $\{\rho(r), \beta_a(r)\}$

Assumptions

- Dynamic equilibrium & spherical symmetry (implicit in Jeans equation).
- Stars are distributed according to a Plummer profile.
- Stars contribute negligibly to the gravitational potential.
- Anisotropy is constant.
- Velocity data samples a Gaussian line-of-sight velocity.
- Stellar velocities are not significantly influenced by the presence of binary stars.

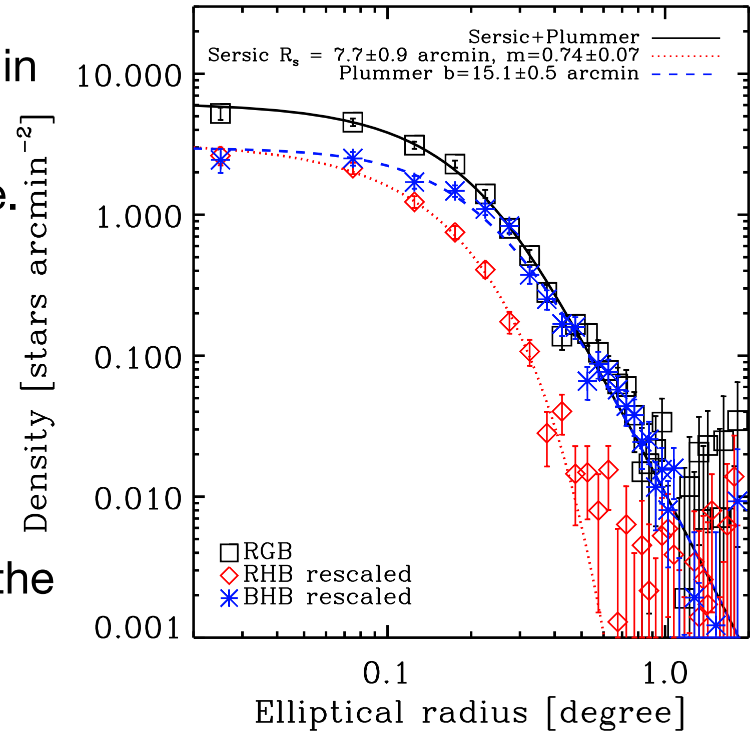

Battaglia et al., 2008

Plummer profile for stellar distribution

$$\nu(r) = \frac{3L}{4\pi R_e^3} \frac{1}{\left(1 + R^2/R_e^2\right)^{5/2}}, \longrightarrow \Sigma(R) = \frac{L}{\pi R_e^2} \frac{1}{\left(1 + R^2/R_e^2\right)^2}$$

Half-light radius

Classical dwarfs

Object	Distance (kpc)	$R_{\rm half}$ (pc)	$N_{\rm sample}$
Carina	105 ± 6	250 ± 39	774
Draco	76 ± 6	221 ± 19	292
Fornax	147 ± 12	710 ± 77	2483
Leo I	254 ± 15	251 ± 27	267
Leo II	233 ± 14	176 ± 42	126
Sculptor	86 ± 6	283 ± 45	1365
Sextans	86 ± 4	695 ± 44	441
Ursa Minor	76 ± 3	181 ± 27	313
Bootes I	66 ± 2	242 ± 21	37
Canes Venatici I	218 ± 10	564 ± 36	214
Canes Venatici II	160 ± 4	74 ± 14	25
Coma Berenices	44 ± 4	77 ± 10	59
Hercules	132 ± 12	330^{+75}_{-52}	30
Leo IV	154 ± 6	206 ± 37	18
Leo V	178 ± 10	135 ± 32	5
Leo T	417 ± 19	120 ± 9	19
Segue 1	23 ± 2	29^{+8}_{-5}	70
Segue 2	35 ± 2	35 ± 3	25
Ursa Major I	97 ± 4	319 ± 50	39
Ursa Major II	32 ± 4	149 ± 21	20

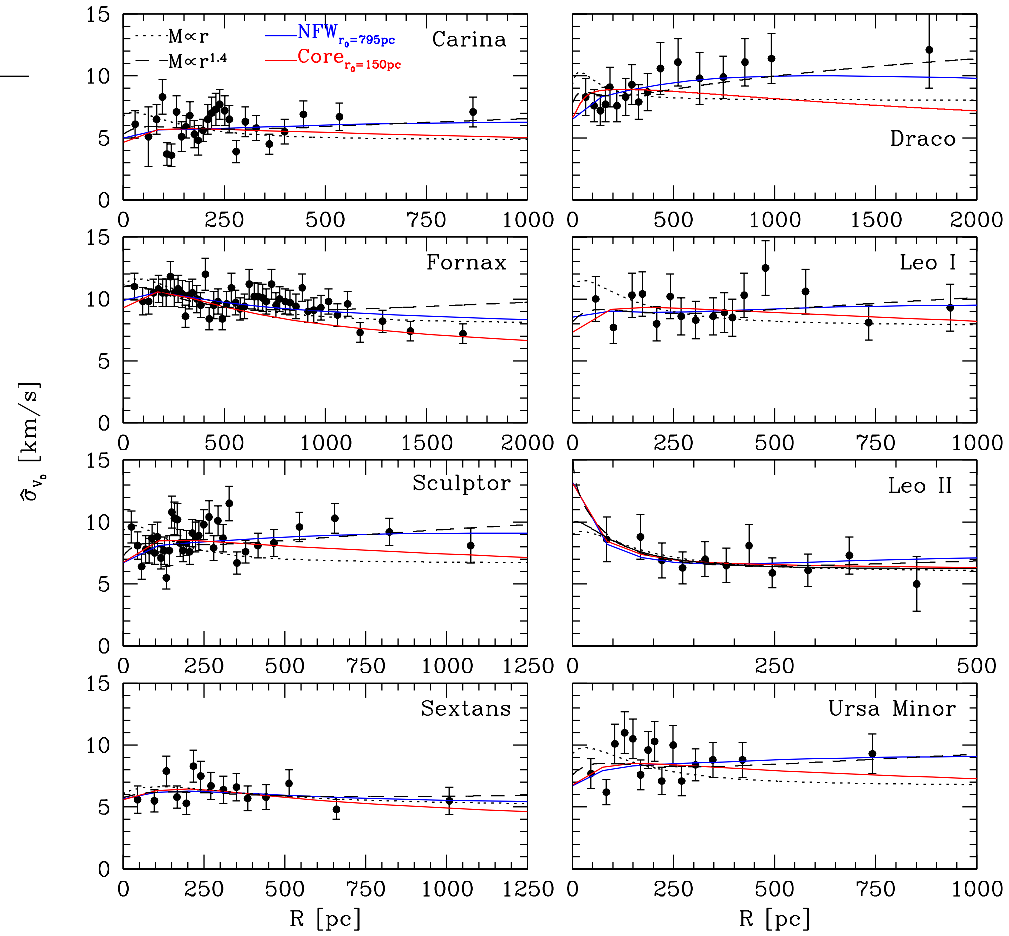

Ultra-faint dwarfs

Object	Distance (kpc)	R_{half} (pc)	N_{sample}
Carina	105 ± 6	250 ± 39	774
Draco	76 ± 6	221 ± 19	292
Fornax	147 ± 12	710 ± 77	2483
Leo I	254 ± 15	251 ± 27	267
Leo II	233 ± 14	176 ± 42	126
Sculptor	86 ± 6	283 ± 45	1365
Sextans	86 ± 4	695 ± 44	441
Ursa Minor	76 ± 3	181 ± 27	313
Bootes I	66 ± 2	242 ± 21	37
Canes Venatici I	218 ± 10	564 ± 36	214
Canes Venatici II	160 ± 4	74 ± 14	25
Coma Berenices	44 ± 4	77 ± 10	59
Hercules	132 ± 12	330^{+75}_{-52}	30
Leo IV	154 ± 6	206 ± 37	18
Leo V	178 ± 10	135 ± 32	5
Leo T	417 ± 19	120 ± 9	19
Segue 1	23 ± 2	29^{+8}_{-5}	70
Segue 2	35 ± 2	35 ± 3	25
Ursa Major I	97 ± 4	319 ± 50	39
Ursa Major II	32 ± 4	149 ± 21	20

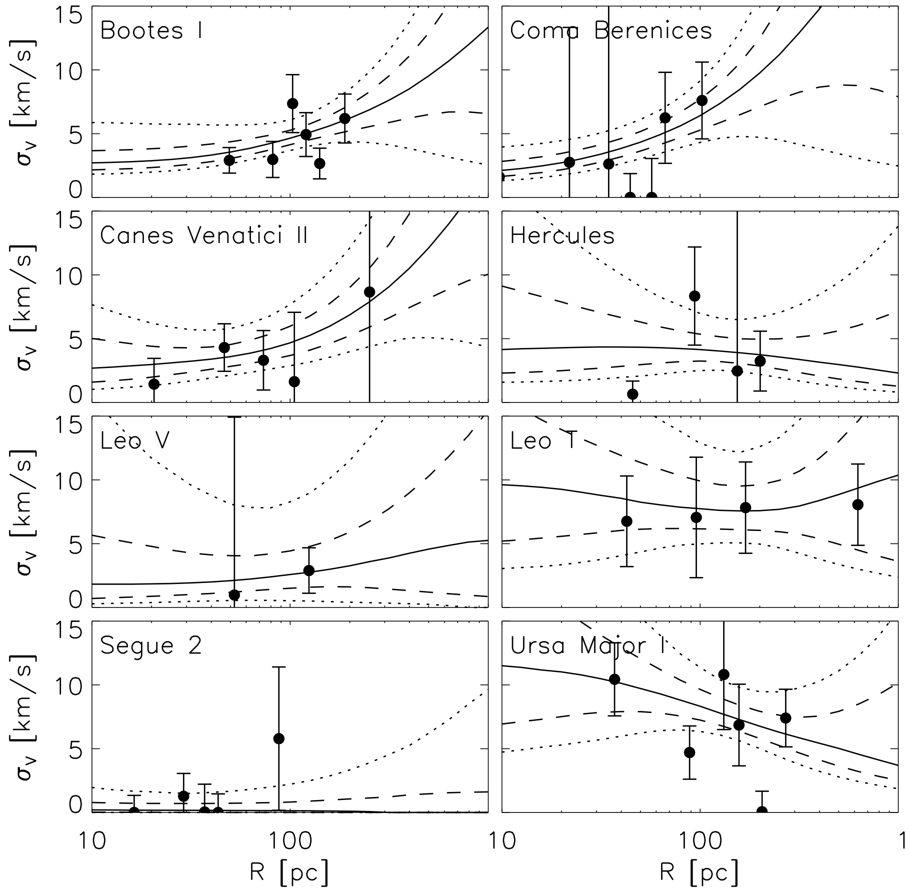

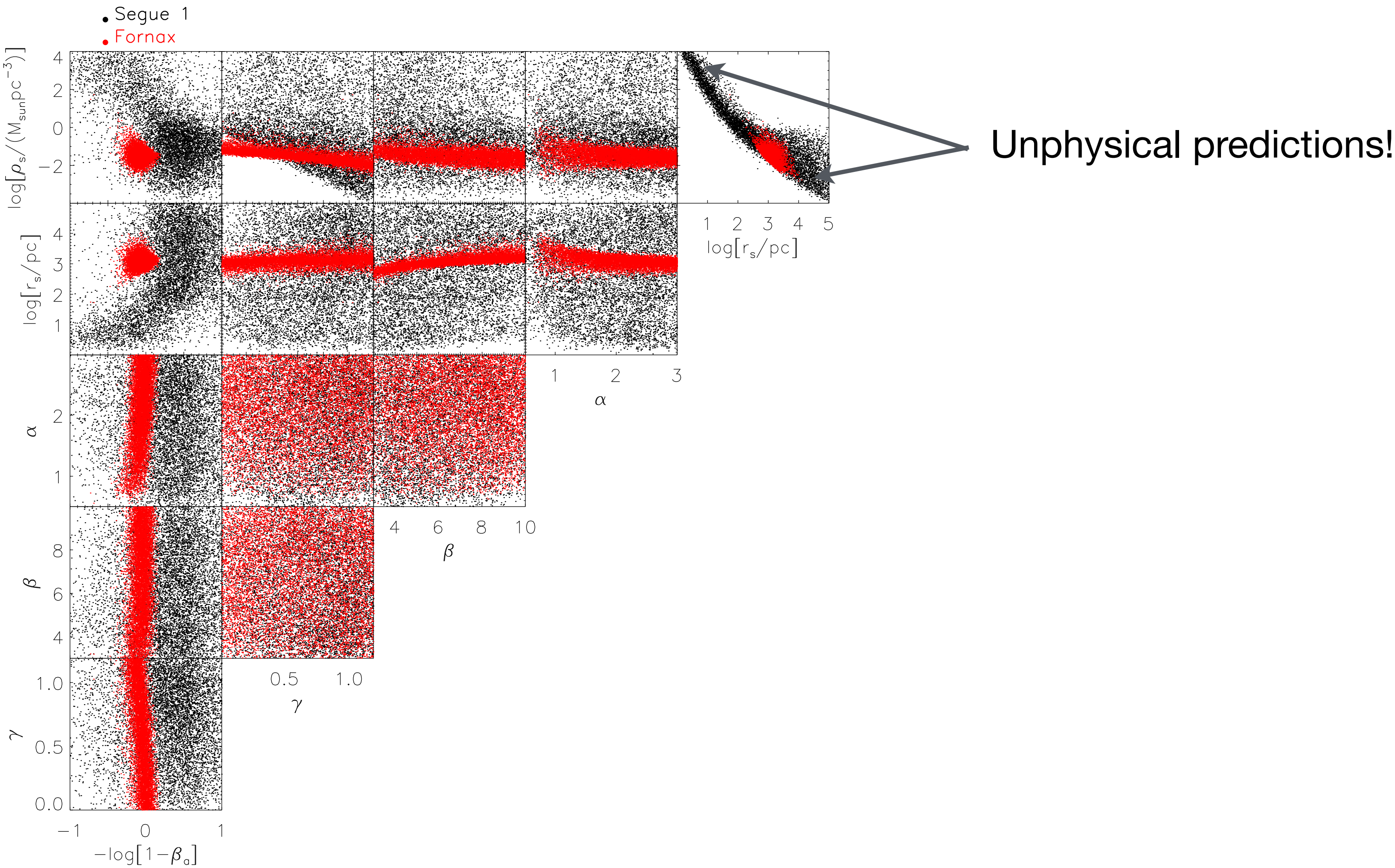

Segue 1
Fornax
log[ρs/(Msunpc−3)]
log[rs/pc]
α
β
γ
−log[1−βa]
Unphysical predictions!

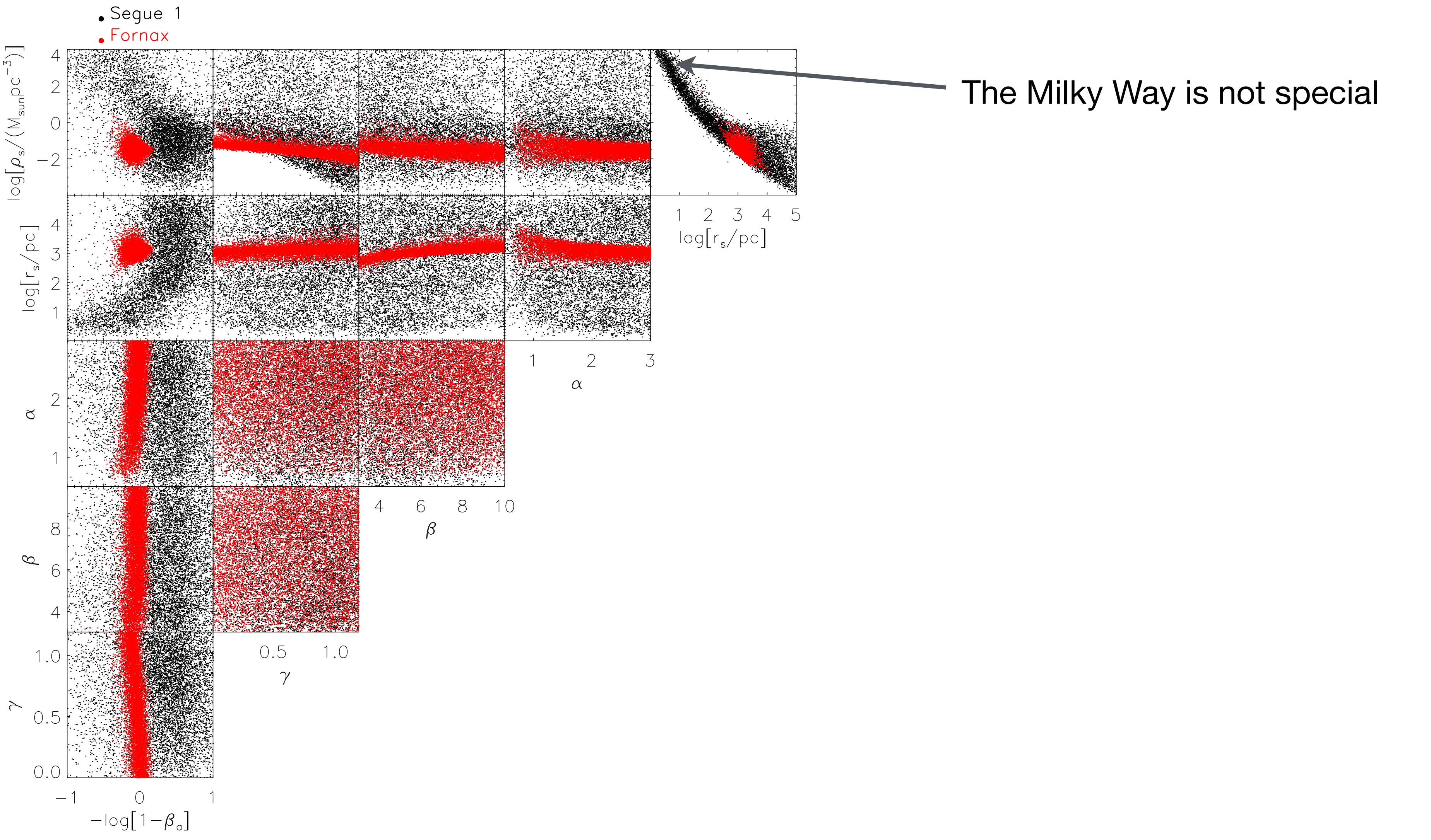

Segue 1
Fornax
The Milky Way is not special
log[ρs/(Msun pc−3)]
log[rs/pc]
α
β
γ
−log[1−βa]

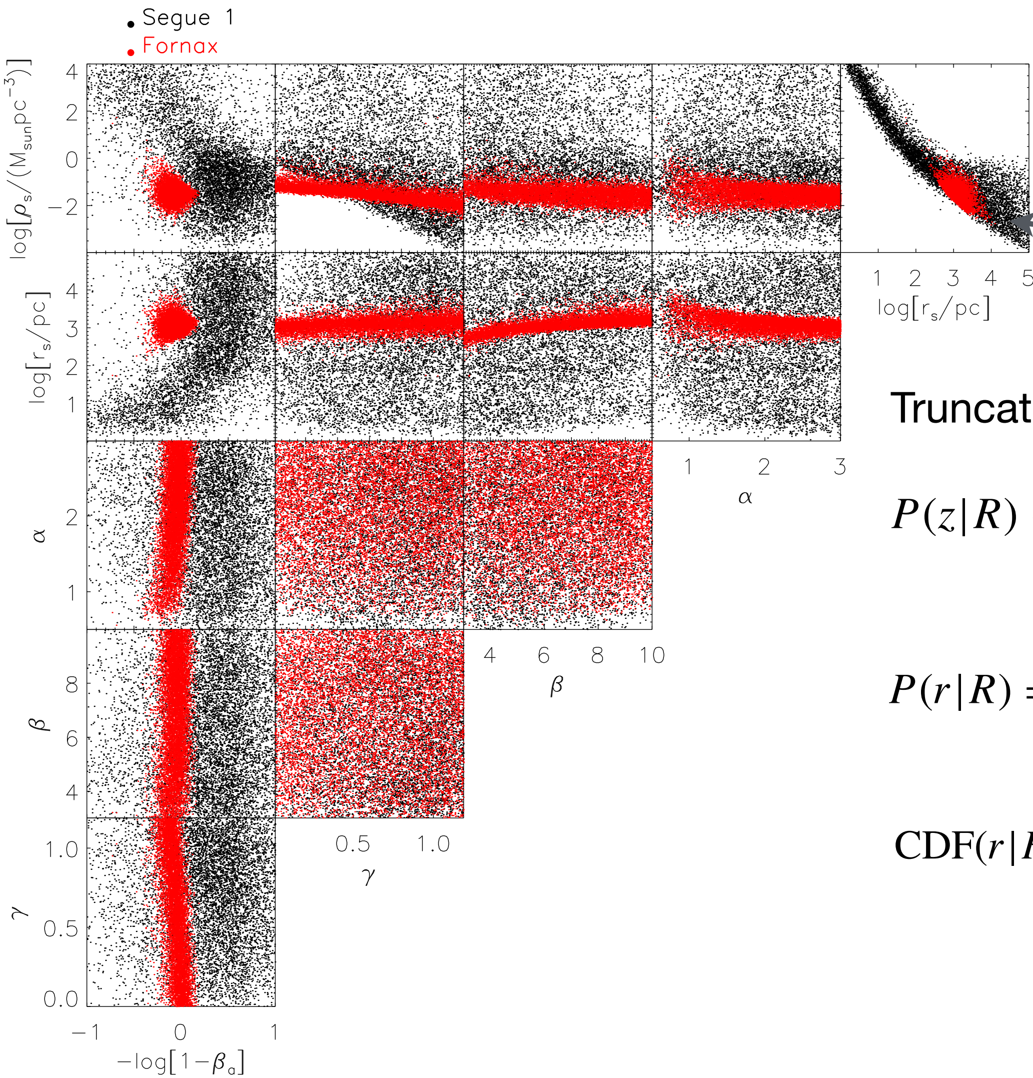

Truncation

Truncation at last star

$$P(z|R) \propto \left(1 + \frac{z^2 + R^2}{R_e^2}\right)^{-5/2}$$

$$P(r|R) = \int_z P(r|z, R)\ P(z|R)\, dz$$

$$\mathrm{CDF}(r|R) = \int_0^r P(r'|R) dr'$$

$$= \frac{\left(r^2 - R^2\right)^{1/2} \left(r^2 + \frac{1}{2}\left(3R_h^2 + R^2\right)\right)}{\left(r^2 + R_h^2\right)^{3/2}}.$$

$$\mathrm{CDF}_{\max}(r|R_1, \ldots, R_n) = \mathrm{CDF}(r|R_1) \cdots \mathrm{CDF}(r|R_n),$$

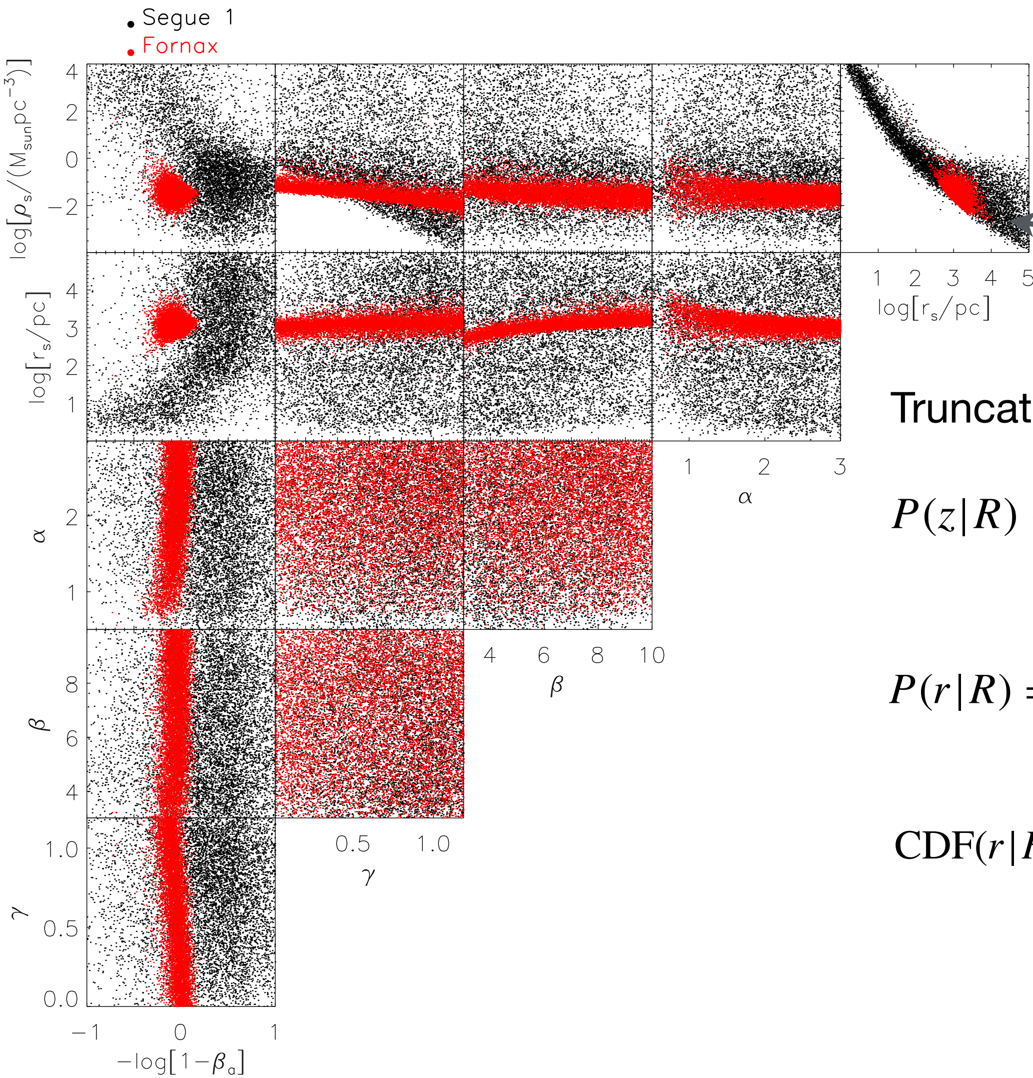

Truncation

Truncation at last star

$$P(z|R) \propto \left(1 + \frac{z^2 + R^2}{R_e^2}\right)^{-5/2}$$

$$P(r|R) = \int_z P(r|z, R)\ P(z|R)\, dz$$

$$\mathrm{CDF}(r|R) = \int_0^r P(r'|R)dr'$$
$$= \frac{\left(r^2 - R^2\right)^{1/2}\left(r^2 + \frac{1}{2}\left(3R_h^2 + R^2\right)\right)}{\left(r^2 + R_h^2\right)^{3/2}}.$$

$$\mathrm{CDF}_{\max}(r|R_1, \ldots, R_n) = \mathrm{CDF}(r|R_1)\cdots\mathrm{CDF}(r|R_n).$$

$$r_t^3 - D^3 \frac{M(r_t)}{M_{\rm MW}(D)}\left[2 + \frac{\omega^2 D^3}{G M_{\rm MW}(D)} - \left.\frac{d \ln M_{\rm MW}}{d \ln r}\right|_{r=D}\right]^{-1} = 0.$$

Alternatively use tidal radius

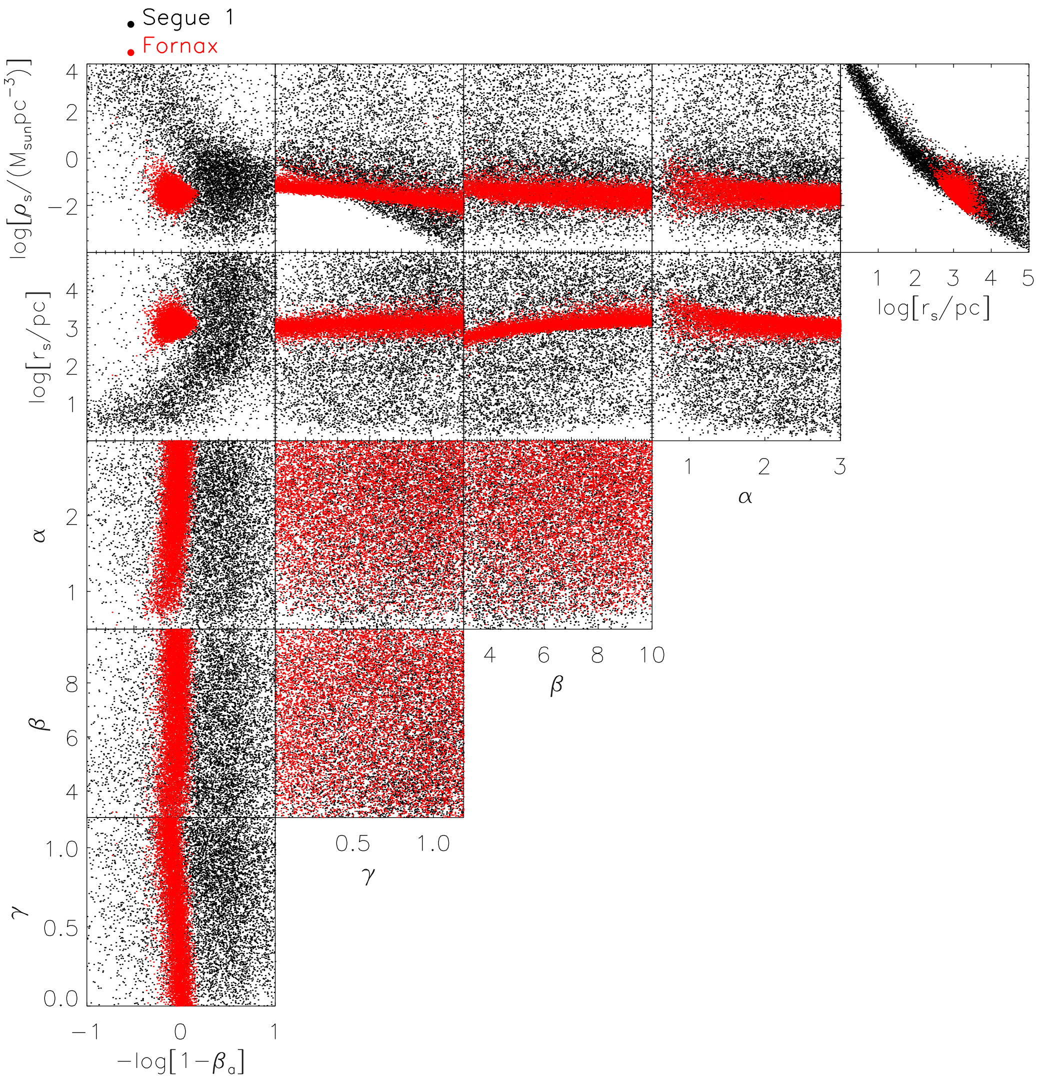

Halo Profile Parameter Constraints

Name	$\log_{10}\rho_s$ $(M_\odot \mathrm{pc}^{-3})$					$\log_{10} r_s$ (pc)					α					β					γ					$-\log_{10}(1-\beta_a)$				
	-2σ	-1σ	Median	$+1\sigma$	$+2\sigma$	-2σ	-1σ	Median	$+1\sigma$	$+2\sigma$	-2σ	-1σ	Median	$+1\sigma$	$+2\sigma$	-2σ	-1σ	Median	$+1\sigma$	$+2\sigma$	-2σ	-1σ	Median	$+1\sigma$	$+2\sigma$	-2σ	-1σ	Median	$+1\sigma$	$+2\sigma$
Carina	−3.74	−2.86	−1.96	−1.28	−0.73	2.61	2.90	3.31	3.96	4.63	0.62	0.87	1.47	2.41	2.89	3.12	3.75	5.60	8.36	9.71	0.13	0.54	0.95	1.13	1.19	−0.41	−0.23	−0.07	0.08	0.25
Draco	−3.36	−2.66	−1.74	−1.09	−0.78	2.85	3.11	3.57	4.34	4.83	0.75	1.18	2.01	2.65	2.95	3.19	4.16	6.34	8.69	9.74	0.06	0.29	0.71	1.02	1.16	0.01	0.25	0.54	0.81	0.97
Fornax	−2.11	−1.83	−1.49	−1.20	−0.76	2.73	2.93	3.09	3.25	3.51	0.86	1.39	2.13	2.73	2.96	3.30	4.54	6.97	9.02	9.84	0.03	0.19	0.61	1.02	1.17	−0.25	−0.15	−0.06	0.02	0.09
Leo I	−3.69	−3.08	−2.18	−1.38	−0.92	2.91	3.23	3.80	4.55	4.91	0.71	1.12	1.93	2.64	2.94	3.16	3.99	6.15	8.70	9.76	0.09	0.41	0.84	1.08	1.18	−0.20	−0.03	0.14	0.37	0.72
Leo II	−3.24	−2.31	−0.92	−0.03	0.47	1.95	2.29	2.89	4.03	4.77	0.64	1.01	1.76	2.53	2.90	3.16	3.89	5.95	8.56	9.73	0.08	0.35	0.82	1.08	1.18	−0.88	−0.51	−0.01	0.51	0.88
...																														

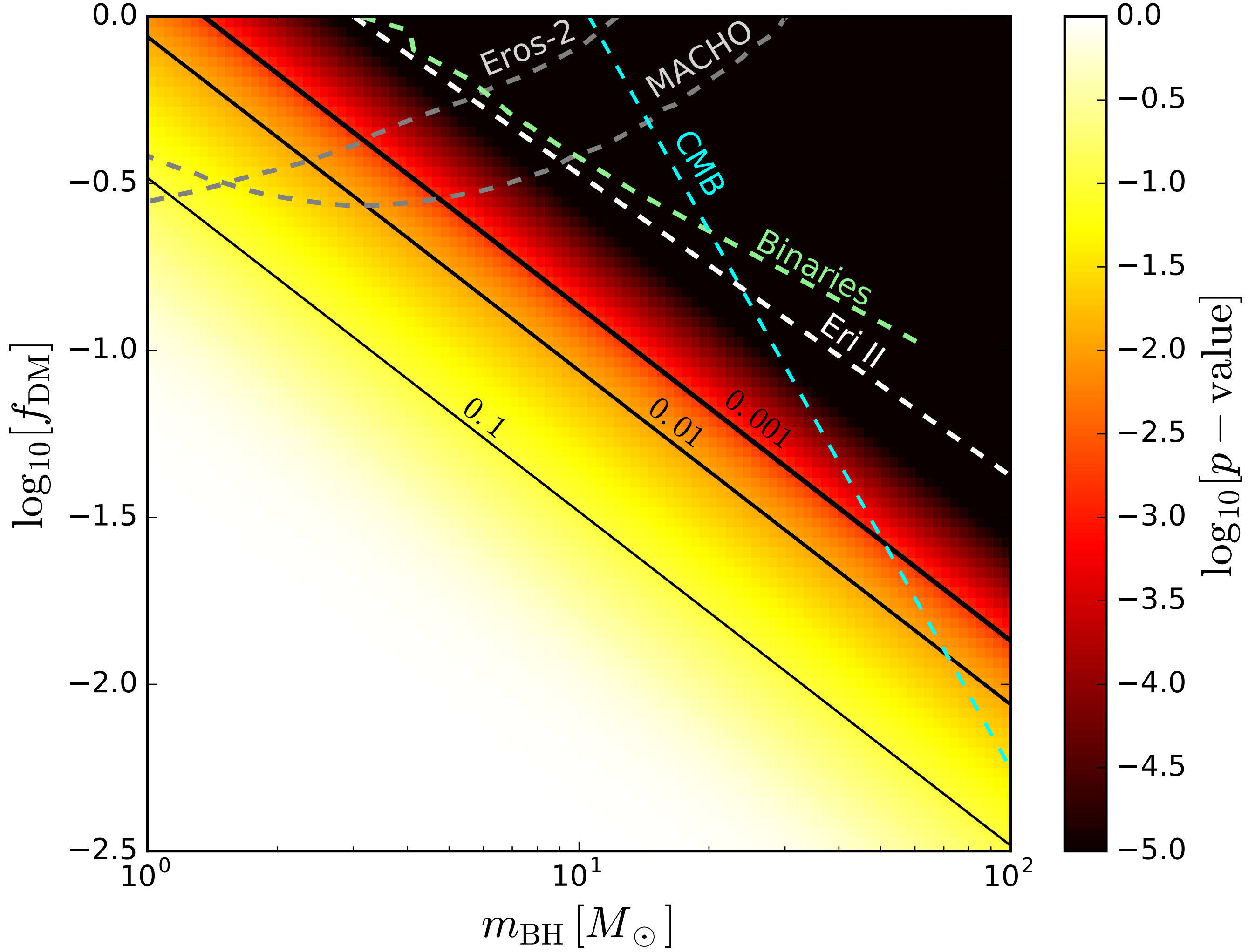

Eros-2
MACHO
CMB
Binaries
Eri II
0.1
0.01
0.001
$\log_{10}[f_{\rm DM}]$
$m_{\rm BH}\,[M_\odot]$
$\log_{10}[p-{\rm value}]$

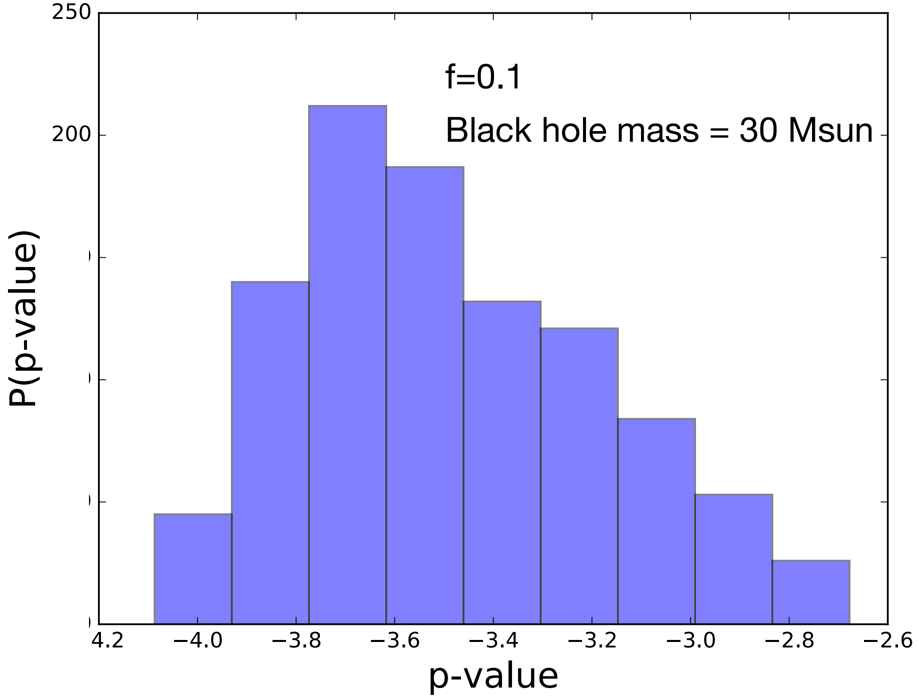

f=0.1
Black hole mass = 30 Msun
250
200
4.2
−4.0
−3.8
−3.6
−3.4
−3.2
−3.0
−2.8
−2.6
p-value
P(p-value)

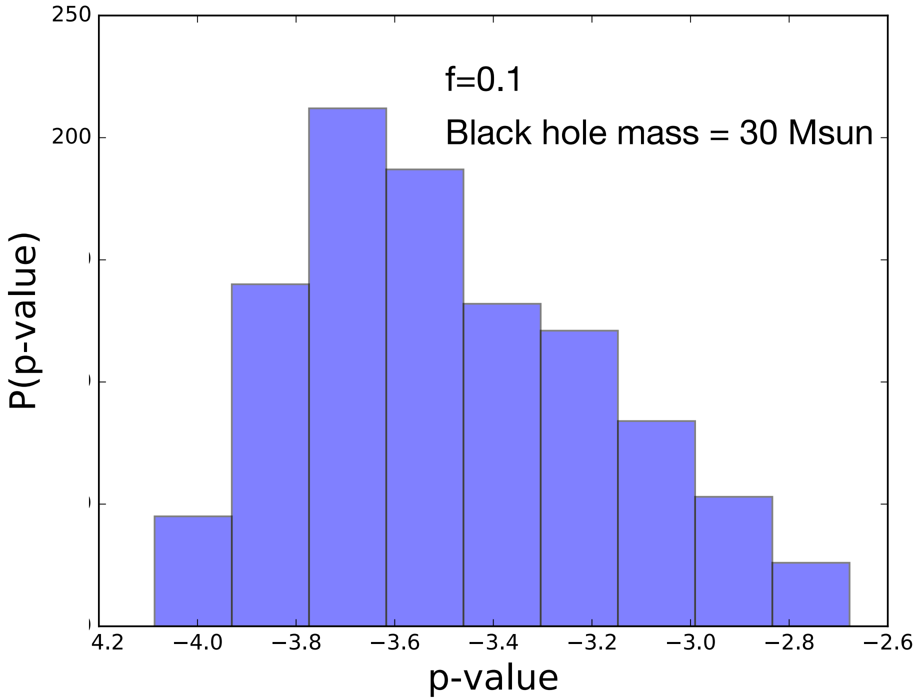

f=0.1
Black hole mass = 30 Msun
P(p-value)
p-value

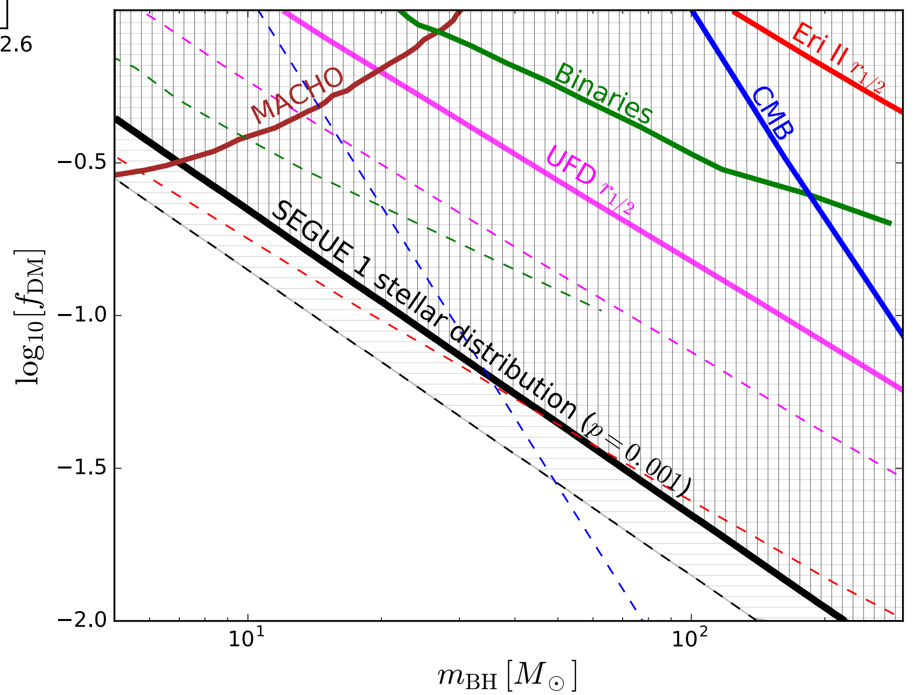

MACHO
Binaries
CMB
Eri II $r_{1/2}$
UFD $r_{1/2}$
SEGUE 1 stellar distribution ($p = 0.001$)
$\log_{10}[f_{\rm DM}]$
$m_{\rm BH}\,[M_\odot]$

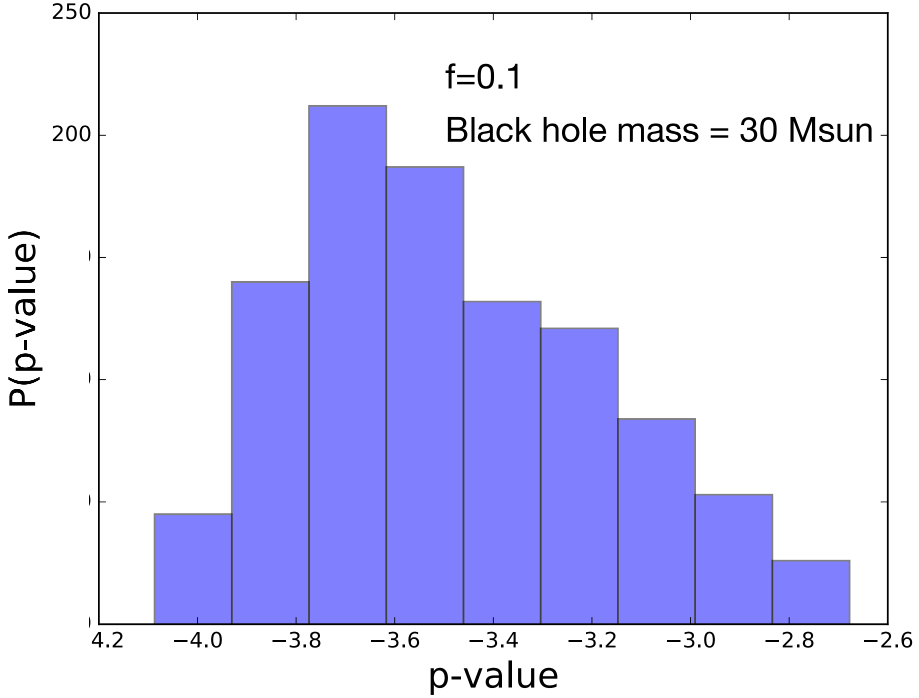

f=0.1
Black hole mass = 30 Msun
P(p-value)
p-value
250
200
4.2
−4.0
−3.8
−3.6
−3.4
−3.2
−3.0
−2.8
−2.6

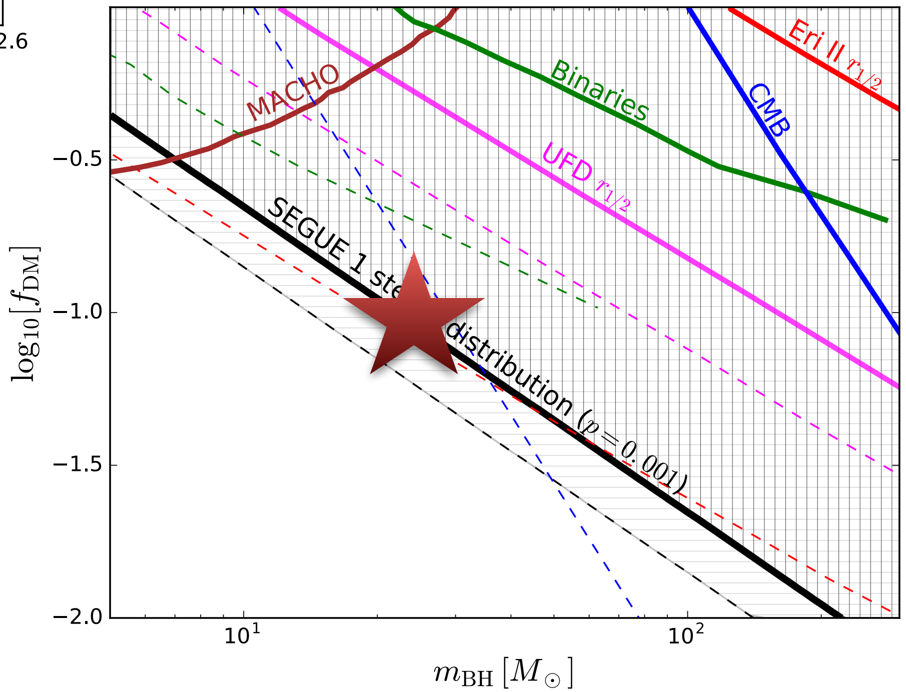

MACHO
Binaries
CMB
Eri II $r_{1/2}$
UFD $r_{1/2}$
SEGUE 1 ste distribution ($p = 0.001$)
$\log_{10}[f_{\mathrm{DM}}]$
$m_{\mathrm{BH}}\,[M_\odot]$
−0.5
−1.0
−1.5
−2.0
10^1
10^2

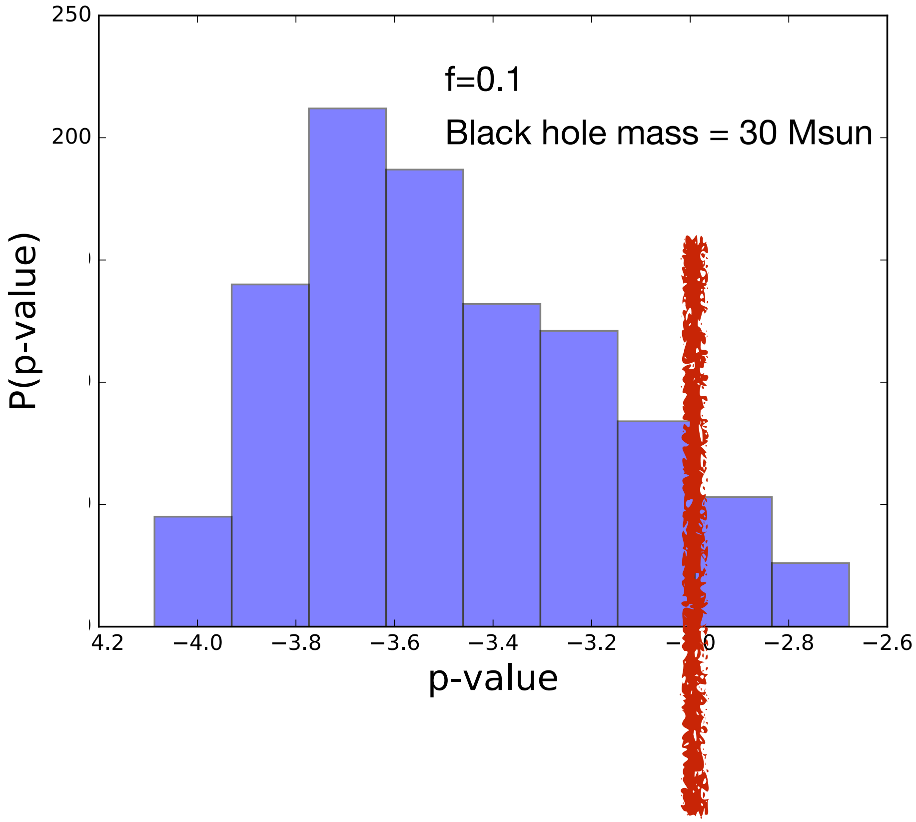

f=0.1
Black hole mass = 30 Msun
P(p-value)
p-value
250
200
4.2
−4.0
−3.8
−3.6
−3.4
−3.2
−2.8
−2.6

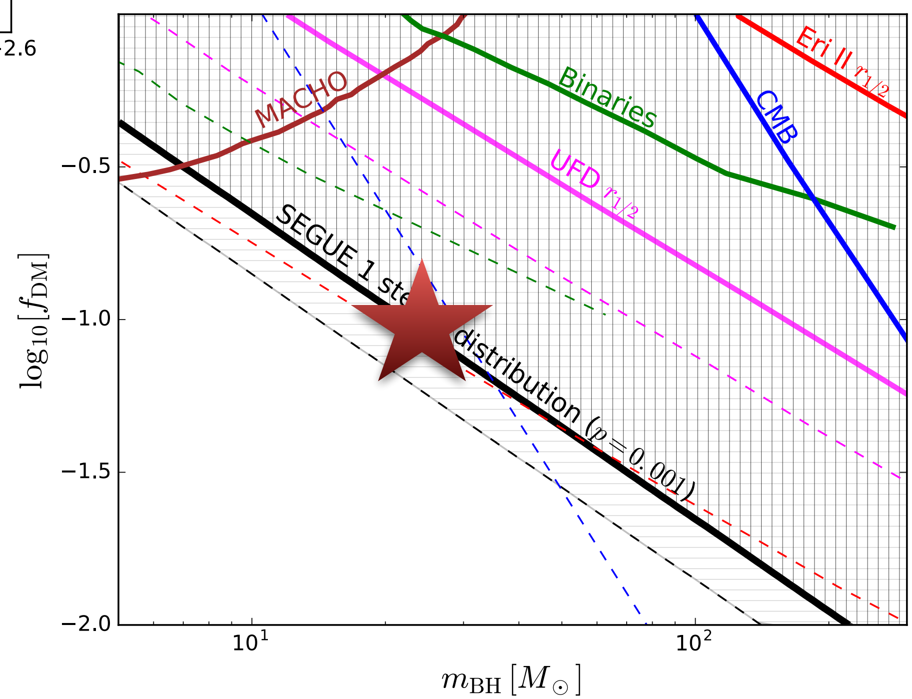

Eri II $r_{1/2}$
CMB
Binaries
MACHO
UFD $r_{1/2}$
SEGUE 1 ste
distribution ($p = 0.001$)
$\log_{10}[f_{\rm DM}]$
$m_{\rm BH}\,[M_\odot]$
−0.5
−1.0
−1.5
−2.0
10^1
10^2

Three things to take away from dwarf constraints

1. Black holes as dark matter lead to a depletion of stars in the center and the appearance of a ring in the projected stellar surface density profile.

2. Current observations rule out the possibility that more than 4% of the dark matter is composed of black holes with mass of few tens of solar masses.

3. Next generation of large aperture telescopes could improve these constraints.

How to distinguish primordial from baryonic black holes

Koushiappas & Loeb, arXiv:1708.07380

Rate of black hole merger events

- Black holes must be formed.
- Black holes must find a way to get close enough so that gravitational waves can take-over as the dominant energy loss mechanism.

Koushiappas & Loeb, arXiv:1708.07380

Rate of black hole merger events

- Black holes must be formed.
- Black holes must find a way to get close enough so that gravitational waves can take-over as the dominant energy loss mechanism.

Both of the above depend on the ability of gas to cool

Koushiappas & Loeb, arXiv:1708.07380

Rate of black hole merger events

$$\mathcal{N}(>z) = \int_z^\infty \frac{d\mathcal{R}}{dz}\, dz$$

$$\frac{d\mathcal{R}}{dz} \equiv \int_{M_{\rm min}(z)}^\infty \frac{dN}{dM\,dV} C_{\rm NG}(M,z) \frac{\langle \epsilon(M,z)\rangle}{(1+z)} \frac{\dot{M}_{\rm g}(M,z)}{2m_{\rm BH}} \frac{dV}{dz}\, dM$$

- Minimum halo mass where gas can cool ($M_{\rm min}(z)$)
- Dark matter halo mass function ($\frac{dN}{dM\,dV}$)
- Effects of non-gaussianity on halo mass function ($C_{\rm NG}(M,z)$)
- Fraction of gas that cools to form black holes ($\langle \epsilon(M,z)\rangle$)
- Rate of gas inflow ($\dot{M}_{\rm g}(M,z)$)
- Black hole mass (monochromatic) ($m_{\rm BH}$)
- Comoving volume ($\frac{dV}{dz}$)
- Integral is over all dark matter halo masses (dM)

Koushiappas & Loeb, arXiv:1708.07380

Rate of black hole merger events

$$\mathcal{N}(>z) = \int_z^\infty \frac{d\mathcal{R}}{dz}\, dz$$

Fraction of gas that cools to form black holes

Rate of gas inflow

$$\frac{d\mathcal{R}}{dz} \equiv \int_{M_{\rm min}(z)}^\infty \frac{dN}{dM\,dV} C_{\rm NG}(M,z)\,\frac{\langle\epsilon(M,z)\rangle}{(1+z)}\,\frac{\dot{M}_{\rm g}(M,z)}{2m_{\rm BH}}\,\frac{dV}{dz}\,dM$$

Minimum halo mass where gas can cool

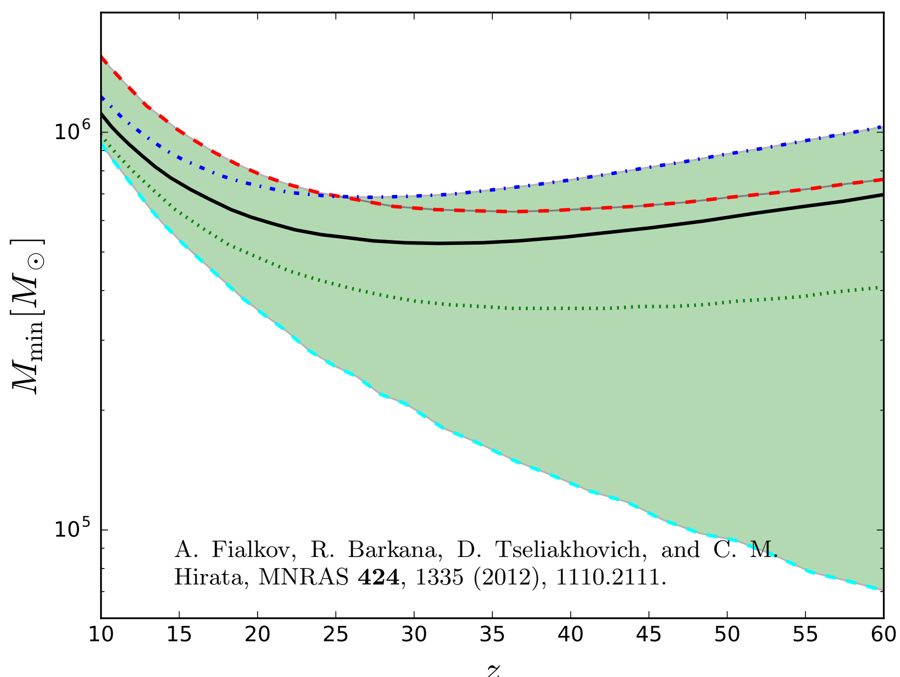

Koushiappas & Loeb, arXiv:1708.07380

Rate of black hole merger events

$$\mathcal{N}(>z) = \int_z^\infty \frac{d\mathcal{R}}{dz}\, dz$$

Fraction of gas that cools to form black holes

Rate of gas inflow

$$\frac{d\mathcal{R}}{dz} \equiv \int_{M_{\rm min}(z)}^{\infty} \frac{dN}{dM dV} C_{\rm NG}(M,z) \frac{\langle \epsilon(M,z)\rangle}{(1+z)} \frac{\dot{M}_{\rm g}(M,z)}{2m_{\rm BH}} \frac{dV}{dz}\, dM$$

Dark matter halo mass function

Effects of non-gaussianity $f_{\rm NL} = 43$ on halo mass function

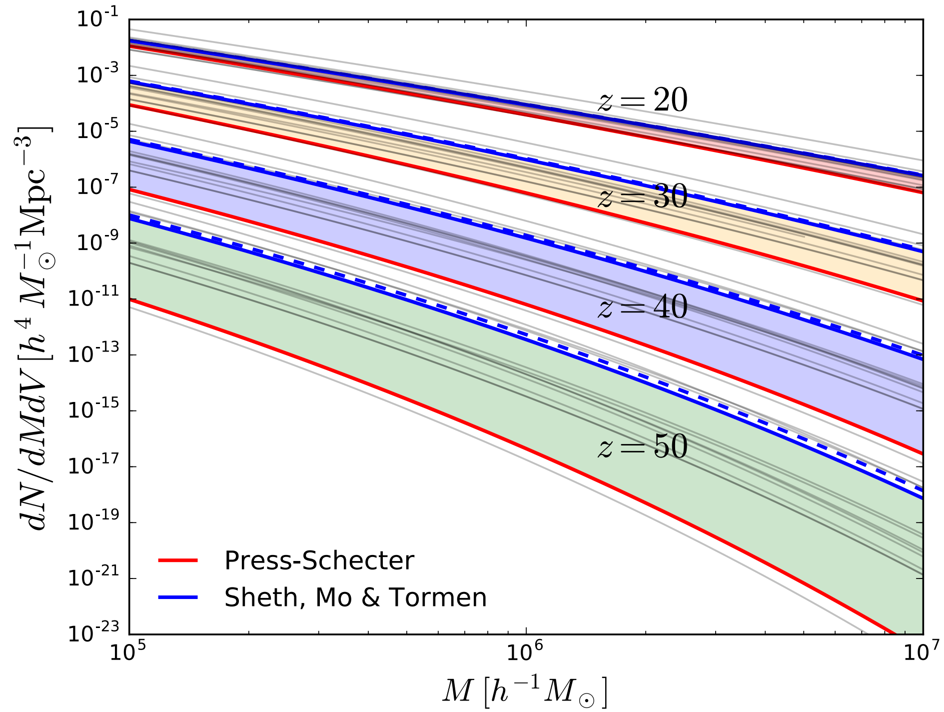

Koushiappas & Loeb, arXiv:1708.07380

S. Matarrese, L. Verde, and R. Jimenez, ApJ **541**, 10 (2000), astro-ph/0001366.

Planck Collaboration, P. A. R. Ade, N. Aghanim, M. Arnaud, F. Arroja, M. Ashdown, J. Aumont, C. Baccigalupi, M. Ballardini, A. J. Banday, et al., A&A **594**, A17 (2016), 1502.01592.

Rate of black hole merger events

$$\mathcal{N}(>z) = \int_z^\infty \frac{d\mathcal{R}}{dz}\, dz$$

Fraction of gas that cools to form black holes

Rate of gas inflow

$$\frac{d\mathcal{R}}{dz} \equiv \int_{M_{\rm min}(z)}^\infty \frac{dN}{dM\,dV} C_{\rm NG}(M,z)\, \frac{\langle \epsilon(M,z)\rangle}{(1+z)}\, \frac{\dot{M}_{\rm g}(M,z)}{2m_{\rm BH}}\, \frac{dV}{dz}\, dM$$

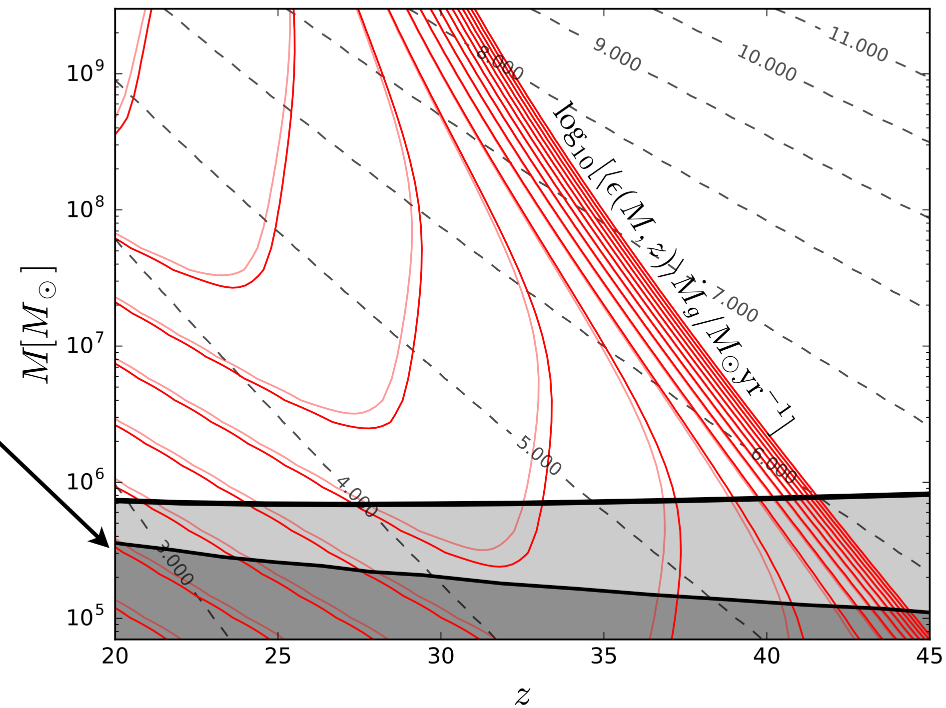

Koushiappas & Loeb, arXiv:1708.07380

Rate of black hole merger events

$$\mathcal{N}(>z) = \int_z^\infty \frac{d\mathcal{R}}{dz}\,dz$$

Fraction of gas that cools to form black holes

Rate of gas inflow

$$\frac{d\mathcal{R}}{dz} \equiv \int_{M_{\min}(z)}^\infty \frac{dN}{dM\,dV} C_{\rm NG}(M,z) \frac{\langle\epsilon(M,z)\rangle}{(1+z)} \frac{\dot{M}_{\rm g}(M,z)}{2m_{\rm BH}} \frac{dV}{dz}\,dM$$

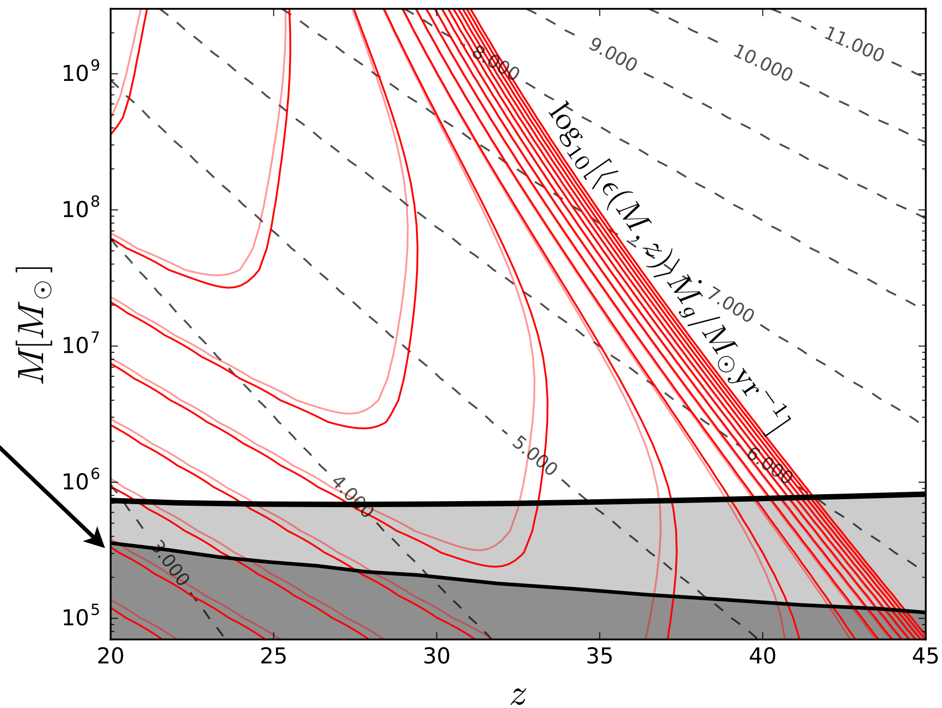

Koushiappas & Loeb, arXiv:1708.07380

E. Neistein and A. Dekel, MNRAS **388**, 1792 (2008), 0802.0198.
T. Goerdt, D. Ceverino, A. Dekel, and R. Teyssier, MNRAS **454**, 637 (2015), 1505.01486.
G. Sun and S. R. Furlanetto, MNRAS **460**, 417 (2016), 1512.06219.

Rate of black hole merger events

Define maximum redshift

$$\mathcal{N}(z = z_{\max}) = 1\,\mathrm{yr}^{-1}$$

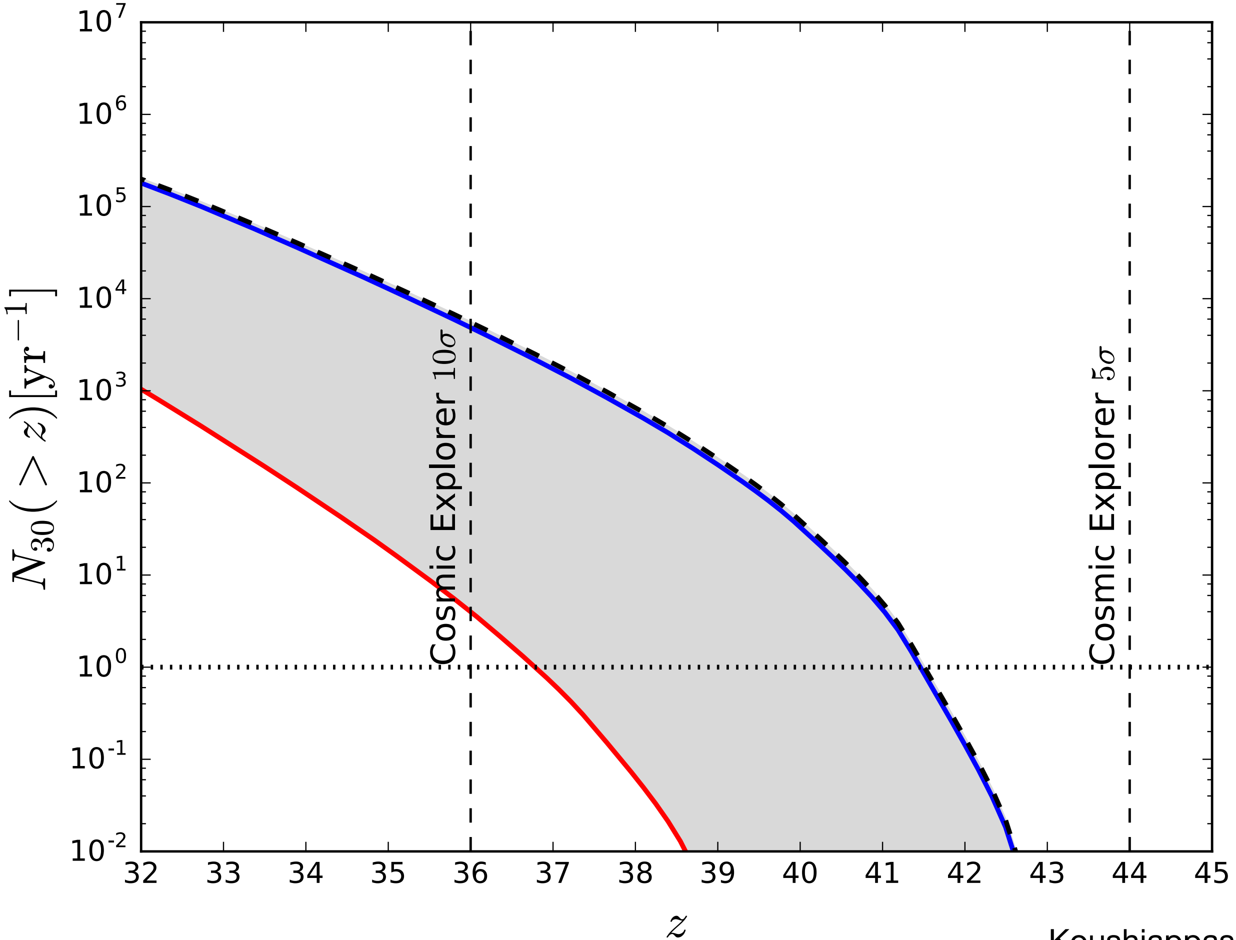

Koushiappas & Loeb, arXiv:1708.07380

Rate of black hole merger events

Define maximum redshift

$$\mathcal{N}(z = z_{\rm max}) = 1\,{\rm yr}^{-1}$$

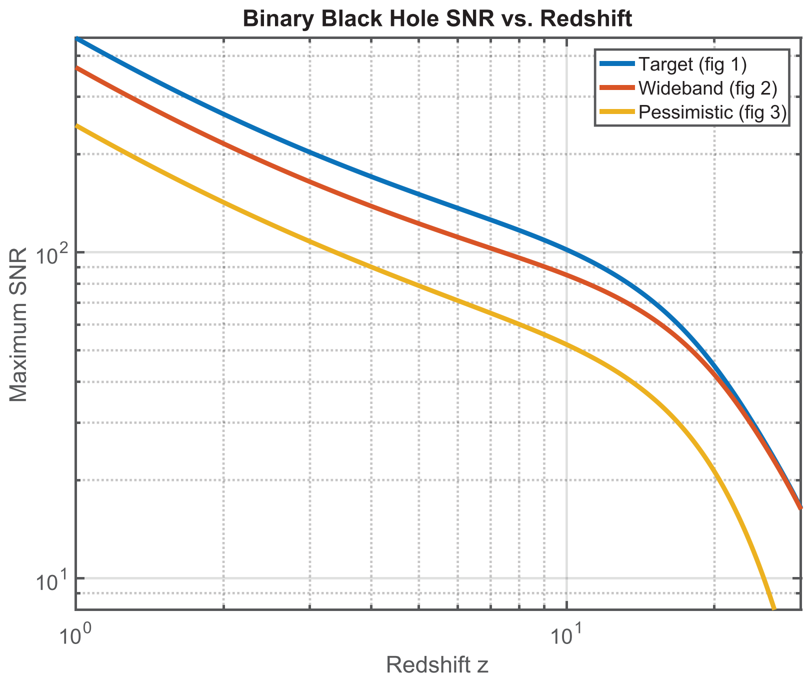

Cosmic Explorer

Koushiappas & Loeb, arXiv:1708.07380

Rate of black hole merger events

Define maximum redshift

$$\mathcal{N}(z = z_{\max}) = 1\,\mathrm{yr}^{-1}$$

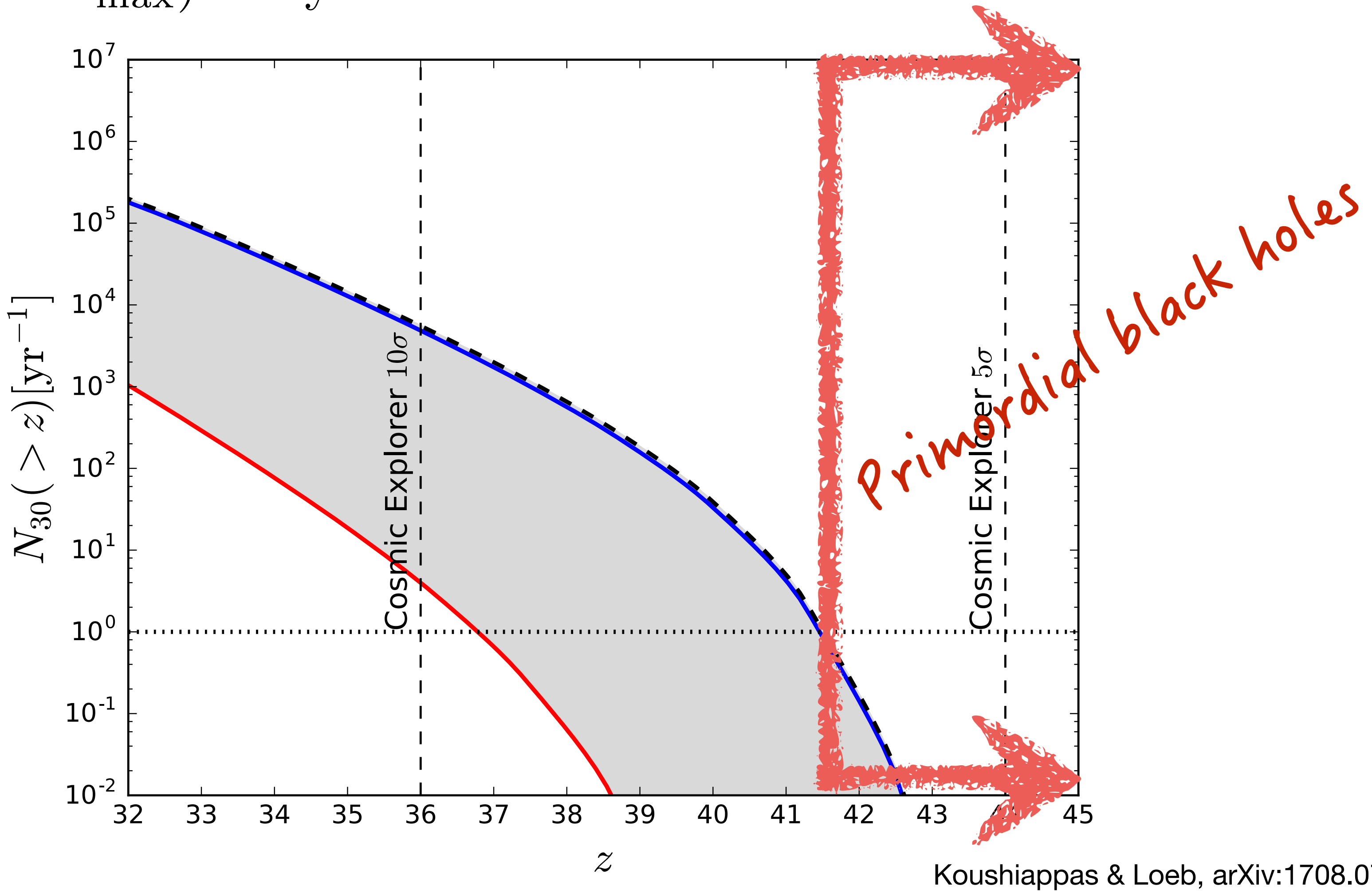

Koushiappas & Loeb, arXiv:1708.07380

The potential primordial black hole - WIMP conflict

The potential primordial black hole - WIMP conflict

- Dark matter gets “locked” onto the black hole at formation.
- There is a central core set by the equilibrium of in-falling and annihilating material
- Search for discrete sources of annihilation today

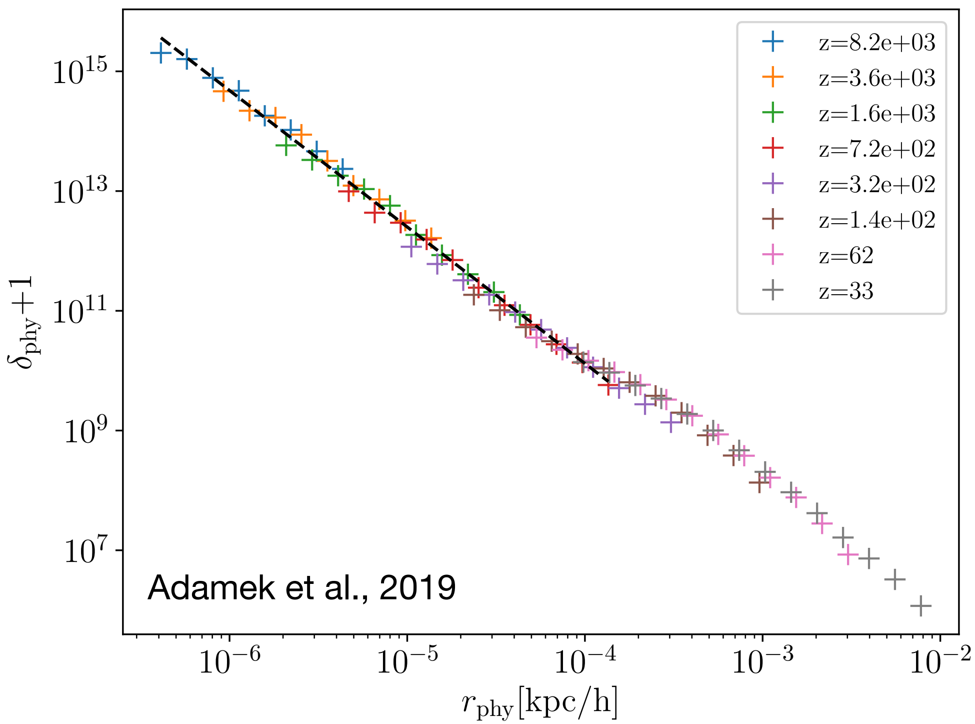

$$f_{\rm PBH} = \frac{\Gamma_{\rm DM}\, M_{\rm PBH}}{\Gamma_{\rm PBH}\, m_\chi}.$$

m_χ	10 GeV	100 GeV	1 TeV
$f_{\rm PBH} \lesssim$	10^{-9}	2×10^{-9}	4×10^{-9}

Primordial black holes and WIMP dark matter cannot co-exist!!!!

The potential primordial black hole - WIMP conflict

Two ways this result can be strengthened

- Use existing measurements of the diffuse gamma-ray background and annihilation constraints.
- Use of the 1-point function.

The potential primordial black hole - WIMP conflict

Two ways this result can be strengthened

- Use existing measurements of the diffuse gamma-ray background and annihilation constraints.
- Use of the 1-point function.

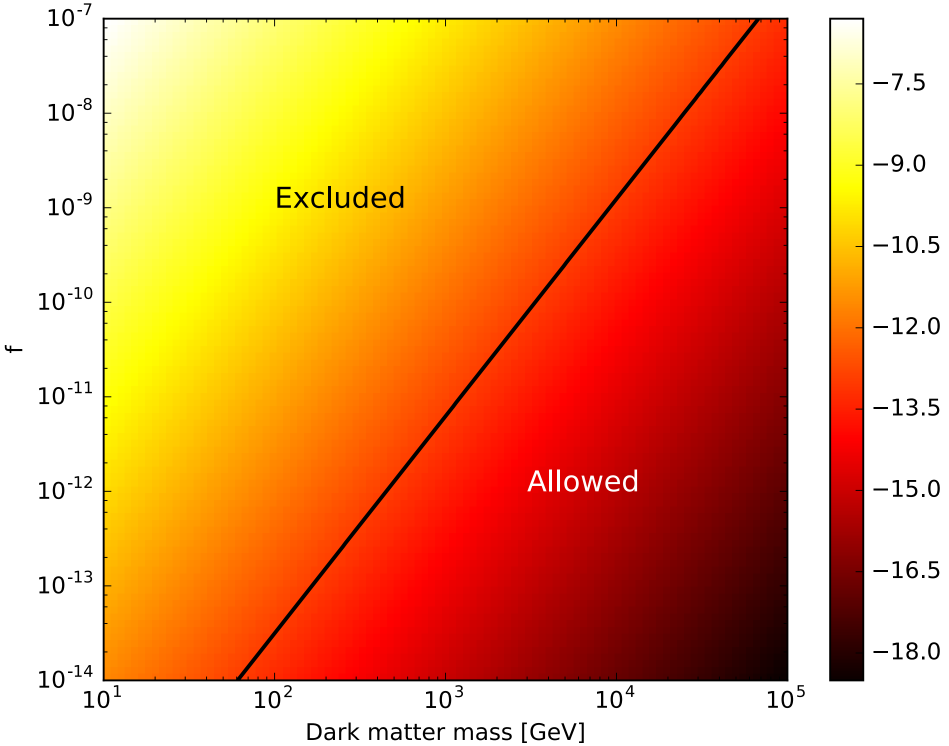

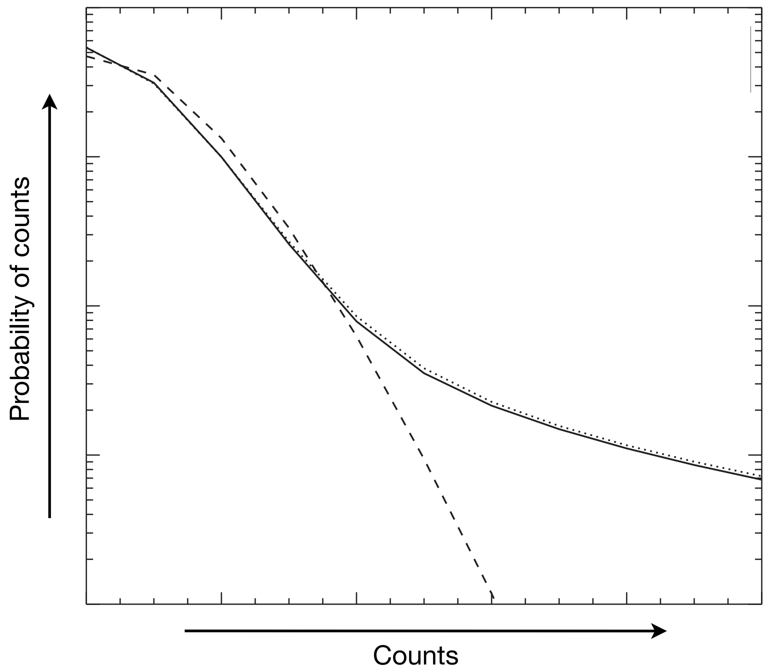

Kliegman & Koushiappas (2020)

The potential primordial black hole - WIMP conflict

Probability of observing flux F from a single black hole

$$P_1(F;\psi_i) \propto \Theta(F_{\max} - F) \int_0^{\ell_{\max}} d\ell\, \ell^4 \int_{M_{\min}}^{M_{\max}} dM \frac{dN[r(\ell,\psi_i)]}{dM dV} \times P[L_{\rm sh} = 4\pi\ell^2 F | M, r(\ell,\psi_i)]. \quad (4)$$

$$dN(r)/dMdV = A \frac{(M/M_\odot)^{-\beta}}{\tilde{r}(1+\tilde{r})^2},$$

Probability of observing total flux F from multiple black holes

$$P_{\rm sh}(F;\psi_i) = \mathcal{F}^{-1}\{e^{\mu(\psi_i)(\mathcal{F}\{P_1(F;\psi_i)\}-1)}\},$$

$$\mu(\psi_i) = \Omega_{\rm pixel} \int d\ell\, \ell^2 \int dM \frac{dN[r(\ell,\psi_i)]}{dM dV}.$$

Mean number of black holes in a given pixel

Kliegman & Koushiappas (2020)

The potential primordial black hole - WIMP conflict

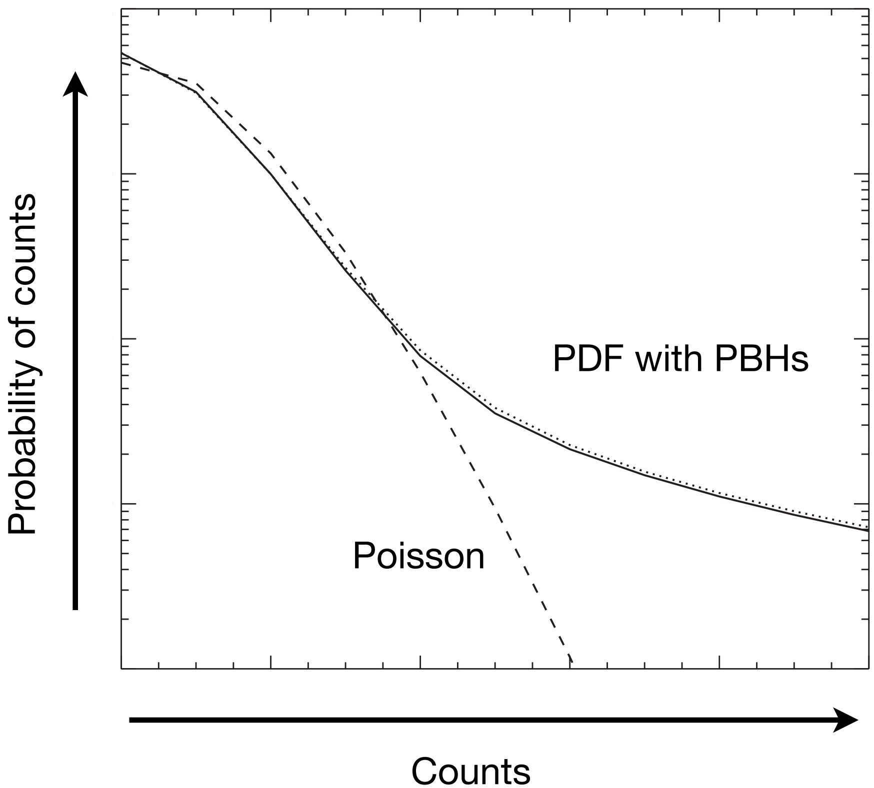

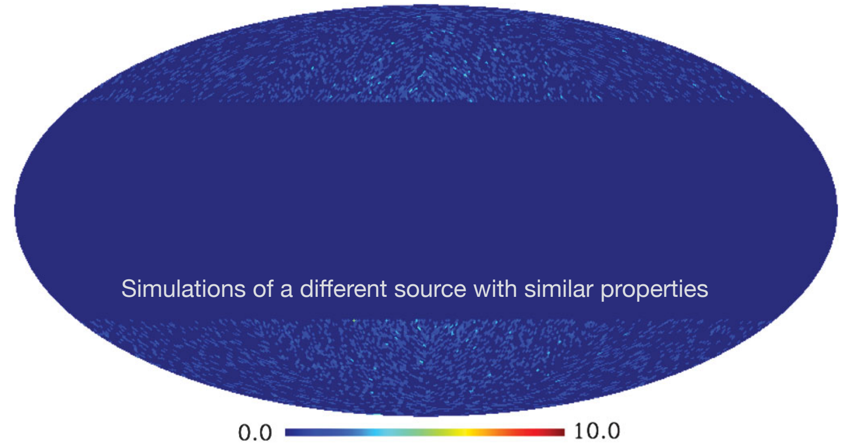

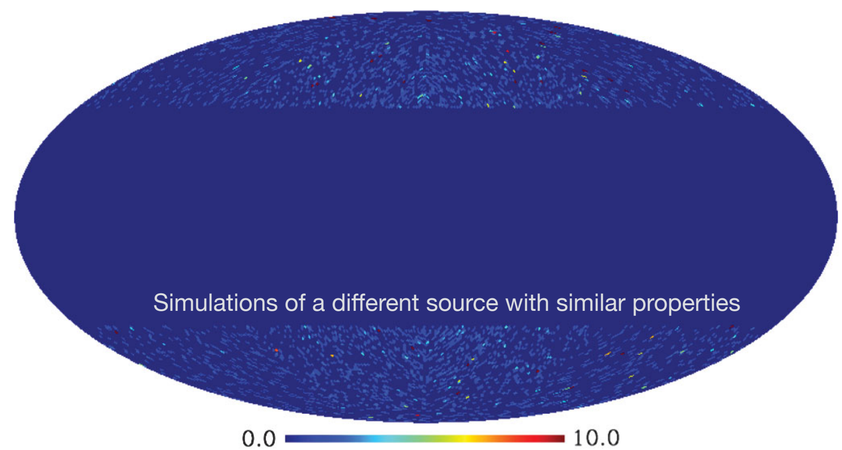

Discrete sources give counts probability function that deviates from Poisson

See Baxter et al., PRD 82, 123511 (2010)

Fin

Where do supermassive black holes come from?

Where do supermassive black holes come from?

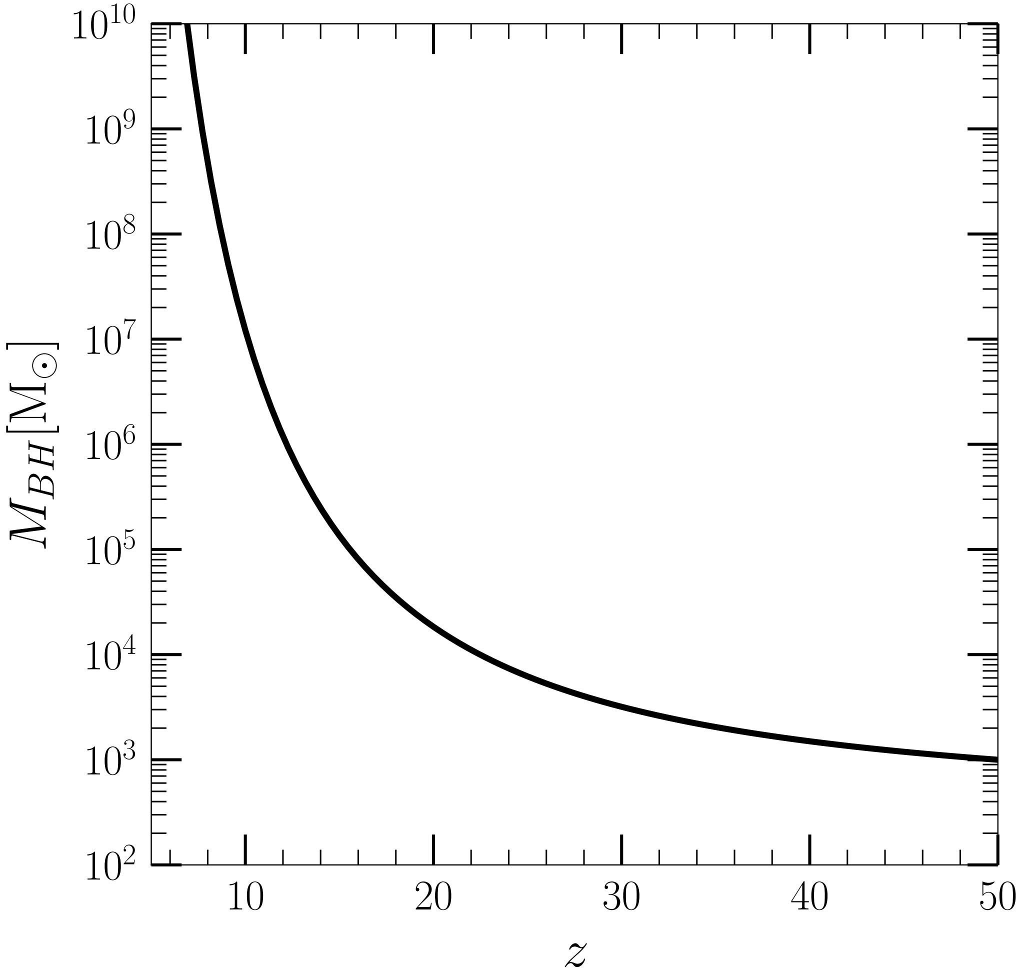

$$L_{Edd} = \frac{4\pi G m_p c M_{BH}}{\sigma_T}$$

$$M_{BH}(z) = M_0 e^{k(t(z)-t_0)}$$

Where do supermassive black holes come from?

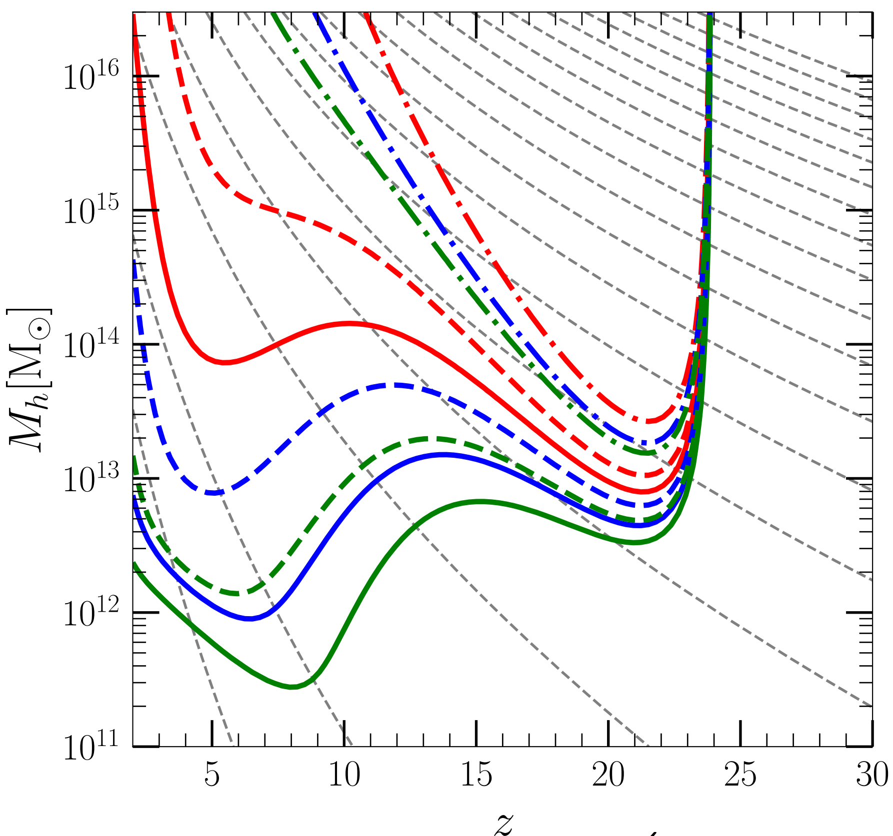

Host halos must be extremely rare

$$\log_{10}\left(F\,\langle f(M_h,z)\rangle\,\frac{\dot{M}_g(M_h,z)}{\dot{M}_{BH}(M_{BH},\epsilon)}\right)=0$$

Vattis & Koushiappas (2020)